POLITECNICO
MILANO 1863

SCUOLA DI INGEGNERIA INDUSTRIALE
E DELL'INFORMAZIONE

Modeling thrombosis in a microfluidic system: the effect of shear stress, microparticles and protein surfaces

TESI DI LAUREA MAGISTRALE IN
BIOMEDICAL ENGINEERING
INGEGNERIA BIOMEDICA

Author: **Eleonora Puce**

Student ID: 968516
Advisor: Prof. Alberto C. L. Redaelli
Co-advisor: Prof. Marvin J. Slepian
Ing. Tatiana Mencarini
Silvia Bozzi, Phd

Academic Year: 2021-22

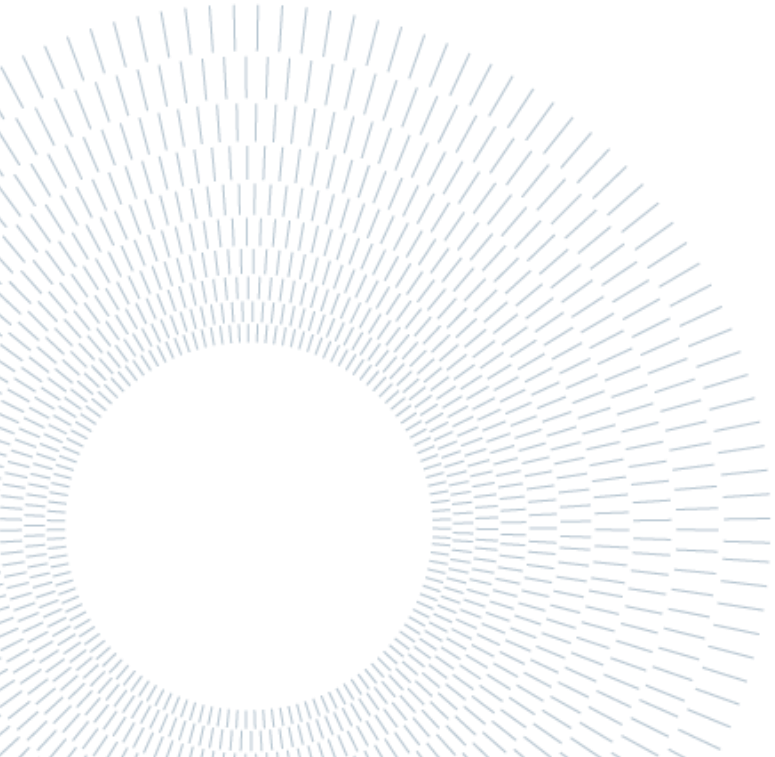

Abstract

Platelets play a central role in hemostasis, but in case of platelet dysfunction, they can lead to excessive bleeding, thrombosis, myocardial infarction, ischemic stroke. It is important to properly monitor platelet activity and, in this regard, many platelet function testing devices are commercially available. However, only few accepted clinical methods evaluate platelet activity under physiological flow conditions. The present work focuses on the characterization of a microfluidic platform to reach two main purposes: assess thrombus formation under in vivo-like flow conditions, simulating the presence of a vessel injury by coating the channels of a microfluidic device with extracellular matrix (ECM) proteins to promote platelet activity; develop an easy-to-use, label-free system, using a pressure sensor to assess platelet activity. The effect of shear stress and different ECM immobilized proteins on platelet adhesion and aggregation has been investigated. Results show how, except for collagen, all the other protein substrates are not able to promote significant platelet aggregation; moreover, high shear stresses allow good platelet adhesion only on collagen and fibrinogen. Platelet activity alteration caused by high levels in blood of platelet-derived microparticles (PDMPs) was evaluated via the same platform. Results show reduced platelet aggregation when PDMPs are present, especially at high shear stress. This altered platelet activity may lead to a high number of circulating activated microaggregates and to further increased levels of PDMPs, that can cause severe complications in vivo, such as microthrombosis or organ failure. The effect of Covid-19 on platelet activity was also investigated. Analysis between the two donor groups (healthy subjects and covid patients) does not highlight relevant differences; however, more experiments should be performed to confirm the absence or presence of any statistically significant difference. The addition of the pressure sensor to the platform allowed to perform the preliminary tests for the design of a bedside point-of-care device, however more precise results are needed to proceed with the device development.

Key-words: thrombosis, extracellular matrix proteins, platelet-derived microparticles, microfluidic device, platelet function testing, pressure sensor.

Sommario

Le piastrine svolgono un ruolo centrale nel processo emostatico, ma disfunzioni piastriniche possono causare sanguinamento, trombosi, infarto, ictus ischemico. È importante quindi monitorare opportunamente l'attività piastrinica; al giorno d'oggi sono disponibili numerosi test di funzionalità piastrinica, tuttavia, solo pochi dei metodi clinicamente accettati operano in condizioni di flusso simil-fisiologiche. A tal proposito, il presente lavoro prevede la caratterizzazione di una piattaforma microfluidica per raggiungere due obiettivi principali: valutare la formazione di trombi in condizioni di flusso simili a quelle in vivo, rivestendo i canali di un chip microfluidico con proteine della matrice extracellulare (ECM) per simulare un danno ai vasi sanguigni e promuovere l'attività piastrinica; sviluppare un dispositivo label-free e di semplice utilizzo, che utilizzi un sensore di pressione per valutare l'attività piastrinica. È stata valutata l'influenza che lo shear stress e le differenti proteine testate hanno su adesione ed aggregazione piastrinica. I risultati mostrano come, ad eccezione del collagene, tutti gli altri substrati, da soli, non siano in grado di promuovere l'aggregazione piastrinica; inoltre, alti shear stress premettono una buona adesione solo su collagene e fibrinogeno. Con la stessa piattaforma è stata valutata l'alterazione dell'attività piastrinica causata da alti livelli nel sangue di microparticelle piastriniche (PDMPs). I risultati evidenziano una ridotta aggregazione in presenza di PDMPs, soprattutto ad alti shear stress. Tale alterazione potrebbe comportare la formazione di numerosi microaggregati particolarmente reattivi in circolo, oltre che causare un ulteriore aumento dei livelli di PDMPs, con il rischio di complicazioni in vivo come microtrombosi o collasso di organi. Si è anche analizzato l'effetto del Covid-19. Le analisi effettuate non evidenziano particolari alterazioni dell'attività piastrinica, ma, per risultati più accurati, è necessario realizzare un maggior numero di esperimenti. L'inserimento del sensore di pressione nella piattaforma ha permesso di realizzare dei test preliminari per la progettazione di un dispositivo bedside; valutazioni più accurate sono però necessari per procedere con lo sviluppo del dispositivo.

Parole chiave: trombosi, proteine della matrice extracellulare, microparticelle piastriniche, dispositivo microfluidico, test di funzionalità piastrinica, sensore di pressione.

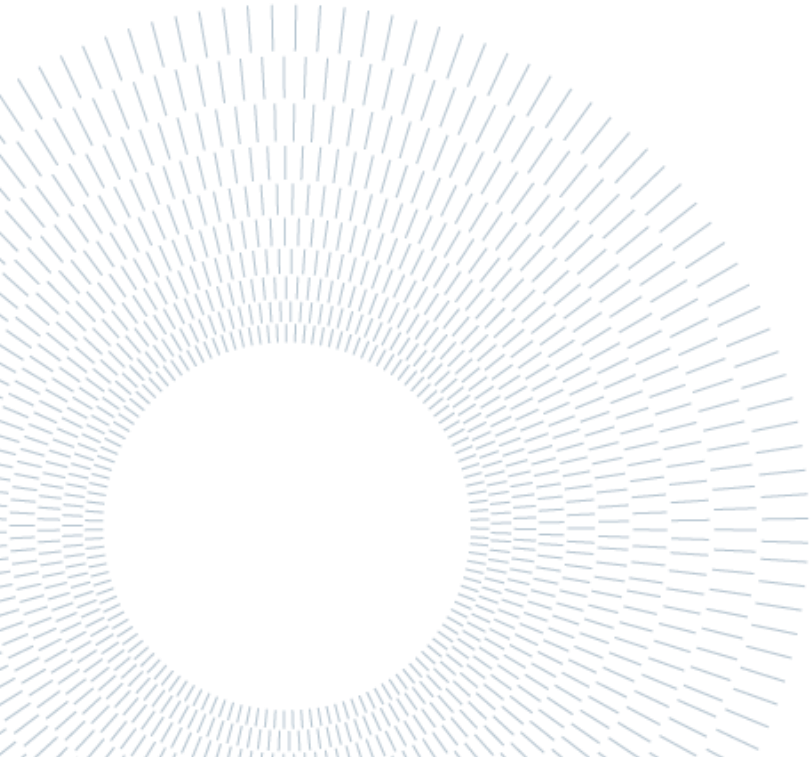

Contents

Introduction

Cardiovascular diseases are a group of heart and blood vessels disorders representing the leading cause of mortality and morbidity worldwide. Thrombosis is a major complication of cardiovascular diseases, it may lead to thromboembolism, ischemia, myocardial infarction. Clinical disorders associated to platelet dysfunction include excessive or even spontaneous bleeding, anomalies in platelet count, or pathological thrombus formation inside blood vessels [1]. Disorders caused by platelet dysfunction can be inherited, and generally linked to other disorders (like immune system abnormalities or kidney problems), or they can be acquired, due to abnormal inflammatory responses, assumption of drugs affecting normal platelet activity, treatments, implantation of biomedical devices or any pathology that alters the physiological hemostatic pathway. Many factors can also alter the blood fluid dynamics, incrementing the risk of thromboembolism or stroke. Blood vessels injuries, surgery and the implantation of devices in contact with blood (heart-supporting systems, grafts, oxygenators, stents, heart valves) may also increase this risk [2]. Antiplatelet therapy is the standard treatment for platelet dysfunction-associated disorders; however, it presents several limitations and it does not consider patients responsiveness individuality to antiplatelet agents: it may lead to excessive bleeding due to an incorrect therapy management whereas many patients continue experiencing cardiovascular events [3]. There is the urge to find new and improved methods to monitor platelet activity, improve treatments and identify individualized antiplatelet therapy. In this respect, the present work aims to better explore the mechanisms behind platelet adhesion and aggregation by means of a microfluidic platform.

This research has a twofold aim: the characterization of the microfluidic platform to assess platelet activation as a function of shear stresses and protein substrates; the

refinement of the platform, to develop a point-of-care device to assess platelet activity by monitoring the pressure inside the channel of a microfluidic device.

The characterized platform was used to evaluate the effects of platelet-derived microparticles (PDMPs) and Covid-19 on platelet activity.

In the first chapter, an overview of the hemostatic process, the disorders caused by platelet dysfunctions, the main actors in the process of thrombus formation and the role of PDMPs will be presented. This chapter also deals with the main complications of Covid-19.

The second chapter presents many ways to test platelet activity, from the early methods to new advances in platelet function testing (PFT) devices. It reports several studies on microparticles as a diagnostic tool for many severe pathologies; it also reports studies on the effect of Covid-19 on platelet activity.

The third chapter focuses on the used materials and methods. The microfluidic platform, the specific protocol defined to assess platelet activation by means of shear stress and protein substrates, the PDMP generation process and the method used for pressure measurements are described in detail.

The fourth and the fifth chapters show, respectively, the results obtained from each set of experiments and the related discussions and comments.

The last chapter presents some future developments that could strengthen and enhance the obtained results.

1 Clinical background

1.1. Blood and platelets

Blood is a specialized body fluid that circulates constantly in the body providing oxygen, nutrients and waste products removal. It is pumped through blood vessels (arteries, veins and capillaries), whose internal walls help preventing blood from clotting.
Plasma represents the liquid portion of blood; it is mainly composed of water, fat, proteins, sugar and salt. Its primary function is to transport blood cells, nutrients, waste products, antibodies, blood proteins, clotting proteins and chemical messengers such as hormones.
The other half of blood volume is made of three types of blood cells:

- Red blood cells (also called erythrocytes), which contain a protein, hemoglobin, that carries oxygen to the tissues;
- White blood cells (also called leukocytes), which provide a response against infections, regulate the immune system and produce antibodies;
- Platelets (also called thrombocytes), that promote, among other functions, blood coagulation process.

Platelets are small cells that contain a considerable number of mediators that regulate not just hemostasis and thrombosis, but also other functions, such as angiogenesis, vasomotor function, cell growth, chemotaxis (cell recruitment), metastasis and inflammation. When vascular injuries occur, platelets provide the initial seal to prevent bleeding, ensuring vessel wall structural integrity [4].
Normal human platelet count is 150–400 billion per liter of blood. Platelets can only be visible under a microscope, in fact, they have a typical diameter of 2–3 μm and a typical thickness of 0.5 μm (platelet volume 6-10 fL). Their lifespan in the human body is about10 days. In their non-active form they have a discoid shape, however, activation

cause a substantial change in shape and they become spheroids with pseudopods, that help platelets adhering both to the subendothelial matrix and to other cells (Figure 1.1) [5].

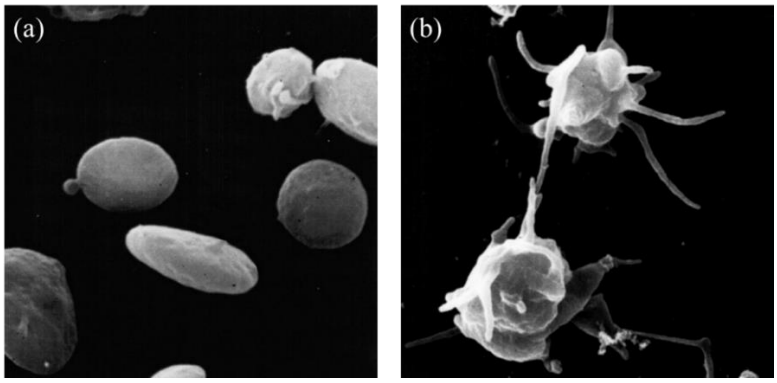

Figure 1.1: *Example of non-activated (a) and activated (b) platelet.*

Platelets are not properly cells, as they lack a nucleus; they are actually circulating fragments of cells, but they contain many structures crucial to the coagulation process. Many types of receptors contribute to the initiation of platelet activation and aggregation pathway. Constituents relevant for thrombosis are present both in the cytoplasm (within platelet granules) and on the cell membrane. The platelet membrane contains glycoproteins that interact with several ligands: either soluble, that activate platelets, or fixed ligands (present within the vessel wall and on other cells) that allow platelet adhesion. The platelet contains some secretory vesicles called granules. The two main types of granules present in platelets during the non-active state are α and δ granules [6].

α granules secrete most of platelet factors involved in coagulation, hemostasis and thrombosis, such as factors IV, V, XI, XII, XIII, fibrinogen, von Willebrand factor (vWF), P-selectin, β thromboglobulins. They also contain adhesion molecules involved in platelet-vessel wall interaction (fibronectin and vitronectin), growth factors (platelet-derived growth factor (PDGF), transforming growth factor-β, vascular endothelial growth factor (VEGF)) and other proteins that are also expressed on the platelet cell membrane (GPIb complex, GPVI, GPIIb/IIIa).

δ granules are small granules containing high concentrations of adenosine diphosphate (ADP, involved in hemostasis), adenosine triphosphate (ATP) and serotonin

(responsible for vasoconstriction), together with small guanosine triphosphate-binding proteins and adhesion molecules.
During platelet activation, granules release their content into the extracellular environment, contributing to the recruit of other platelets, hence aggregation.

1.2. Hemostasis

Hemostasis is the physiological process that allows maintaining blood vessel integrity when an injury occurs. The hemostatic process activates promptly, forming a hemostatic plug to stop the blood loss; it is tightly regulated to allow a localized action: a balance between the procoagulant and anticoagulant system is required to stop the bleeding at the site of the injury while maintaining blood fluidity elsewhere. After a vessel wall injury, some subsequent steps occur: vasoconstriction, platelet adhesion, activation and aggregation, clot formation and clot retraction (lysis) [7].
The two main events in the hemostatic process, that happen simultaneously, are primary and secondary hemostasis: primary hemostasis is related to platelet adhesion to the site of the injury and to one another (aggregation) forming a platelet plug; secondary hemostasis refers to the formation of an insoluble fibrin mesh, incorporated around and into the plug [8].

Primary hemostasis

Primary hemostasis creates a primary platelet plug: in case of a vessel injury, the subendothelial matrix is exposed to blood flow, and platelet adhesion and activation processes begin (Figure 1.2).

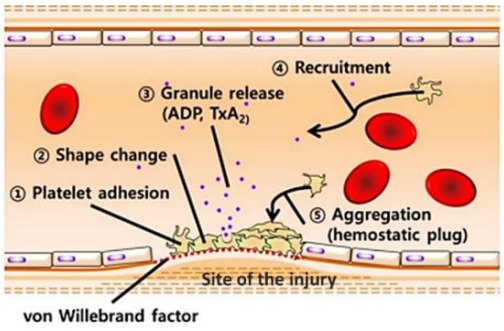

Figure 1.2: *Primary hemostasis: platelet adhesion, activation and aggregation.*

Thrombus formation process starts when multiple adhesive proteins, present in the ECM, target receptors on platelets surface [9]. Examples of these proteins are collagen, laminin, fibrinogen, fibronectin, vitronectin and vWF.

vWF is a large protein present both in the plasma and in the subendothelial matrix. Through the GPIbα-vWF interaction, the receptor GPIb-IX-V binds to vWF present on the immobilized collagen fibrils; high shear stress conditions present at the vessel wall, especially in arterioles, promote the high affinity interaction between GPIbα and immobilized vWF, allowing the initial link between platelets and the matrix. Another receptor critical for adhesion is GPVI that binds to the exposed collagen, present in the subendothelial matrix.

Following activation, αIIbβ3, α2β1 and αvβ3 integrins present on the surface of platelets, undergo conformational changes exposing the ligand binding sites, promoting platelet-platelet connections, strengthening the aggregation.

To allow further aggregation, the activation of neighboring platelets is needed: ADP, Thromboxane A_2 (TXA2) and serotonin are released in the cytosol from platelet granules, promoting platelet activation. Furthermore, activated platelets release some agonists that stimulate G protein-coupled receptors that mediate the activation of surrounding platelets.

Thus, when ligated, receptors initiate cell-signaling pathways, resulting in platelet granule secretion, activation of integrins and platelet cytoskeleton remodeling.

Secondary hemostasis

Secondary hemostasis consists in the ultimate fibrin formation, through the cascade of coagulation serine proteases that leads to the cleavage of soluble fibrinogen by thrombin (Figure 1.3). The generated insoluble fibrin forms a crosslinked fibrin mesh at the site of an injury. Secondary hemostasis includes two different coagulation pathways (intrinsic and extrinsic) which end up forming the common pathway.

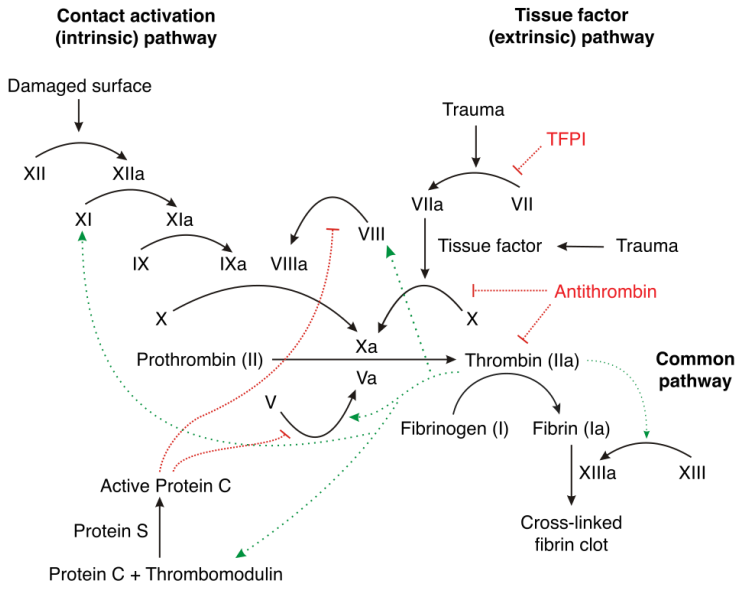

Figure 1.3: *Secondary hemostasis (intrinsic, extrinsic and common pathways) and regulation of clotting (in red).*

The extrinsic pathway begins when, due to the vessel damage, the endothelial cells release tissue factor (TF) which starts a cascade activating factor VII to factor VIIa. Factor VIIa acts then as a catalyst to activate factor X.

The intrinsic pathway starts when exposure to endothelial collagen activates factor XII (an inactive serine protease). This first activation triggers a cascade leading to the activation of factor XI and IX. The complex IXa-VIII activates factor X.

At the factor X activation level, extrinsic and intrinsic pathways converge in the common pathway. In the presence of its cofactor Va, factor Xa activates factor II (also known as prothrombin) to factor IIa (thrombin), leading to prothrombin cleavage into thrombin and subsequent fibrinogen cleavage into fibrin.

Thrombin is pivotal in hemostasis, as it acts both as a thrombotic and antithrombotic agent.

As a thrombotic molecule, thrombin activates, in the intrinsic pathway, factor XIII and cofactors V and VIII. The formation of fibrin strands, from fibrin subunits, leads to the creation of an insoluble fibrin mesh, needed to stabilize the platelet plug [10].

As an antithrombotic molecule, instead, it binds to thrombomodulin present on the endothelial cells, activating C and S anticoagulant proteins. Tissue factor pathway

inhibitors limit thrombin activation by inhibiting factor V and VIII activation; thus, thrombin mainly acts as its own inhibitor.

Fibrinolysis

The fibrinolytic system takes action in wound healing process, dissolving blood clots, it also plays an important role in preventing blood from clotting in healthy blood vessels. It is composed of three serine proteases (tissue-type plasminogen activators, urokinase-type plasminogen activators and plasmin), that ultimately cleave fibrin leading to blood clot retraction.

1.3. Thrombosis

While hemostasis maintains blood vessel integrity providing a physiological response that prevents bleeding, thrombosis, instead, refers to a pathological clot formation within blood vessels. Thrombosis is, in fact, a blood clot formation that causes partial or complete blockage of the vessels, limiting, altering or stopping the blood flow. That blood clot is called a thrombus, and it forms when platelets, fibrin, red and white cells stick together forming a solid mass. It is a serious disorder, especially for its complexity in diagnosis and management. Thrombosis can create further complications in clinical diseases like stroke, myocardial infarction, deep venous thrombosis. Moreover, in some cases, a thrombus, or part of it, may detach from its site of origin, flow in the bloodstream and occlude small vessels causing an embolism. The two main types of thrombosis are arterial and venous thrombosis [11] (Figure 1.4).

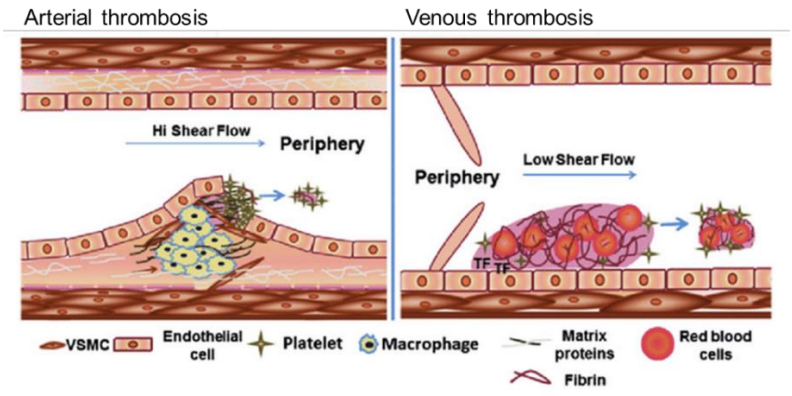

Figure 1.4: *Arterial and venous thrombosis.*

Arterial thrombosis consists in the formation of thrombi mainly made of platelets and fibrin (called "white" thrombi); its main consequences include stroke and myocardial infarction. Arterial thrombi usually form over an atherosclerotic plaque (especially if there is a plaque rupture or if the plaque presents superficial endothelial erosion), in a high shear and flow rate environment. In fact, under the high arterial shear stresses, platelets provide adhesion to the damaged wall, thanks to many platelet agonists and adhesion molecules present in the plaque. Atherosclerosis and vascular anomalies are common risk factors for arterial thrombosis, as they damage the vessel wall inducing turbulences that alter the blood flow, promoting platelet adhesion.

Venous thrombosis is characterized by red blood cells and fibrin-rich thrombi (called "red" thrombi). Some of the common risk factors (both intrinsic and acquired) include surgery, medications, stroke, cancer and inherited hypercoagulable states. In venous thrombosis, the activation of coagulation factors plays a major role; this is in contrast with what happens in arterial thrombosis, where the high flow rate removes these factors preventing their activation cascade.

Several studies highlight that the risk of arterial thrombotic complications is higher in patients with venous thromboembolism, meaning that both arterial and venous thrombosis are triggered by similar biological stimuli that activate coagulation and inflammatory pathways [12]: risk factors common to both of them include obesity, age, smoking, blood hypertension, surgeries, infections, cholesterol, metabolic syndrome, infections, implanted devices [13]. In particular, implanted devices can trigger thrombus formation (leading to the implanted device failure) [14]: when blood flow comes in contact with these devices, protein (especially fibrinogen) absorption to their artificial surface mediates blood cells adhesion, activating the intrinsic pathway of coagulation. Some surfaces (like glasses, silica, collagen) may, instead, activate factor XII leading to the activation of the extrinsic pathway of coagulation. From here, the importance of bioengineered surfaces to avoid blood cells adhesion and thrombus formation.

Pathogenesis is highly triggered by platelet hyperactivity. Antiplatelet (antiaggregant) therapy is a common tool used to prevent vascular events in arterial thrombosis, targeting specific receptors or enzyme that are crucial for the action or the synthesis of some important mediators that allow platelet response. They mainly interfere with key pathways of platelet activation, but, in some cases, this can lead to harmful effects

compromising platelets physiological functioning. If the antiplatelet regimen is not tailored, it may lead to a thrombosis enhancement (caused by under-anticoagulation) or to hemorrhagic bleeding (caused by over-anticoagulation) [15]. Antiplatelet drugs are not very successful in preventing venous thrombosis. Venous thromboembolism, in fact, is mainly treated administrating anticoagulants, that target procoagulant factors.
Arterial and venous thrombosis are the most studied, but thrombosis may also occur within the microcirculation [16]. A large number of severe diseases involve microvascular thrombosis, such as sepsis, thrombotic thrombocytopenic purpura, antiphospholipid syndrome, intravascular coagulation, Covid-19. Microvascular thrombi structure varies from "white" to "red" thrombi, and they can form in organs and microvessels. Microvessels refer to capillaries, arterioles and venules; they all differ for vascular wall structure and function, morphology of endothelial cells, expression of endothelial vWF. Due to these differences, especially between arterioles and venules, there are different ways to treat and prevent microvascular thrombosis [11] [17]. However, it is still not fully understood how differences between thrombotic responses in arterioles and venules can be accounted for.

1.4. Platelet activity

Under physiological conditions, platelets do not adhere to healthy blood vessel walls; however, when vascular injuries occur the subendothelial matrix is exposed to blood flow and platelets initiate primary hemostatic mechanisms providing the initial seal to prevent bleeding, maintaining the integrity of the vessel wall. Platelets initiate both activation and aggregation pathway thanks to many types of receptors, such as glycoproteins (GPIb-IX-V, GPVI) and integrins (αIIbβ3, α2β1, α5β1, α6β1, αvβ3, $P2Y_{12}$, $P2Y_1$, $P2X_1$, PAR1 and PAR4), that respond to specific stimuli [5]. In particular, vWF plays a critical role in tethering platelets to the vessel wall, especially at arterial flow rates (ranging between 3-26 mL/min), by interacting with the receptor GPIb-IX-V. This interaction allows the activation of β1 and β2 integrins and subsequent platelet aggregation.

1.4.1. Platelet-protein interaction

The above-mentioned receptors are fundamental to promote platelet adhesion to the surface and platelet-to-platelet aggregation. Adhesion and aggregation are primarily achieved by the binding of the receptors to specific ligands. These ligands mainly include ECM proteins (such as collagen, fibronectin, laminin) and plasma proteins (such as vitronectin, fibrinogen, vWF). Different proteins have different effects on platelet adhesion, activation and aggregation. The proteins tested in the present work are described below.

Collagen

Collagen represents almost half of the vessel wall protein content. It provides strength and structural support to the vessel wall, but it also contributes initiating the coagulation pathway. It is characterized by a triple helix structure that forms fibrils. There are 28 different collagen types. In particular, fibrillar collagen type I and III are found in the interstitial membrane; fibrillar collagen type VI create a link between the interstitial matrix and the basement membrane; fibrillar collagen type IV, XV and XVIII are found in the basement membrane (Figure 1.5) [18].

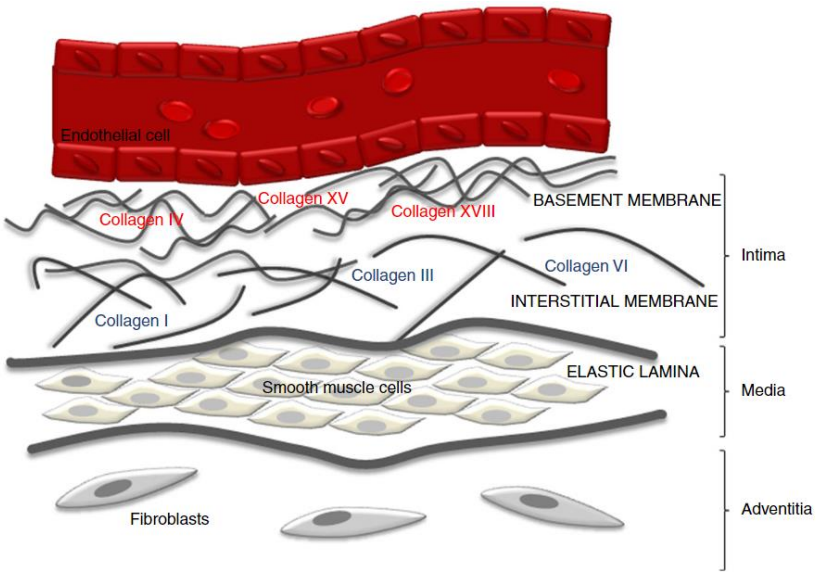

Figure 1.5: C*ollagen distribution in the interstitial matrix and basement membrane surrounding the vascular vessel.*

Collagen I is the most abundant collagen type and can also be found in the connective tissue of skin, intestine, liver and lungs. It is also the collagen type mainly implicated in vascular disorders, in particular thrombosis, when deep vessel injuries occur.
Collagen plays an important role in hemostasis and thrombosis [19]. It is the main agonist that mediates the coagulation pathway in the subendothelial matrix; it binds to many platelet receptors, such as α2β1, αvβ3, α5β1 and α6β1 and chiefly αIIbβ3, which is one of the most abundant receptors present on platelet surface. Moreover, during endothelial injury, the exposed collagen binds to GPVI, triggering a signaling that initiate platelet adhesion; the interaction between collagen and the integrin α2β1 further enhance platelet adherence to collagen itself.

Fibronectin

Fibronectin is a large molecule found both in plasma and in the subendothelial matrix. It is one of the ECM proteins essential for hemostasis and wound healing; fibronectin is involved in the regulation of cell adhesion processes and, during damage repair, it forms a three-dimensional matrix creating a scaffold that provides structural support [20]. It helps mediating homeostasis, in fact, upon vessel injury, the soluble form of fibronectin found in plasma is incorporated into the fibrin clots. Once platelets are activated, platelet adhesion and platelet-to-platelet aggregation is promoted by the binding of platelet receptors to several ligands; in particular, αIIbβ3 and α5β1 bind to fibronectin [21]. Moreover, under both static and flow conditions, adhesion to fibronectin is mediated and promoted by GPIb-vWF binding mechanism [22].

Laminin

Laminin is a large glycoprotein and, together with collagen type IV, one of the major components of the basement membrane of the blood vessels. It is made of three polypeptide chains: α, β and γ; α chains contain most of the sites for cell interaction [23]. Laminin helps create a scaffold for cell migration and it regulates cellular functions [24]; it also participates in the hemostatic process, in fact, upon a vessel injury, laminin becomes an adhesive surface for platelets. Platelet adhesion to this glycoprotein depends

on laminin prior binding to the integrin α6β1. This interaction allows then laminin to bind to the collagen receptor GPVI and to promote platelet spreading [25].

Fibrinogen

Fibrinogen is a soluble glycoprotein abundant in the plasma; it is synthetized by the liver and it is composed of three polypeptide chains (α, β, γ). During inflammations, fibrinogen levels significantly increase; thus, it can be used as a biomarker for coronary artery diseases and myocardial infarction [26]. Fibrinogen is also involved in the coagulation pathway, as its cleavage into insoluble fibrin creates a firm clot to repair vessel damages. In its soluble native conformation it does not bind to platelets, but, once activated, it acts as a coagulation factor binding to αIIbβ3 integrin, promoting platelet adhesion and increasing platelet reactivity.

Vitronectin

Vitronectin is a multifunctional glycoprotein found mainly in plasma as a folded monomer, but also present in the ECM [27]. It is an adhesive glycoprotein that participates in many regulatory processes; in particular, it helps regulate blood coagulation forming complexes with both thrombin and antithrombin.
αIIbβ3 integrin can bind to vitronectin, producing adherence of activated platelets to this adhesive protein. Moreover, vitronectin-αvβ3 interaction can induce platelet adhesion and aggregation [28].

1.4.2. Platelet-derived microparticles

Microparticles are subcellular particles with a size in the range 0.1-1 μm and can originate from the membrane of many cells. They can be involved in many processes (both physiological and pathological) because they inherit some proteins from the surface of the cells they derive from.
Platelets also release membrane macrovesicles (originated from platelets membrane blebs), called platelet-derived microparticles (PDMPs) [29]. They are present in human blood both in physiological and pathological conditions: they are shed and released upon activation, apoptosis, inflammation, implantation of cardiovascular devices,

cardiovascular diseases, high shear stresses (like arterioles shear stresses); they can also form spontaneously during platelet storage. In pathological conditions, PDMPs concentration in blood significantly increase; for this reason, high PDMP count in blood is used as a marker for several diseases, such as stroke, thrombo-embolisms, myocardial infarction, hereditary thrombophilia, sepsis, acute coronary syndromes [30]. Platelet microparticles are involved in processes like homeostasis, intracellular signal transduction, inflammatory responses and angiogenesis. They have a procoagulant surface with multiple active components like TFs, many signaling receptors (P-selectin, GPIIb-IIIa and GPIb), phosphatidylserines. The phosphatidylserines on their surface promote the aggregation of prothrombin complexes, fundamental for coagulation. A damage to the vascular wall also induces PDMPs adherence, which contributes to platelet activation [31]. High PDMP concentrations in blood may lead to microthrombosis, arterioles occlusion and, ultimately, organ failure.

1.4.3. Platelet activity in COVID-19 patients

SARS-CoV-2, or Covid-19, is an acute respiratory syndrome, associated with lungs dysfunctions and lung tissue inflammation, neurological and cardiac disorders [32] and, as main complications, multiorgan failure and thromboembolic events [33] [34]. Covid-19 patients displayed increased platelet adhesion, aggregation and higher thrombin concentrations; the infection can alter platelet activity facilitating thrombus formation [35] [36]. In fact, Covid-19 infection may induce neutrophils activation, which triggers hypercoagulability and may also cause severe endothelial damage, that can lead to an exaggerated thrombus formation and subsequent thrombosis or thromboembolism, despite antiaggregant and anticoagulant administration [37].

These coagulopathies are mainly due to endothelial disfunctions that promote a procoagulant state either activating coagulation mechanisms or producing a deficit in the antithrombotic mechanisms. Furthermore, recent studies [38] associate Covid-19 with the phenomenon of microvascular thrombosis, that can lead to organ dysfunction; moreover, in many cases, thrombosis and microvascular thrombosis caused by this infection are accompanied by inflammations, therefore, these conditions can be defined as immunothrombosis.

In this chapter, the clinical background behind platelet activity and thrombosis has been presented. Considering the morbidity and mortality of disorders caused by platelet dysfunction, together with their diffusion rate, there is the urge to find new diagnostic methods to test platelet function and to better understand the mechanisms behind thrombosis to administer individualized and more adequate antiplatelet therapies.

2 State of the art

2.1. Platelet function testing

Platelet disorders or defects, if not promptly diagnosticated, may lead to severe complications. In the last few decades, PFT in the clinical setting has become essential for the assessment of platelet dysfunctions, to diagnose patients bleeding disorders, evaluate patients' response to antiplatelet therapy and to assess perioperative hemostasis in case of surgery [39]. Considering the importance of PFT in clinics to monitor platelet activity and reduce complications related to platelet dysfunctions, prospects see the use of PFT also in general laboratories.

In this context, there is the need for the development of new easy-to-use devices to evaluate platelet activity and the actual effects of antiplatelet therapies at the point-of-care (POC). Some of the most common POC devices are Platelet Function Analyzer (PFA)-100, VerifyNow System, TEG-5000 Multiplate Electrode Aggregometry, (MEA); these devices are easy-to-use and they mainly use whole blood (WB), which eliminates the necessity of processing the blood samples [40]. However, they also have some disadvantages: most of them are expensive, time consuming, they lack of clinical studies and they are poorly standardized. Some of the most common PFT methods are reported in Table 2.1, grouped by their methodological principle, but they are mainly used in specialized laboratories to monitor the effect of antiplatelet therapies [41].

Method	Sample	Method application	Method principle
Bleeding time	Native WB	Screening test (obsolete)	In vivo measurement of bleeding block
Tests based on platelet aggregation			
Light transmission platelet aggregation (LTA)	Citrated PRP	Screening test for bleeding tendency Diagnostic for platelet defects Monitoring antiplatelet treatment effect	Photo-optical measurement of light transmission increase in relation to agonist-induced platelet aggregation
Impedance platelet aggregation	Citrated WB	Screening test for bleeding tendency Diagnostic for platelet defects Monitoring antiplatelet treatment effect	Measurement of electrical impedance increase in relation to agonist-induced platelet aggregation
Lumiaggregometry	Citrated WB	Detection of storage/release disorders	LTA or WB aggregometry combined with luminescence
Plateletworks	Citrated WB	Monitoring of the platelet response to antiplatelet agents	Platelet counting pre- and postactivation in whole blood
Tests based on platelet adhesion under shear stress			
PFA-100; Innovance PFA-200	Citrated WB	Assessment of bleeding risk and drug effects Searching severe platelet dysfunctions, revealing of VWD	Time evaluation of high shear WB flow blocked by platelet plug into a hole in activated surface
Impact; Cone and Plate(let) Analyzer	Citrated WB	Screening of primary hemostasis	Shear-induced platelet adhesion–aggregation upon specific surface
Global thrombosis test (GTT)	Native WB	Evaluation of platelet function and thrombolysis	Measurement of time cessation of WB flow by high shear-dependent platelet plug formation
Platelet function methods combined with viscoelastic test			
TEG/platelet mapping system	Citrated WB	Assessment of global hemostasis plus monitoring antiplatelet treatments effect	Evaluation of rate of clot formation based on low shear-induced and agonist addition
ROTEM platelet	Citrated WB	Assessment of global hemostasis plus diagnostic of platelet defects plus monitoring antiplatelet treatments effect	Measurement of electrical impedance increase in relation to agonist-induced platelet aggregation
Platelet analysis based on flow cytometry			
Flow cytometry	Citrated WB, PRP, W-Plt	Cell counting, detection platelet activation by extent of expression of surface and/or cytoplasmic biomarkers	Engineering laser-based detection of suspending fluorescent label platelets in a flowing solution

Table 2.1: *Common Platelet Function Testing methods with brief description* [41].

There are several methods to evaluate platelet functioning; the PFT methods reported in Table 2.1, plus another method that is worth mentioning, are described in detail in the

following subsections. As they work according to different operating principles, the described methods are divided in subgroups.

2.1.1. Early methodology

Bleeding time

Bleeding time (BT) is a laboratory test that evaluates platelet function by creating an incision in the patient's arm (IVY method) or finger (Duke method) and measuring the time required for the creation of a hemostatic plug that stops the bleeding. Normal BT is less than 3 minutes for the Duke method and less than 8 minutes for the IVY method; times greater than 5 and 10 minutes, for the Duke and IVY methods, respectively, may indicate the presence of abnormalities or coagulopathies [42].
The test is quick and easy to perform and was used to diagnose congenital and acquired diseases and to monitor antiplatelet therapies; however, it carries the risk of local scarring, hematoma, excessive bleeding, infection and especially misdiagnosis. The test, in fact, has low specificity and sensitivity, and it has proven to poorly predict bleeding in clinical settings [43] [44].

2.1.2. Tests based on platelet aggregation

Light transmission platelet aggregation

Light transmission aggregometry (LTA) allows to determine several agonists ability to stimulate in vitro platelet activation and induce platelet-to-platelet aggregation [45]. The test analyses the stirred platelet-rich plasma (PRP) placed in a cuvette, at 37°C, between a photocell and a light source. Due to the high platelet content suspended in plasma, the fluid allows only little light transmission. Once the agonist is added, the solution becomes less cloudy due to platelet aggregation, and light can more easily pass through. The photocell detects the light transmission and records it as a function of time. A wide range of agonists can be used, and this allows to investigate different platelet activation pathways; the most used agonists are ADP (low and high dose), collagen, ristocetin (low and high dose), adrenaline, thrombin (low and high dose), arachidonic acid, TXA2 [46]. A typical resulting aggregation curve is shown in Figure 2.1: the percentage maximum

aggregation is evaluated dividing the distance between the baseline (which represents the PRP, so 0% aggregation) and the maximal aggregation by the 100% aggregation (platelet poor plasma (PPP)).

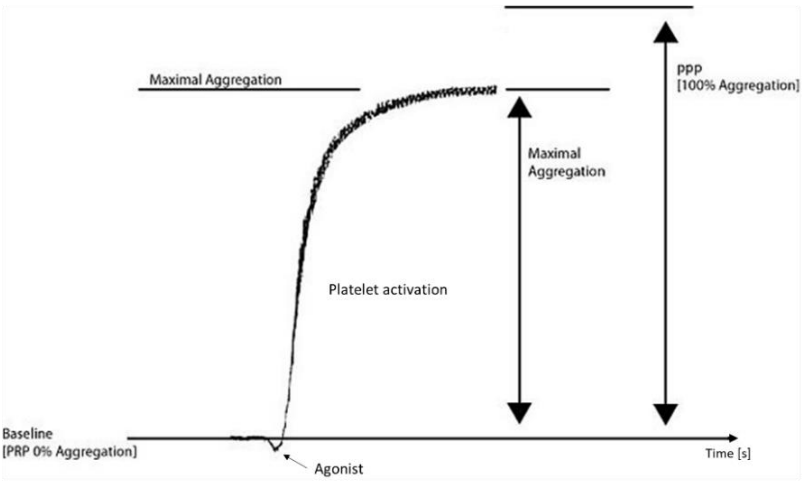

Figure 2.1: *Typical LTA aggregation curve.*

The formula for the maximum aggregation percentage is:

$$Maximum\ aggregation\ [\%] = \frac{Aggregation\ at\ start - Maximal\ aggregation}{Aggregation\ at\ start - PPP} * 100\%$$

Other measured parameters are:

- the slope of the curve;
- the area under the curve;
- the lag phase [s].

Depending on the added agonist and on the shape of the resulting aggregation curve, LTA allows to evaluate platelet disorders, discriminate between healthy subjects and pathological conditions, and evaluate major adverse cardiovascular events [47]. Originally, this device was highly operator dependent; however, recent developments have simplified and automated this method. In fact, adding a dedicated software (the Sysmex CS-2x00 series, Norderstedt, Germany) to the instrument, experiments can be run without trained operators. The software allows to select the agonist used and its concentration, then it performs the test and shows the results more readily than with the traditional LTA [48]. The automated acquisition also reduces the quantity of PRP needed

(140 µL of PRP are now required with respect to the 200-500 µL previously needed) and allows to increase the numbers of aggregation tests that can be run simultaneously, enabling to get a high-throughput method.
The disadvantages that were not eliminated by the improvements in automation are the need to process WB to produce PRP, the high cost of the reagents, and the fact that this method does not evaluate platelet aggregation in physiological conditions (i.e. under flow).

Impedance platelet aggregation

Impedance platelet aggregometry evaluates platelet response to multiple agonists by measuring platelet aggregation in WB using electrodes. Impedance platelet aggregometry with PRP can also be performed, but the use of WB avoids the need for PRP generation [49]. According to its working principle (shown in Figure 2.2), two electrodes are immersed in the blood sample, kept at 37°C; when the agonist is added, platelet aggregation begins and a change in the electrical impedance [Ohm] between the two electrodes occurs and is continuously recorded.

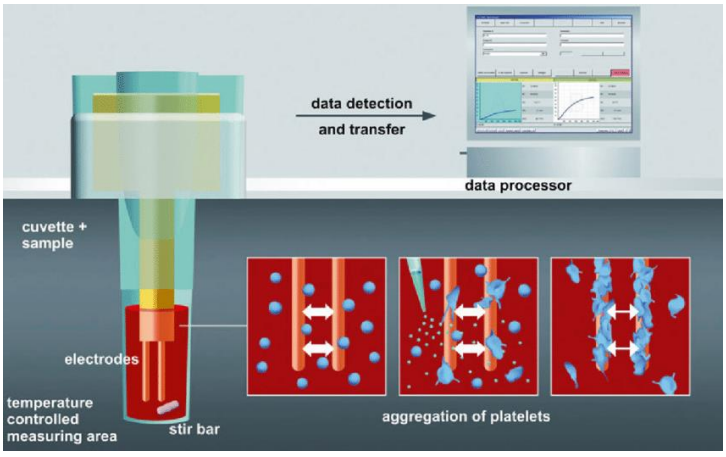

Figure 2.2: *Impedance platelet aggregometry working principle.*

The most used model of the impedance WB aggregometer is the Multiplate Analyzer (Roche diagnostic, Basel, CH): it has five independent channels that allow to simultaneously test either different blood samples or the effect of different agonists (using the same blood sample). For each analysis, the device requires 300 µL of

anticoagulated-whole blood mixed with 300 µL of saline and provides two almost overlapping aggregation curves (an example of typical curves is shown in Figure 2.3). The output parameters are:

- the aggregation unit (AU), which is the maximum height of the curve;
- the area under the curve, which is the integral of the aggregation curve starting from the agonist addition;
- velocity, defined as the maximum slope of the curve.

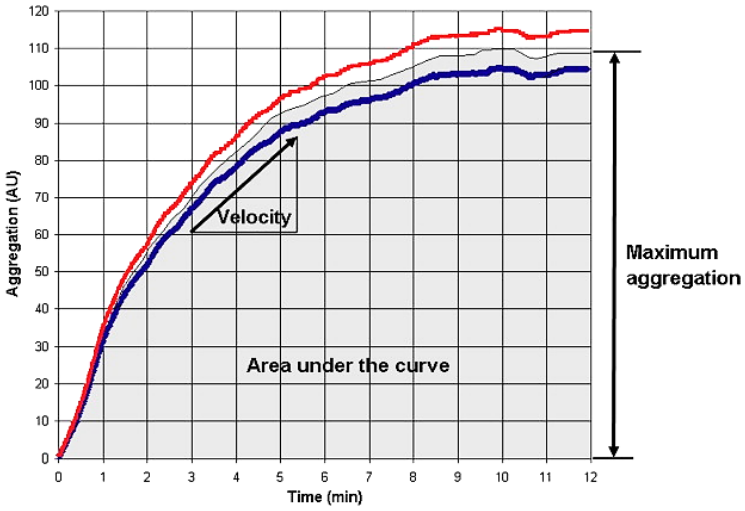

Figure 2.3: *Typical multiplate aggregation curve.*

This PFT device is rapid, semi-automated and, due to the use of WB, allows to assess platelet function in more physiological conditions. It allows to identify platelet disorders and diagnose sepsis and systemic inflammatory response syndrome [50] [51].

Lumiaggregometry

Lumiaggregometry allows to simultaneously measure platelet aggregation and ATP secretion from activated platelets (ADP released from platelet δ granules converts into ATP upon platelet activation). This test can be performed both using PRP and WB, and it is based on the detection, amplification and recording of a chemiluminescence generated by the reaction between ATP, released from activated platelets, and the added luciferin-luciferase reagent [52]. The emitted light is proportional to the ATP concentration. This

method is useful to identify defects in degranulation, that is deficiencies in δ granules number and content [53].
Due to its poor standardization, lumiaggregometry is recommended to be used as a first screening test for patients at risk of platelet dysfunctions [54].

Platelet aggregometry

The plateletworks methodology is the main example of this working principle. Plateletworks is a POC platform used to measure platelet count, diagnose platelet dysfunctions and monitor platelet response to all the common antiplatelet agents. This method uses WB (1 mL), an impedance cell counter, some EDTA baseline tubes and some reagent tubes (citrate tubes with agonists). The agonists commonly used are ADP, collagen and arachidonic acid. This system provides fast results and also allows a measurement of platelet count, platelet aggregation and inhibition activity, together with a pre-surgical and trauma screening [55]. Platelet count is measured in the control sample baseline tube, then, this result is compared with the platelet count measured in the citrated WB with the agonist after the aggregation; the fall in platelet count provides information about platelet aggregation. The use of WB avoids the need for any blood manipulation, making the assay rapid; in fact, results are provided within 10 minutes. However, the need to perform the test within few minutes from the blood withdrawal limits the use of this method in laboratories.
Despite this, it is a useful tool to monitor antiplatelet therapies effect and to avoid bleeding risk and any cardiovascular adverse event, especially for people with stent implants or that undergo surgery [56].

2.1.3. Viscoelastic based methods

Viscoelastic based methods evaluate different characteristics of the clot, such as strength (stability), elasticity and adhesive ability.

Thromboelastography (TEG) and Rotational Thromboelastometry (ROTEM)

TEG platelet mapping system (Haemonetics Corpoation, Braintree, MA, USA) and ROTEM platelet test (Instrumentational Laboratory, Bedford, MA, USA), have many similarities:

both provide quantitative information on the mechanisms of clot formation, stabilization and degradation. To perform both tests, a blood sample (340μL) is placed in a heated (37°C) cuvette. TEG involves non-anticoagulated WB, while ROTEM employs citrated WB. A pin, connected to a detector system, is introduced within the sample cup; the detector is a torsion wire for the TEG analyzer and an optical detector for the ROTEM analyzer. The two devices monitor and display the viscoelastic forces produced in the blood sample during clot formation. The force is then transmitted to an electromechanical transducer [57].

The TEG device consists of a cylindrical cup that oscillates of 4° 45′ every 5 sec, while the pin is suspended from the torsion wire in the blood sample. The amplitude of the pin motion increases with the clot viscoelastic strength; this motion is transmitted to the torsion wire and detected by the electromechanical transducer. Standard TEG devices can analyze two samples at a time.

For the ROTEM device, instead, the pin is suspended on a ball bearing mechanism and, due to the application of a constant force, it starts oscillating (initially of 4° 75′ every 6 sec) while the cup is fixed. As the clot grows, the clot viscoelastic strength increases and the pin motion is damped; during the clot lysis, instead, the pin moves more freely. The pin rotation impediment is monitored using the optical detector. This device can analyze four different samples at a time.

TEG and ROTEM working principles are shown in Figure 2.4 [58].

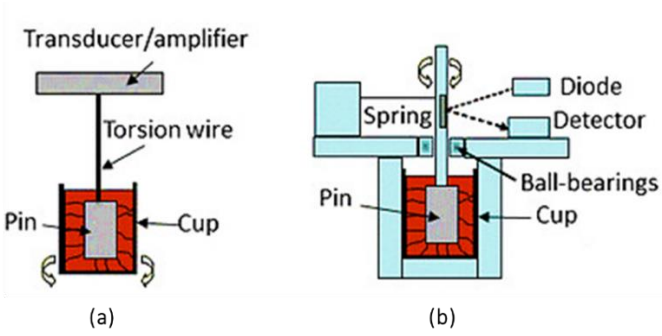

Figure 2.4: *TEG (a) and ROTEM (b) working principle.*

In both cases coagulation is the result of the imposed shear stress and the addition of an activator (agonist). Both devices provide the same information regarding the clot generation, clot strength and clot lysis but the resulting parameters are different. They

both evaluate the time needed for the clot to form and the strength of the clot. In both cases, all these information are provided by means of a graphical representation [59]. The two tests reflect the in vivo hemostatic process, including the platelet-fibrinolytic agents interaction, and are useful tools to prevent thrombotic and hemorrhagic episodes and to monitor the effect of antiplatelet agents. They are well established methods in cardiovascular surgery and TEG is a commonly used POC test in trauma settings, in major surgery and blood transfusions [60] [61] [62].

2.1.4. Shear stress-induced platelet activation

These systems stimulate platelets using shear stress and measure, in different ways, the shear-mediated platelet activation.

Platelet Function Analyzer – PFA

The PFA-100 analyzer (Dade Behring, Marburg, Germany) is a PFT device which simulates primary hemostasis through the presence, in the system, of an agonist that stimulate platelet adherence and aggregation under high shear conditions [63]. To perform this POC test, citrated WB is drawn in collagen coated cartridges through a capillary. At the end of the cartridge a collagen coated membrane with a 147 μm aperture, filled with either epinephrine (EPI) or ADP, is present (Figure 2.5). Due to both the applied shear stress and the agonist, platelets will form a plug that will eventually occlude the hole, stopping the blood flow. The time needed to create this occlusive plug is defined as closure time and is a measure of the platelet-related hemostasis. The availability of two different cartridges (ADP filled or EPI filled) allows to discriminate between intrinsic platelet defects i.e. vWF defects (using a cartridge with ADP) and defects due to antiplatelet therapy that uses acetylsalicylic acid (using a cartridge with EPI) [64] [65] [66].

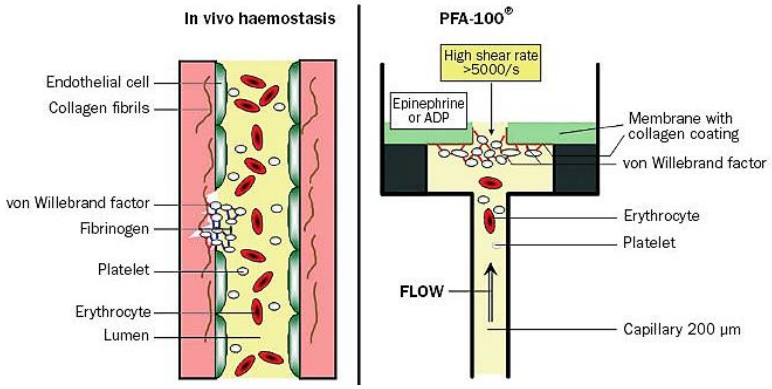

Figure 2.5: *PFA-100 analyzer functioning principle.*

Cone and plate analyzer

The IMPACT: Cone and Plate(Let) Analyzer (CPA) (Image Analysis Monitoring Platelet Adhesion Cone and Plate Technology), (DiaMed, Cressier, Switzerland), is an innovative POC device that uses a computerized automatic system to evaluate primary hemostasis [67]. It uses citrated WB in a system made of a cone and plate device, a staining device and an image analysis software: platelets on a polystyrene covered plate are activated by the spinning of a cone on the plate; they adhere on the polystyrene surface forming aggregates, and the surface covered by these aggregates and the average aggregates size are measured.

This method is useful for platelet defects diagnosis and to test the efficacy of antiplatelet therapy by adding some agonists (arachidonic acid or ADP) to the system [68] [69].

Global thrombosis test (GTT)

The global thrombosis test (GGT) (Montrose Diagnostics Ltd, London, UK) differs from the PFA and CPA methods for using non-anticoagulated WB [41]. In this test platelet activation is achieved by applying a high shear stress, similar to the one in coronary artery stenosis. In this system WB flows into a plastic tube holding a conical component where two ceramic balls are present (Figure 2.6).

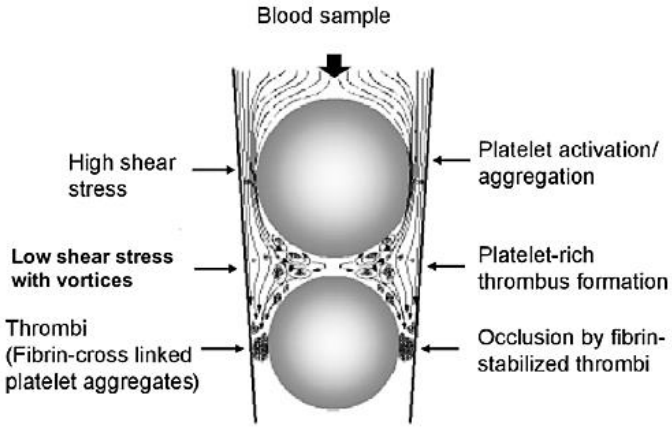

Figure 2.6: *GTT functioning principle.*

The presence of some flat segments along the inner wall of the tube avoids the complete occlusion of the tube lumen. According to the test, under the force of gravity, blood flows through the narrow gaps created by the first ball and the high shear stress activates platelets; between the first and the second ball, the turbulent flow and the low shear stress promote platelet aggregation, creating some platelet plugs that occlude the gaps created by the second ball, at the end of the tube. This occlusion causes blood to slowly come out of the tube in the form of blood drops. Some parameters are then evaluated:

- the occlusion time [s], which is the time needed to occlude the tube;
- the time interval between two consecutive blood drops (d) [s], this parameter is recorded until an arbitrary endpoint is reached (usually when d is higher than 15 s);
- the lysis time [s], which is the time needed to have again a blood flow at the end of the tube, due to spontaneous lysis of the plug.

This POC device is used both for general screening and in critical care settings, as it rapidly provides information on the patient thrombotic status [70] [71]. GTT has an important clinical value, however, evaluations of GTT results, in association with clinical outcomes, are still in progress.

Total thrombus formation analysis system

Total thrombus formation analysis system (T-TAS 01) (ZACROS, Tokyo, Japan) uses microchips with collagen and thromboplastin coated flow paths, to simulate a blood vessel damage and promote the thrombus formation process. This new and innovative

automated system, in fact, recreates inside flow chambers the entire hemostatic process, quantitatively measuring thrombus formation under physiological flow conditions [72]. Anticoagulated WB (320-480 µL) flows inside the flow chamber at a defined flow rate. A portion of the flow path is coated with either collagen or a combination of collagen and thromboplastin, depending on the assay used. The wall shear stress activates platelets, and thrombus formation on the coated portion of the capillary begins. The thrombi block the flow causing a pressure increase.

The T-TAS measures the change of flow pressure thanks to a pressure sensor located upstream in the flow chamber. The thrombus formation inside the capillary creates a partial occlusion, causing a flow resistance increase, hence a pressure increase. The pressure increase is monitored and recorded, and the pressure-time curve is reported. The evaluated parameters are:

- the occlusion start time, which represents the lag time needed for the pressure to reach 10kPa;
- the occlusion time, which is the time needed for the pressure to reach 60kPa;
- the area under the curve, which represents the overall thrombus formation.

This easy-to-use system has the main advantage of performing tests under in vivo-like flow condition. It uses WB, which avoids sample processing, and different shear rates can be tested (600, 1200 and 1500 s^{-1}).

2.1.5. Platelet Flow cytometry

Flow cytometry (FC) is a laser-based technique used to define different cell types in a heterogeneous population and to characterize and analyze cells or particles. This powerful tool has many applications: it can be used in cancer biology, virology, immunology or to detect the response to infectious diseases [73]. In studies of hemostasis, platelet FC allows to monitor the efficacy of antiplatelet agents, to diagnose both inherited and acquired platelet disorders, to provide important platelet phenotypic data and information on their physical (such as size and volume) and antigenic properties (such as platelet granules secretion and platelet conformational changes following activation) [74]. Both WB and PRP can be used, but using WB leads to many advantages: it allows performing the analysis in more physiological conditions, only a

small blood volume is required (2-10 µL), it allows simultaneous analysis of different platelet receptors, the effect of thrombin on platelet activation can be assessed and directly measured, it can be used in patients with acute thrombocytopaenia [75].

To be characterized, cells in suspension need to be labeled, usually with a fluorescently conjugated monoclonal antibody. In the flow cytometer, cells pass through a flow chamber first, and then through a laser focused beam, at a varying shear rate of 1000-10000 cells per minute. When a labeled cell is crossed by the light, the dye fluorochrome activates and emits a light energy at a specific wavelength. Then, the fluorescent dye-conjugated antibodies in the cell, emit an energy at a specific emission wavelength, which is measured by a detector.

This allows to obtain several information about the sample and the cells in suspension and to perform cell counting and cell sorting processes. A schematic diagram of the FC working principle is shown in Figure 2.7.

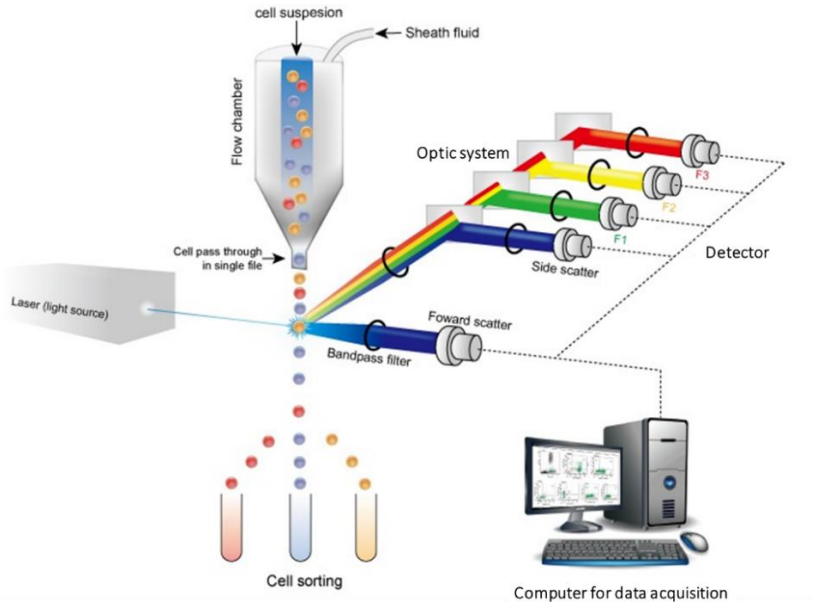

Figure 2.7: *Flow Cytometry working principle.*

In whole blood, by performing a double labeling, distinction between platelets, platelet-derived microparticles or cell aggregates can be performed [76]. FC is also a useful tool to determine if any platelet pathological activation occurs and to recognize the efficacy of antiplatelet therapies [77]. Despite these advantages, FC presents some issues: the preparation of the sample is complicated, requires time and a trained operator is needed;

flow cytometers are expensive and the tests need to be run within 45 minutes from the sample collection to avoid platelet activation ex vivo.

All the above-mentioned methods are clinically accepted, however, only the T-TAS evaluates thrombus formation under physiological flow conditions. Flow assays are indispensable research tools that allow to replicate the vasculature hemodynamic conditions.

2.1.6. Microfluidic devices and microfluidic flow assays

Over the last decade, microfluidic systems extensively developed, growing from specialized research areas to numerous fields that include many research groups and companies. Microscale systems allow a precise control of the confined fluid behavior, avoid wasting huge amounts of reagents or solvents and enable the investigation of phenomena non-visible at the macroscopic level. Microfluidic flow assays (MFA) are able to evaluate and measure shear-dependent platelet activity, allow a good control of the flow inside the microchannels and, for these reasons, they have the potential to substitute in vivo mouse models of thrombosis. The use of microfluidic channels with protein micropatterning to assess platelet adhesion has become, in the last few years, a useful tool to overcome the high volume requirements of the early flow devices and to obtain controlled cell adhesion [78] [79]. MFA could, potentially, be used in clinical applications to diagnose and treat platelet disorders (like thrombosis or excessive bleeding).

The first studies on blood cells-vessel wall interaction date back to the ‘60s, when an annular perfusion chamber was developed. Based on this device, combined efforts of many researchers allowed the design of parallel plate and annular assays. The first flow devices that actually assess hemostasis and platelet function under physiological flow conditions go back to the 1970s, when platelet adhesion to ECM components, in particular vWF, was investigated [80]. These studies allowed basic knowledge of hemostasis [81]; however, these early devices never became common practice in clinical settings or were translated into clinical assays, mostly due to the large amount of blood needed and to the low throughput.

Early studies investigate thrombotic events on glass or polyurethane surfaces coated with collagen, and on polycarbonate membranes with collagen fibers [82]. Initial research highlights the importance of a controlled flow rate environment to evaluate thrombotic events, and shows how the shear rate may modify platelets, their activity and their response to several stimuli; moreover, increasing shear rate causes increasing platelet adhesion [83].

Nowadays, the use of fibrillar collagen type I immobilized on a surface has become a standard for the assessment of platelet adhesion under flow conditions. Commercial systems for in vitro studies are available, but many laboratories design their own customized perfusion chambers. Shear-mediated platelet activity is largely investigated using microfluidic devices: the use of polydimethylsiloxane (PDMS) microchannels coated with a micropatterned protein surface (especially collagen, fibrinogen and vWF) has become very popular to produce local platelet adhesion and simulate the presence of a vessel wall injury. The photo lithography technique is used to fabricate some micropatterned templates on a silicon wafer; the desired features are then transferred on PDMS via soft lithography, which is used to stamp the ECM protein pattern on a flat surface, usually a glass slide [84] [85].

Using this technique, Hansen *et al.* proposed a method to identify platelet function defects and monitor and dose antiplatelet drugs [86]. The study addresses the effect of the size of the collagen nanofiber spot on platelet adhesion capability by perfusing WB in multi-shear microfluidic devices. Recent studies propose the use of stenosis models within the microchannels to assess both the effect of the vessel partial occlusion on thrombosis [87], and the efficacy of antiplatelet therapy [88].

Akther *et al.* investigated the effect of atherosclerotic plaque components on platelet aggregation, at multiple shear rates, through the site-specific introduction of some atherosclerotic plaque components into stenosed channels. The authors also tested the antiplatelet efficacy of aspirin at two different concentrations (50 and 100 μM), reporting the two dose response curves [89].

To study shear-dependent platelet adhesion, Gutierrez *et al.* proposed a microfluidic device consisting of parallel microchannels with either one or multiple inlets and outlets [90]. By changing the height of the channels, different flow rates are achieved; moreover, within the same device, in each channel a different flow rate can be also obtained by

introducing resistance channels in series with the test channels, allowing to simultaneously test different flow rates in a single experiment. They used anticoagulated WB to investigate the mechanisms of platelet adherence to the vessel wall by evaluating platelet adhesion on three ECM proteins: vWF, fibrinogen and collagen. Neeves *et al.* used MFA to assess shear-dependent platelet activity, using WB perfused through four channels coated with fibrillar collagen type I, at four shear rates [91]. The study aims to determine how genetic factors, phenotypic factors and experimental conditions affect platelet accumulation on the collagen substrate.

Fluorescence microscopy is a largely used tool to visualize thrombus formation, obtain images and analyze the number of thrombi and their morphological features to evaluate platelet adhesion ad aggregation capability [92] [93] [94]. However, microscopy presents some disadvantages: first of all, fluorescence microscopes are expensive and they are found only in specialized laboratories; second of all, the method is not easy-to-use, requires trained operators and is operator dependent.

For this reason, another method, proposed by Hosokawa *et al.* to assess white thrombi formation, without the use of microscopy, is worth mentioning. It uses a microfluidic device coupled with a flow pressure sensor: thrombus formation is evaluated by monitoring the pressure drop in the channel [95].

Despite their usefulness in the platelet activity and thrombus formation assessment, the main issue of MFA and microfluidic devices consist in the lack of standardization. Numerous laboratories measure platelet activation, adhesion and thrombus formation by performing blood perfusion assays but, despite several attempts, no standardized protocol is yet available [96].

2.1.7. Point-of-care devices

Nowadays, POC devices are emerging in the healthcare industry. They are bedside diagnostic instruments which rapidly provide diagnostic results. They have the potential to revolutionize healthcare as they can replace expensive and time-consuming laboratory tests. They are mostly handheld devices, and they are usually based on immunosensors, such as electrochemical, optical, piezoelectric, electromechanical or thermoelectric transducers [97].

They can be used in many research fields including hematology: POC devices are more and more advanced, as a result of the continuous progress made in biomedical devices development.

Useful hematology POC devices were developed over the past decades, including devices that evaluate blood clots. Unlike laboratory PFT, POC devices are smaller, faster, cheaper and user-friendly.

In the hemostatic field, nowadays, one of the most common POC device is the CoaguCheck Xs (Roche Laboratory, Meylan, France). It is a coagulometer and it works by measuring the prothrombin time (PT). A small amount of WB is collected using some test strips with a peptide substrate containing activators. When WB is in contact with the strip, thromboplastin (used as the reagent) dissolve and thrombin generation begins. The device performs an amperometric determination of the PT, by using electromagnetic sensors; it also allows to monitor anticoagulation therapies [98]. Another POC device is the Protime Microcoagulation System (International Technidyne Corporation, NJ, USA): a sample of WB is pumped through a capillary tube when a coagulation reagent is added; the PT is obtained through an optical detection of the amount of time needed to generate a clot that stops the blood flow. The PT can also be measured as the time after which the blood sample, placed in a cuvette, creates a coagulum that allows the immobilization of a rotating ball, moved by a rotating magnetic field. The ball movements are detected by a sensor [99]. Another anticoagulation monitoring system is CoaguSense (CoaguSense, Inc., Fremont, CA, USA). This method only requires a small blood sample which must be placed on a heated test strip, containing a spoked wheel. By rotating, the wheel pulls the sample in the reaction well, where the blood is activated due to the presence, in the test strip, of recombinant rabbit thromboplastin. The device evaluates the PT by using an optical detector: a light beam detects the blood moving in the reaction well and when a clot forms the light beam is interrupted; this interruption is identified by the optical detector. The PT goes from when the blood is pulled in the reaction well, until the light beam is blocked [100] [101].

An innovative device that provides rapid and accurate information about the coagulation process is ClotChip (CWRU, Cleveland, OH, USA). This POC device, proposed by a research group from Case Western Reserve University, uses miniaturized dielectric spectroscopy to monitor clotting by applying an external electric field to a blood drop. It

evaluates blood clotting capability by quantitatively measuring how much the field is affected by the blood [102].

2.2. Effect of platelet-derived microparticles in blood

The interest in PDMP studies has increased in the last decades. They are the most abundant microparticles type present in the human body and their role in diseases is still being investigated. PDMPs play a big role in the transport and delivery of active molecules and promote and participate in several processes such as hemostasis, angiogenesis and immunomodulation but also thrombosis, infection transfer, inflammation, tumorigenesis and metastasis [103]. Many disease states are characterized by a high concentration of PDMPs in blood and they may affect many disease processes such as cardiovascular diseases, tumor formation, rheumatoid arthritis, hepatitis [104]. Several methods can be used to detect and analyze PDMPs, such as immunofluorometric assays, microscopy, flow cytometry, spectroscopy, dynamic light scattering [105] [106]; however, a standardization is still required. Many studies have reported that platelets were highly altered in cancer patients, hence also PDMPs. A research study conducted by Sabrkhany *et al.* [107] reports that, in patients with early-stage lung and pancreatic cancers, 85 platelet proteins were notably changed, and VEGF and PDGF significantly increased. Therefore, both platelets and PDMPs may have, on their surface, protein biomarkers that discriminate, with high specificity, patients with cancer from healthy controls. It's still uncertain how platelets are modified by tumor cells.

PDMPs are procoagulants, therefore are likely involved in cardiovascular diseases such as arterial thrombosis. Michelsen *et al.* reported an increased levels of PDMPs in both patients with coronary diseases and myocardial infraction survivors [108]. Increased levels of PDMPs also indicate endothelial injuries [109], that can be extremely dangerous during myocardial ischemia as may enhance platelet adhesion and thrombus formation [110]. As PDMP levels largely increase in diseases with an inflammatory component, monitoring the PDMP concentration in blood represents an important diagnostic tool [111].

Despite their pathogenic potential, the bioactive substances contained in platelet granules or in the cytoplasm allows PDMPs to play a key role in vascular remodeling and tissue repair; α granules, in fact, contain several growth factors that promote tissue regeneration [112]. In vitro studies show that the addition of PDMPs to endothelial outgrowth cells (EOCs) enhance proangiogenic factor release and EOCs recruitment, migration and differentiation [113].

2.3. COVID-19 and platelet activity

Together with severe respiratory syndromes, another main complication of Covid-19 infection is arterial thrombosis. This infectious disease, in fact, causes an increase of some biomarkers such as vWF and P-selectin while keeping a normal platelet count. Platelet activation can follow either an inflammation-mediated pathway or a SARS-CoV-2 specific pathway. The latter is characterized by the virus spike protein binding to its receptor present also on platelet surface, leukocytes and vascular endothelial cells. Therefore, these proteins exert a procoagulant and thrombogenic function [114]. Ercan *et al.* and Schrottmaier *et al.* [115] [116] investigated changes in platelet reactivity in Covid-19 patients, together with other different aspects of platelet functioning, and the outcomes reveal that, in Covid-19 patients, platelet activation mechanisms change, that the virus spike proteins induce platelet activation causing prothrombotic states and that the virus can replicate inside platelets. Moreover, Schrottmaier *et al.* assessed platelet activity throughout the course of the disease, monitoring platelet activation in both patients with fatal outcome and survivors [117]: the former presented significantly higher P-selectin expression and GPIIb-IIIa activation, suggesting an increased platelet degranulation. Platelet responsiveness was also assessed and, despite the higher activation, in fatal disease cases platelets were less responsive to agonist stimulation suggesting an association between fatal outcome and platelet hyper activation and hypo reaction. Therefore, coagulation tests may be a useful tool to identify severe Covid-19 cases.

2.4. Motivation and aim of the work

In this chapter, a description of the most common PFT devices and respective advantages and disadvantages have been reported.

The numerous complications following platelet dysfunction contribute to morbidity and mortality especially in patients with cardiovascular diseases. Often, platelet disorders are not properly treated, and antiplatelet drugs, if wrongly administered, may lead to further complications like excessive bleeding or thrombosis. These issues have led to the urgent need of developing new PFT devices that can evaluate platelet activity and monitor platelet adhesion to determine suitable and personalized antiplatelet treatments.

In the framework of an ongoing collaboration between Politecnico di Milano and Università degli studi di Milano (San Paolo Hospital campus), a microfluidic platform for the study of platelet activity and thrombus formation under flow was designed. By a joint collaboration between Politecnico di Milano and the University of Arizona, this platform was then refined. This benchtop instrument is highly customizable and allows to reproduce in vivo-like conditions to assess platelet functionality.

This work has two main purposes: the characterization of the platform to assess platelet activation as a function of shear stress and protein substrates; start developing a label-free system, with a smaller footprint and less operator dependence, that uses a pressure transducer to evaluate platelet activity, providing automated and repeatable measurements.

The platform was used to assess the effect of platelet-derived microparticles on platelet adhesion and aggregation. High PDMP concentrations represent a risk factor for cardiovascular diseases and may lead to severe consequences; monitoring their effect on platelet activity, at different shear stress levels, represents a tool to properly assess this disorder. Altered platelet function is also associated with covid-19 infection, therefore its effect on platelet activity was investigated.

The addition of a pressure sensor allows a refinement of the microfluidic platform, to start developing a POC device. The system now comprises only a pressure transducer,

placed at the outlet of a microfluidic device, but future developments may include small changes in the design of the device.

The study and refinement of the platform aim to provide a suitable tool to assess the effects of several phenomena on platelet activity and reduce the associated risks of complications.

3 Materials and methods

3.1. Blood samples and generation of microparticles

On each trial day, blood from healthy volunteers was collected. Only donors who abstained from any medication affecting platelet activity for the two weeks prior to the blood withdraw were included in the study. All tests under flow were performed using hirudin-anticoagulated WB. To be able to observe platelet aggregation under the fluorescence microscope, blood was tagged with fluorescent lipophilic platelet dye DiOC6 (1 μM, Sigma Aldrich) and incubated at room temperature for 15 minutes (protocol in appendix B).

Platelet-derived microparticles are obtained adding calcium chloride (2.5 mM CaCl2) to 350 μL of gel-filtrated platelets (GFP) (100000 platelets/μL), sonicating the solution (50% of power, 10 s, Branson Ultrasonics™ SLPt Sonifier) and centrifuging it twice at 2000rpm for 15 minutes to sediment platelets and obtain PDMP fraction. Then the supernatant containing PDMPs is collected, aliquoted and frozen at -80°C.
When needed, microparticles were thawed and added to whole blood, 10 minutes before each test, at a ratio blood:PDMPs of 10:1. The effect of microparticles was only tested on the collagen substrate.

3.1.1. Microparticles activity validation

To validate platelet derived microparticles activity and their ability to adhere to the collagen substrate some preliminary tests were run. Tests under flow using PDMPs only were performed: PDMPs were stained with wheat germ agglutinin (membrane dye, FITC conjugated) and they were perfused alone in the channel, without blood, for 4 minutes. These trial experiments were carried out for all shear stress levels (13.5, 49.5 and 72 dyne/cm^2).

3.2. Microfluidic platform for thrombi formation studies under flow

The effects of flow on blood cell adhesion, coagulation and thrombus formation are studied, ex vivo, using flow chambers and microfluidics [118]. Flow chambers mimic a physiological scenario that, together with flow assays, allow to recreate the hemodynamic conditions of the vasculature to investigate platelet activity under flow conditions. Flow assays usually see the use of a syringe pump to perfuse blood through a channel, allowing the perfusion of small blood volumes. Therefore, to study platelet adhesion, aggregation and thrombus formation under flow, a microfluidic platform was designed to control the flow rate and the channel geometry, hence the shear stress at the channel wall. The platform used in the present work (Figure 3.1) consists of a syringe pump, a fluorescence microscope and a PDMS chip containing 6 parallel channels coated with different ECM proteins. Platelet activity was investigated at venous, arterial and pathological shear stresses [119]. Furthermore, the impact of a high concentration of circulating platelet-derived microparticles in blood was evaluated.
In addition, further studies on collagen substrates ([120] [91], [121]) were performed: the microfluidic platform was modified, introducing a pressure sensor, to search for a correlation between thrombus formation and pressure increase inside the microfluidic channel.

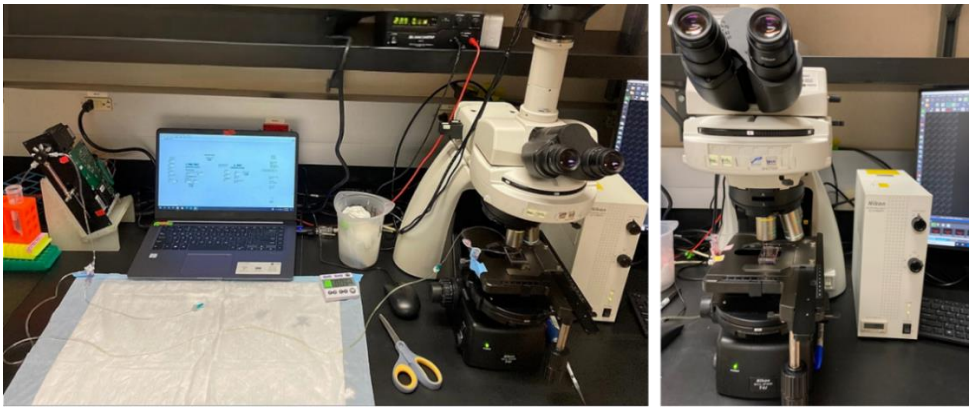

Figure 3.1: *Microfluidic platform set-up. (a) One tube of the pump is placed inside the PBS reservoir, whereas the other one (which presents a fork) is alternatively connected to the inlet and the outlet of the chip, respectively. (b) The chip is placed on the microscope stage.*

3.2.1. Chip production

The microfluidic chip (Figure 3.2) is made of a rectangular PDMS layer with 6 parallel microchannels with rectangular cross section (width = 1 mm, height = 100 μm, length = 3 cm) and a microscope slide.

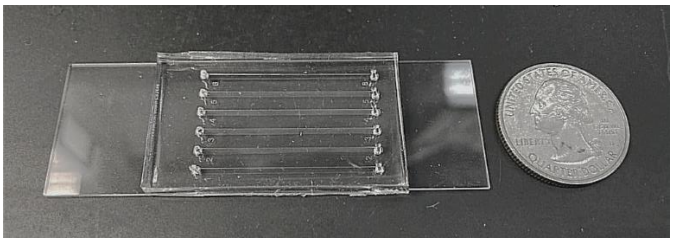

Figure 3.2: *Microfluidic PDMS chip*

The capillaries do not replicate the real geometry of the blood vessels, but their high aspect ratio is ideal both to work with small volumes and to create a quasi-2D flow in the central region, away from the side walls ([122]), this avoid turbulences in the channel and allow a more simple evaluation of parameters such as the shear stress.

The PDMS layer is produced using the soft lithography technique, that allows the replica of the designed features on a PDMS layer, starting from a silicon wafer master mold. The silicon wafer is produced using a common patterning process called photolithography: a light sensitive polymer, placed on top of a silicon substrate, is selectively exposed to ultraviolet light allowing the creation of a pattern. The whole fabrication process is shown in Figure 3.3. Prior to the PDMS chip manufacture, the molds need to be treated with chlorotrimethylsilane (Sigma Aldrich, Saint Louis, MO, USA) to avoid the adhesion of PDMS to silicon wafer.

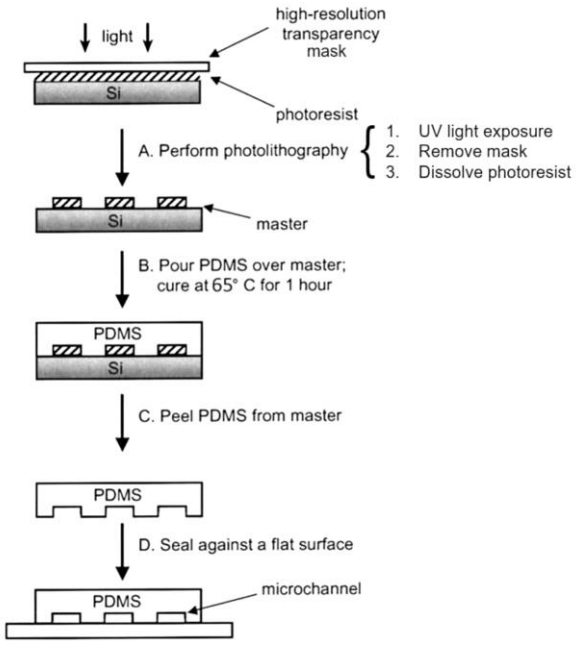

Figure 3.3: *Photo and soft lithography technique*

The PDMS chips can finally be produced using the SYLGARD™ 184 Silicone Elastomer KIT: Base and Curing at a mixing ratio of 10:1. The liquid PDMS is poured into the molds, put in the vacuum bell to remove air bubbles and let set on a horizontal surface at 65 °C for two hours or at room temperature overnight. After the PDMS is crosslinked, the chips can be peeled off the molds and cut to remove the jagged edges. Then, the inlets and outlets of each channel are pierced with a 1.5 mm biopsy punch. As a final step, the PDMS layer is bonded on a glass slide using the Plasma Cleaner machine (Harrick Plasma, Ithaca,NY, USA).

Plasma cleaning is a process that uses an ionized gas, plasma, to both remove organic contaminants and activate the PDMS surface to allow the bonding of the chip with the glass slide. The process takes place in a vacuum chamber and when a gas is under a sufficiently low pressure (200-600 mTorr) and is subjected to a high frequency oscillating electromagnetic field the accelerated ions in the gas and the gas molecules collide creating ionized molecules, which is the plasma. This allows all surfaces exposed to plasma being cleaned; the process further enhance the physical and chemical characteristics of the exposed surfaces. Therefore, the plasma cleaning technique is used to promote the adhesion between the glass slide and the PDMS layer, placed in the plasma cleaner machine with the features facing upwards. After the two elements are

bonded together, the chips are placed in the oven at 65°C for 15 minutes to make the bonding permanent.

3.2.2. Channel coating

The day before each test the channels of the microfluidic chip are coated, for 1/3 of their length starting from the end, with one of the following ECM protein: fibrillar collagen type I (CHRONO-PAR® P/N 385), recombinant vitronectin (MilliporeSigma™ CC130), mouse laminin purified protein (MilliporeSigma™ CC095), fibrinogen from human plasma (MilliporeSigma™ F3879), pure fibronectin (MilliporeSigma™ FIBRP-RO). The chips are left at 4°C overnight, then the channels are rinsed with phosphate buffered saline (PBS) and treated with bovine serum albumin (BSA), a native blood protein used to passivate all the uncoated surfaces to avoid factor XII activation, which could initiate the intrinsic pathway of blood coagulation. The chips are left at room temperature for 30 minutes, before starting the experiment under flow, to saturate uncoated parts of the channel. All proteins were used, after proper diluting, at a concentration of 100 µg/mL (protocols in Appendix B). Only for the experiments involving the use of the pressure sensor, two collagen concentrations were used: 10 and 100 µg/mL.

3.2.3. Syringe pump

The device used to perfuse blood inside the microchannels is the Hamilton PSD/8 Precision Syringe Pump. (Figure 3.4). It is a high precision pump that allows to dispense and aspirate small sample volumes with a constant flow rate.

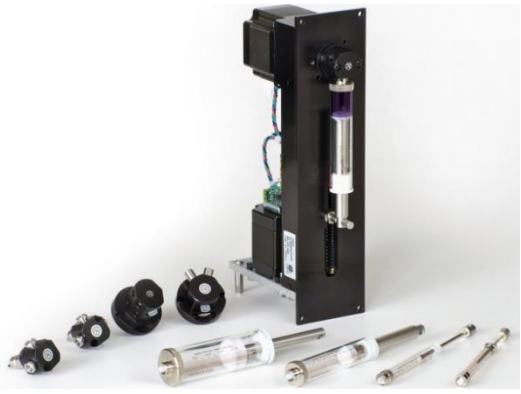

Figure 3.4: *Hamilton PSD/8 Precision Syringe Pump*

According to the syringe volume, different flow/shear rates can be achieved. Compatible syringes go from a volume of 50 μL to 25mL. To achieve the required shear stresses, in this work, two different syringes were used: a syringe with 0.5mL volume to get a shear rate of 300 s^{-1}, so a shear stress of 13.5 dyne/cm^2; a syringe with 1mL volume to get 900 s^{-1} and 1600 $^{s-1}$ shear rates, so, respectively, 49.5 and 72 dyne/cm^2 shear stresses. Main technical specifications of the pump are reported in Table 3.1.

General specifications	
Accuracy	±1%
Precision	≤ 0.05%
Weight	5.4 lbs (2.4 kg)
Dimensions	Height: 10.00 inches (254.0 mm) Width: 2.56 inches (65.0 mm) Depth: 4.51 inches (114.6 mm) Edge connector: 0.25 inches (6.35 mm)
Power Requirements	
Supply voltage	24 VDC
Power rating	850 mA max
Syringe volume	50μL to 25mL
Resolution	3000 steps (standard), 24000 steps (high)
Syringe drive mechanism	DC stepper motor
Stroke length	60mm
Syringe speed	1.2 seconds to 20 minutes stroke

Table 3.1: *Hamilton PSD/8 Precision Syringe Pump technical specifications.*

The PSD/8 is easily controllable using simple command programming; the pump, in fact, is controlled through the software Laboratory Virtual Instrument Engineering (LabVIEW, National Instruments, USA). LabVIEW is a graphically-based software development environment. It can be used to perform several mathematical and logic functions; the graphical language is called “G”. The software allows the user to define different parameters of interest, including the wall shear stress and the channel geometry. In this work, tests were performed at constant shear stress, i.e., at constant flow rate.

The front panel of the virtual instrument is shown in Figure 3.5. The code performs the following operations:

- initialization: initializes the pump and empty the syringe bringing it to the starting position, the initialization button must be clicked before each operation;
- pre-wash phase: used to fill the tubing and the channels with PBS, user can set the number of loops;
- stimulation: allows to aspirate the blood at specific flow rates according to the imposed shear stress value.

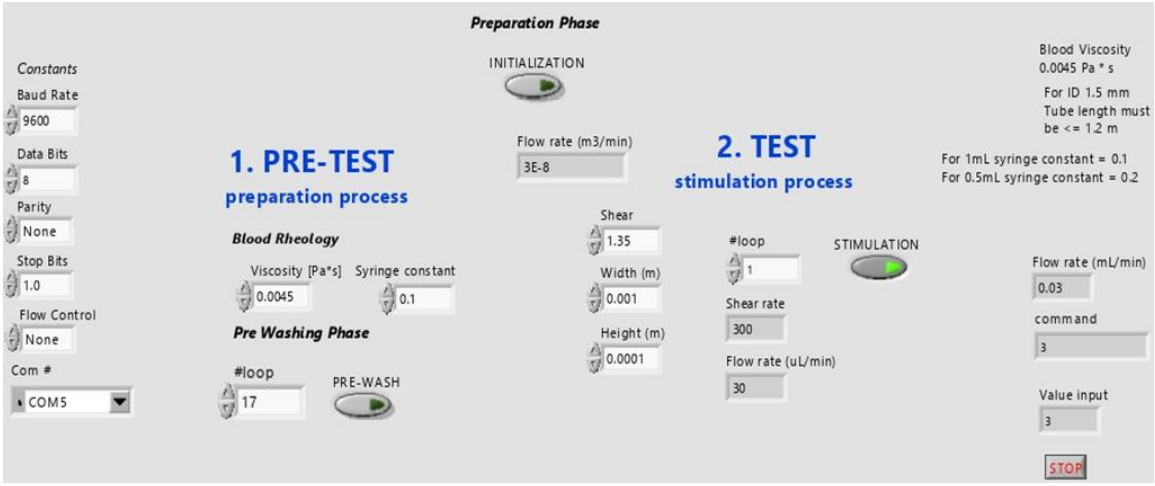

Figure 3.5: *Front panel window of the LabVIEW code.*

Assuming a parabolic pattern, the wall shear rate computed by the pump comes as:

$$\gamma = \frac{6Q}{wh^2}$$

where w [m] is the channel width, h[m] the channel height and Q [m^3/s] is the flow rate. The blood viscosity for the use of this pump is μ=0.0045 Pa*s = 0.045 dyne/cm^2s. Therefore, the shear stress is:

$$\tau = \gamma\mu$$

where μ [dyne/cm^2s] is the fluid dynamic viscosity, γ [s^{-1}] is the shear rate and τ [dyne/cm^2] is the wall shear stress. The following table (Table 3.2) shows the shear rate values and the respective shear stresses and flow rates used in this work. The tested shear stress levels are, respectively, representative of a venous flow, a flow typical of

large arteries and a flow in arterioles or a slightly pathological flow condition (stenotic vessels).

Shear rate [s^{-1}]	Shear stress [dyne/cm^2]	Flow rate [µL/min]
300	13.5	30
1100	49.5	110
1600	72	160

Table 3.2: *Tested experimental conditions*.

The Reynolds number for the three shear stress values is evaluated as follows:

$$Re = \frac{\rho v D}{\mu}$$

where ρ [kg/m^3] is the fluid density, v [m/s] is the average fluid velocity, D [m] is the hydraulic diameter and µ [Pa*s] the fluid dynamic viscosity. The Reynolds numbers corresponding to the above-mentioned shear stresses are equal to 0.214, 0.792 and 1.152, respectively. The found values indicate that the flow inside the microfluidic channels is laminar.

3.2.4. Image acquisition and analysis

During tests under flow conditions, platelet aggregation was monitored in the coated portion of the channel. After four minutes, a picture of the beginning of the coated part of the channel was captured using a fluorescence microscope (Nikon ECLIPSE Ni) with 10X objective, connected to a 14-bit CCD camera (Nikon DS-Qi2), with an exposure time of 200ms and 57.7x analog gain. Images were exported as greyscale TIFF for analysis. Then, they were postprocessed using a MATLAB script, described hereafter (full text is reported in Appendix C).

The user selects a first folder containing the original grayscale image and then a second one containing the same image manually thresholded using the software imageJ (National Institutes of Health, Bethesda, Maryland, USA). The code crops both images to remove the borders, removes any isolated cluster of pixels smaller than a single platelet

area (considering a platelet diameter of 2 μm), then overlaps the 2 images and, using the modified image as a mask, it removes the background from the original image and gives the value of the thrombi mean fluorescence intensity (FI). Afterwards, the code also evaluates:

- surface coverage (SC) [%], defined as the percentage of the area covered by platelets;
- number of thrombi (Nth) [-];
- mean thrombus area (Ath) [μm^2], defined as the SC divided by the number of thrombi.

SC and Nth parameters are useful tools to evaluate platelet adhesion to the substrate; FI and Ath, instead, are parameters mainly related to platelet aggregation. *Figure 3.6* shows an example of image conversion from the original greyscale image to the modified binary one.

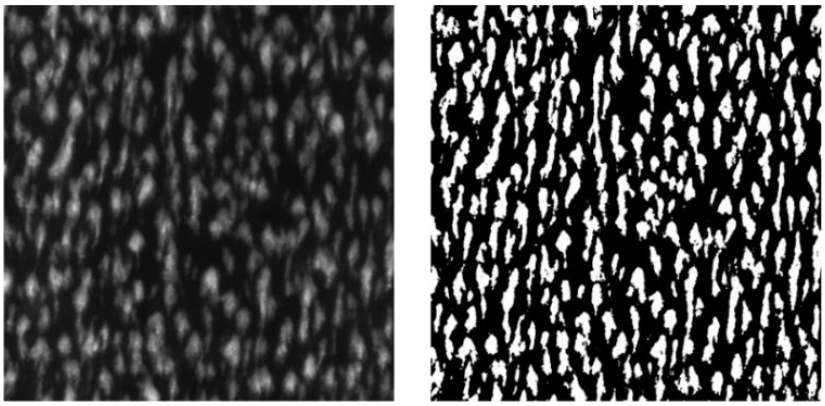

Figure 3.6: Example of image conversion. (a) Grayscale image. (b) Binary image.

3.3. Pressure measurements

Another way to evaluate platelet aggregation was tested by using a micro pressure sensor, with the aim to develop an easy-to-use platform, disengaged from the use of the microscope that can be usually found only in specialized laboratories. A pressure sensor was introduced in the set-up, at the outlet of the microfluidic channel, with the purpose of measuring pressure increase inside the collagen coated channel due to head losses caused by platelet aggregation.

The pressure drop, due to distributed head losses in the tubes and in the microfluidic channels (Δp_d [Pa]), can be evaluated as:

$$\Delta p_d = \sum \xi \frac{l}{D_{eq}} \frac{\rho v^2}{2}$$

where v [m/s] is the fluid velocity, ρ [kg/m^3] is the fluid density, l [m] is either the tubes length or the channel length, D_{eq} is the equivalent diameter [m] and ξ is the friction coefficient (equal to $64/Re$ in case of laminar flow).

The pressure drop due to minor head losses (Δp_m) comes as:

$$\Delta p_m = \sum K \frac{\rho v^2}{2}$$

where K is the minor loss coefficient. The set-up, with the pressure sensor, is reported in Figure 3.7.

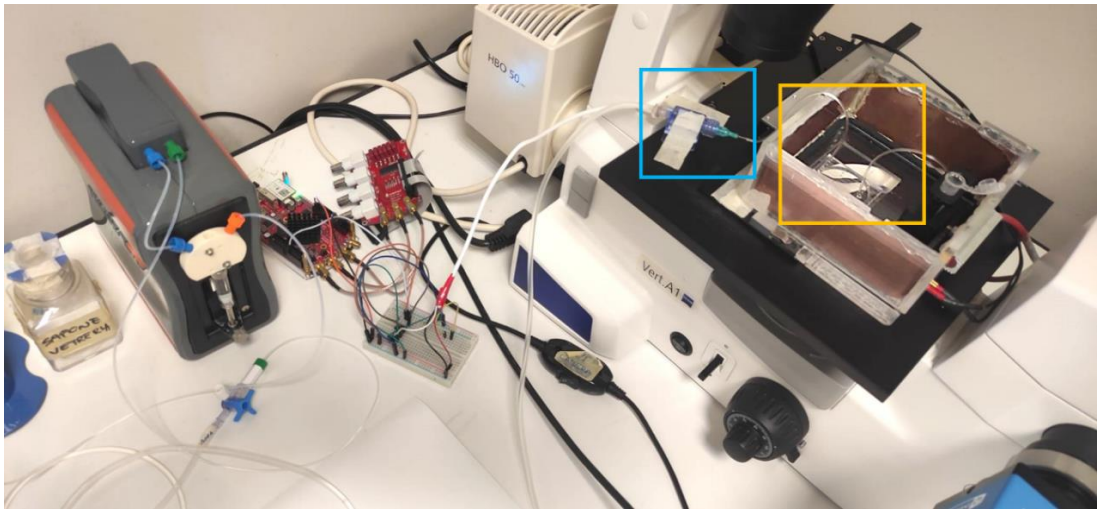

Figure 3.7: *Experimental set-up with the pressure sensor (blue box), connected to the outlet of the microfluidic channel (yellow box).*

The pressure sensor used is the PendoTECH™ PRESS-S-000 [123]. It's a differential pressure sensor and it measures (as output) a voltage drop, that represents the channel pressure drop (Figure 3.8).

Figure 3.8: *PendoTECH™ pressure sensor (PRESS-S-000).*

Main technical specifications are reported in Table 3.3.

Accuracy	Suction (0 to -362 mmHg) ±3% Discharge (0 to 1551 mmHg) ±2%
Pressure range	-594 to 3878 mmHg (-0.79 to 5.2 bar)
Biocompatibility	All materials in contact with product fluid path meet UPS Class VI requirements
Operating temperature	-25°C to 65°C
Input/Output impedence	270 Ohms to 400 Ohms
Excitation voltage	2.5 to 10 Volts
Sensor Output	0.2584 mV/psi/Volt
Connector	Custom molded 4 pin connector; signal +/- and excitation +/-
Shelf life	5 years
Syringe speed	1.2 seconds to 20 minutes stroke

Table 3.3: *PendoTECH™ pressure sensor technical specifications.*

For these experiments the tested shear stress values are reported in Table 3.4. The lowest shear stress value (13.5 dyne/cm^2) was not tested because preliminary experiments showed that the pressure increase caused by this shear stress is not high enough to be appreciated by the pressure sensor.

Shear rate [s^{-1}]	**Shear stress [dyne/cm^2]**	**Flow rate [µL/min]**
950	42.75	95
1600	72	160

Table 3.4: *Experimental conditions for pressure evaluations.*

3.3.1. Pressure data acquisition

The output signal is amplified through an electronic circuitry containing an instrumentation amplifier (INA) (AD627NZ Amplifier). Data are acquired by the STEMlab 125-10 (Figure 3.9), a single board computer by Red Pitaya Company (Solkan, Slovenia) [124]. The STEMlab is flexible and user friendly: by simply connecting it to the computer, this device can perform many electronic tasks in a reproducible and reliable way (signal generator, oscilloscope, spectrum analyzer, bode analyzer, logic analyzer, impedance analyzer, vector network analyzer). All the tasks can be performed through different web-based applications, preinstalled on the board. The software is open source, hence, the board can be controlled through MATLAB, Labview, Scilab or Pyton™. RedPitaya acquires the data and sends them to a calculator that process them through one of the above-mentioned software.

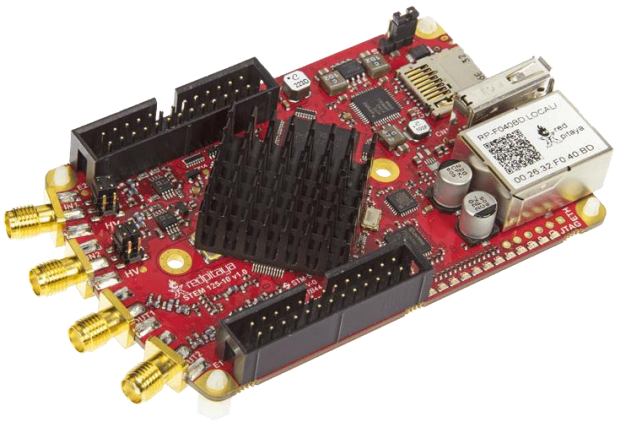

Figure 3.9: *RedPitaya STEMlab 125-10.*

To obtain pressure measurements, a specific circuitry is needed. The INA has height connection pins (power supply pins, reference pin, pins connected to a resistance and input and output pins) that represent the interface between the amplifier and the rest of the circuit. The circuit diagram is shown in Figure 3.10: pin 7 and pin 4 are power supply pins (pin 7 is connected to +3.3V power provided by RedPitaya, pin 4 is grounded); pin 5 is referenced to ground; pin 1 and pin 8 are connected to the resistance (Rg) ends to set the gain of the amplifier; pin 2 and 3 are the input pins for the signal coming from the

pressure sensor; pin 6 is connected to the analog pin 2 of RedPitaya and, from here, the amplified output signal is then processed through MATLAB.

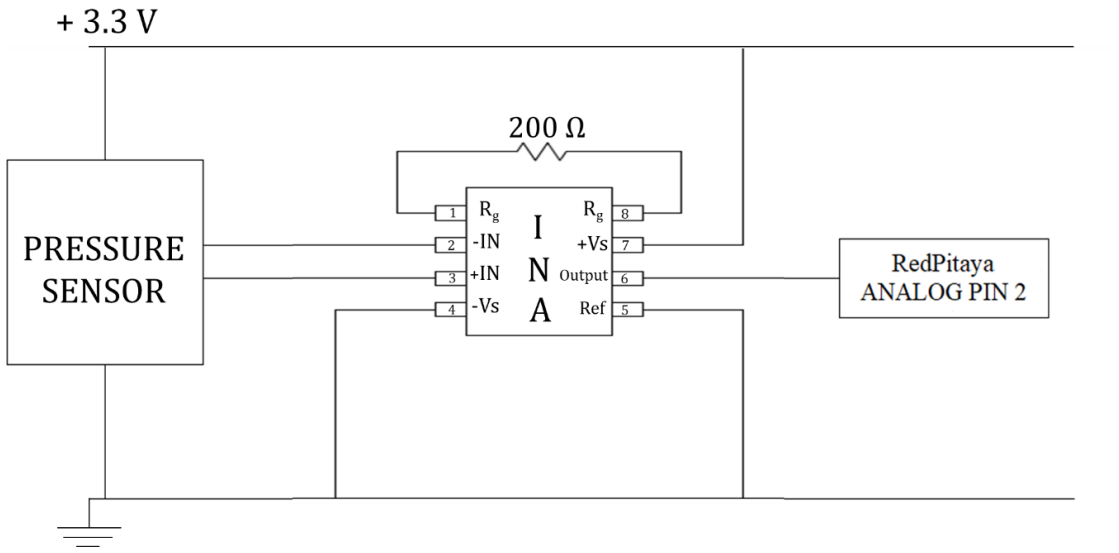

Figure 3.10: *Circuitry which includes the pressure sensor, the INA AD627NZ amplifier and the RedPitaya analog pin 2.*

MATLAB code

MATLAB software allows the connection between a computer and STEMlab 125-10. Once the computer is connected to the RedPitaya wifi network, just by typing the RedPitaya IP address in the browser, it would be possible to connect the two hardware together by SCPI connection.

The customized MATLAB code used (full text in Appendix C) asks the user to introduce information regarding the test conditions, to properly name the output text file containing the measured pressure data. The code acquires the voltage values, and converts them in pressure values, thanks to a preliminary sensor calibration. The code plots, real-time, the pressure-time curve and also reduces the noise by applying a 5-point moving average filter, smoothing the signal.

The moving average filter equation is:

$$y[i] = \frac{1}{M} \sum_{j=0}^{M-1} x[i+j]$$

where *x* is the measured pressure (input signal), *y* is the filtered pressure (output signal) and *M* is the number of points of the sliding window (equal to 5 in this case). At the end of the test, by clicking on the STOP button, the user can stop the acquisition and the code will automatically save the pressure measurements in a .txt file and the pressure-time plot in a .png file.

3.3.2. Pressure data postprocessing

After acquisition, pressure data are postprocessed using a MATLAB script (full text in Appendix C). It takes as input a .txt file containing the raw pressure measurements and plots the pressure-time curve. Then it asks the user to select the test starting point. According to that, the curve is shifted in time and pressure setting time [s] = 0 and pressure [mmHg] = 0 in the selected point. Then the code applies again the 5-point moving average filter to further smooth the signal. Then, the code identifies the aggregation point ($t_{aggregation}$ [s], $P_{aggregation}$ [mmHg]): at the beginning of the test under flow, pressure starts rising due to the change of viscosity moving from PBS to blood flowing into the channel; then a change in the curve concavity occurs (baseline), followed, eventually, by a short pressure plateau; platelet aggregation actually starts and pressure rises again. The time at which aggregation starts ($t_{aggregation}$) depends on the imposed shear stress, so the user is asked whether the shear stress is 42.75 or 72 dyne/cm^2 and then the code automatically divides the curve into two parts, a stabilization curve and the actual aggregation curve. As a final step the code plots the time-pressure curve and saves the output parameters in a .txt file. These parameters are: the maximum pressure (P_{max}), the area under the curve (AUC), and the pressure difference (ΔP). In particular, the ΔP is referred to the difference between P_{max} and $P_{aggregation}$, which represents the actual pressure drop caused by minor head losses due to platelet aggregation and thrombus formation. For the same reason, AUC is the area between the baseline and the aggregation curve (Figure 3.11).

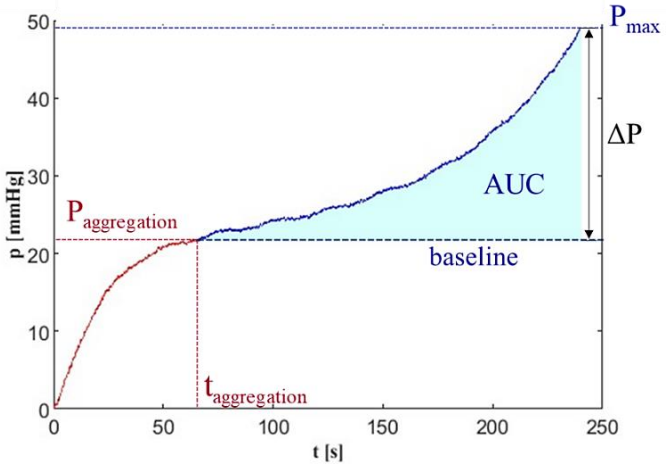

Figure 3.11: *Typical pressure curve showing aggregation parameters.*

3.4. Confocal microscopy acquisition

To correlate pressure measurements to platelet aggregation, thrombus height and thrombus volume need to be assessed, to compute the occlusion degree of the channel. These parameters are evaluated analyzing images of the channel, captured using a confocal microscope. Right after the test under flow, channels were washed with PBS for approximately 1 minute, at a flow rate of 30 μL/min; channels were then observed using a confocal inverted fluorescence microscope (Leica DM IRE2) (Figure 3.12) with a 20X objective. A set of image stacks was captured along the coated portion of the channel.

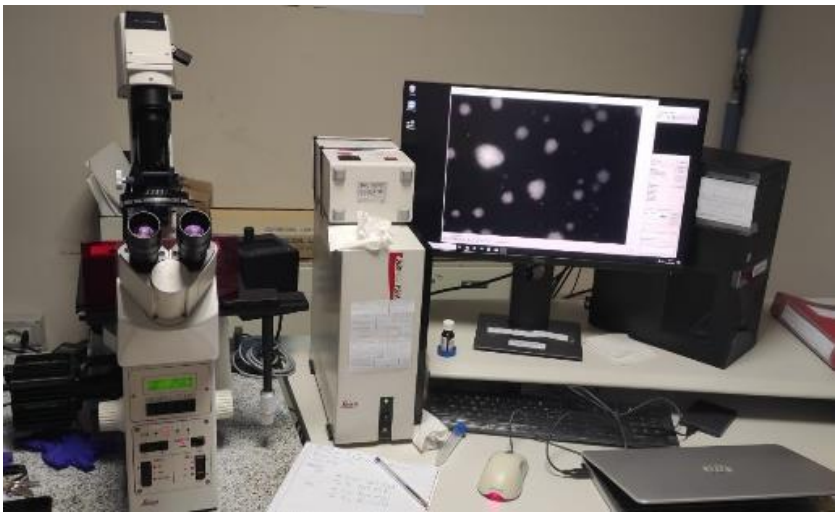

Figure 3.12: *Confocal microscope (Leica DM IRE2) used for thrombus height and volume evaluations.*

3.4.1. Thrombus height and volume measurements

At first, any correlation between thrombus height and pressure difference is sought; then, thrombus volume is taken into account to assess pressure-channel occlusion dependence. Using the software imageJ, per each test, the heigh of the highest thrombus in the channel was evaluated. The highest thrombus should be the one to cause a pressure increase due to minor head losses caused by a local partial channel occlusion.
Using the same software, the volume of the thrombi formed inside the channel was measured. Volume results were then used to calculate the channel occlusion percentage to determine any correlation between pressure and channel occlusion due to thrombus formation and platelet aggregation.

4 Results

4.1. Effect of immobilized adhesion proteins

In this section, the effects of immobilized adhesion proteins on platelet activity will be presented. Experiments under flow were performed in a microfluidic system and platelet adhesion was investigated on all protein substrates at a same shear stress level using blood from a same donor. As collagen is considered to play a major role in the coagulation process [125] and, in literature, platelet adhesion on collagen substrate has been widely studied [126] [127], platelet activity on all the different proteins will be evaluated having as reference the collagen substrate. A total of three shear stress levels (13.5, 49.5 and 72 dyne/cm^2) were tested. Figure 4.1 shows representative images of platelet activity on each substrate at each shear stress level.

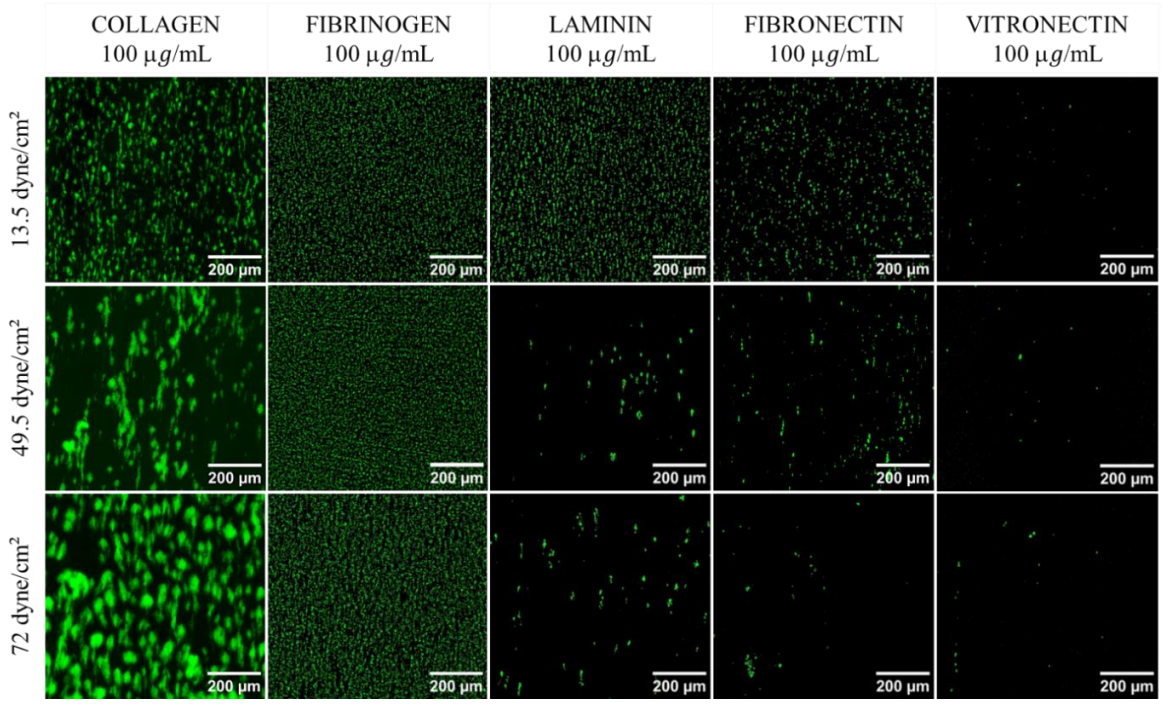

Figure 4.1: *Platelet activity under flow on each protein substrate at each shear stress level. Images captured by fluorescence microscope with 10X objective.*

As shown by the images above, vitronectin elicits almost no adhesion under flow at all shear stress levels; for laminin and fibronectin, instead, platelet adhesion drastically reduces with shear. On collagen and fibrinogen substrates good platelet adhesion is visible at every shear stress level.

Quantitative results of surface coverage, number of thrombi, mean thrombus area and fluorescence intensity are shown in Figure 4.2 as mean ± SD, over a 7 donors sample per each shear stress value. Analyzing the surface coverage graph (Figure 4.2a), at low shear stress, collagen, fibrinogen and laminin are the substrates that allow the highest platelet adhesion; lower but still present is the adhesion to fibronectin, where a statistically significant difference was found ($p<0.05$) compared to the collagen substrate; almost null is the adhesion to vitronectin, where a statistically significant difference with respect to collagen was also found ($p<0.001$). At increasing shear stress, especially at the highest value, the adhesion to laminin, fibronectin and vitronectin reduces, as illustrated by the presence of statistically relevant differences with respect to the collagen substrate. Nth (Figure 4.2b) shows that, for all substrates but fibrinogen, the number of aggregates reduces as shear increases. Ath (Figure 4.2c) show a statistically relevant difference at all shear stress levels, between collagen and the other substrates. At low shear stress, FI (Figure 4.2d) is almost the same for all substrates, and no statistical difference is highlighted by statistical analysis. However, at increasing shear, FI values for collagen increase; at the highest shear level, relevant statistical differences are present between collagen and all the other substrates, suggesting that only collagen is involved in shear-induced aggregation.

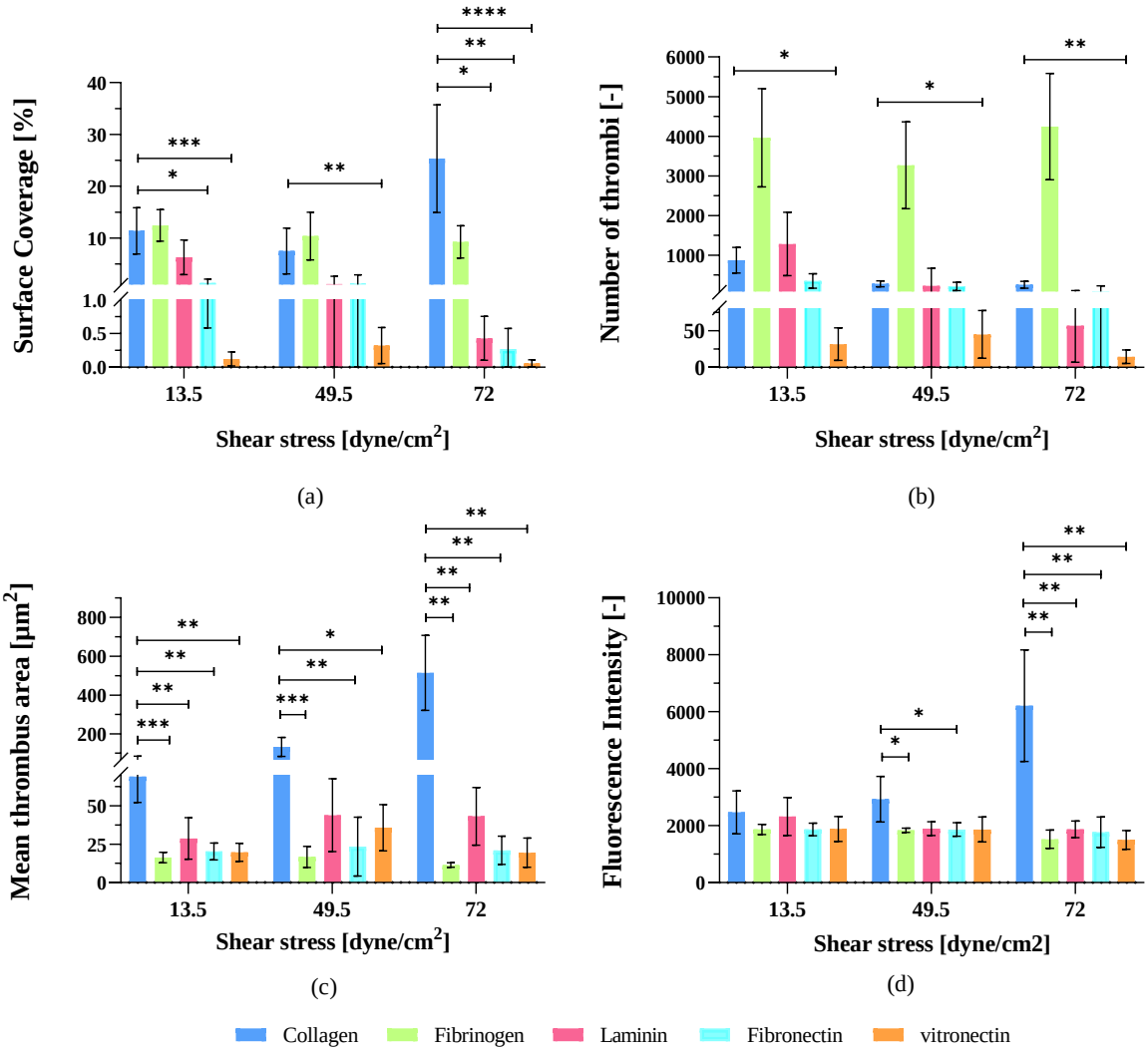

Figure 4.2: *Results of shear induced adhesion and aggregation in whole blood on five different proteins substrates organized by shear stress value: (a) SC, (b) Nth, (c) Ath, (d) FI. Data from 7 donors are shown as mean ± SD. Normally distributed data were analyzed by one-way ANOVA, non-normally distributed data by Friedman test. *p <0.05, **p <0.01, ***p <0.001, ****p <0.0001.*

The same data about the effect of shear stress for each protein substrate is also shown in Figure 4.3, but arranged differently to compare variations within a protein substrate. In particular, thrombus growth both in area and height on the collagen substrate can be better appreciated here (mean Ath ± SD on collagen substrate: 69 ± 16.8, 132.9 ± 48.5 and 514.2 ± 193.6 µm² at shear stress values of 13.5, 49.5 and 72 dyne/cm² respectively; mean FI ± SD on collagen substrate: 2467 ± 754, 2927 ± 800 and 6211 ± 1957 at shear stress values of 13.5, 49.5 and 72 respectively). In fact, statistical analysis highlighted

significant differences among the three shear stress values for Ath (Figure 4.3c) and FI (Figure 4.3d).

The shear dependent platelet adhesion on laminin and fibronectin can be better observed as well. SC (Figure 4.3a) in fact shows how adhesion to these two substrates reduces at increasing shear stress (SC [%] ± SD on laminin substrate: 6.3 ± 3.3, 1.1 ± 1.5 and 0.42 ± 0.33 at shear stress values of 13.5, 49.5 and 72 dyne/cm^2 respectively; SC [%] ± SD on fibronectin substrate: 1.34 ± 0.76, 1.2 ± 1.7 and 0.27 ± 0.31 at shear stress values of 13.5, 49.5 and 72 dyne/cm^2 respectively). Statistically significant differences were found going from low to high shear stress.

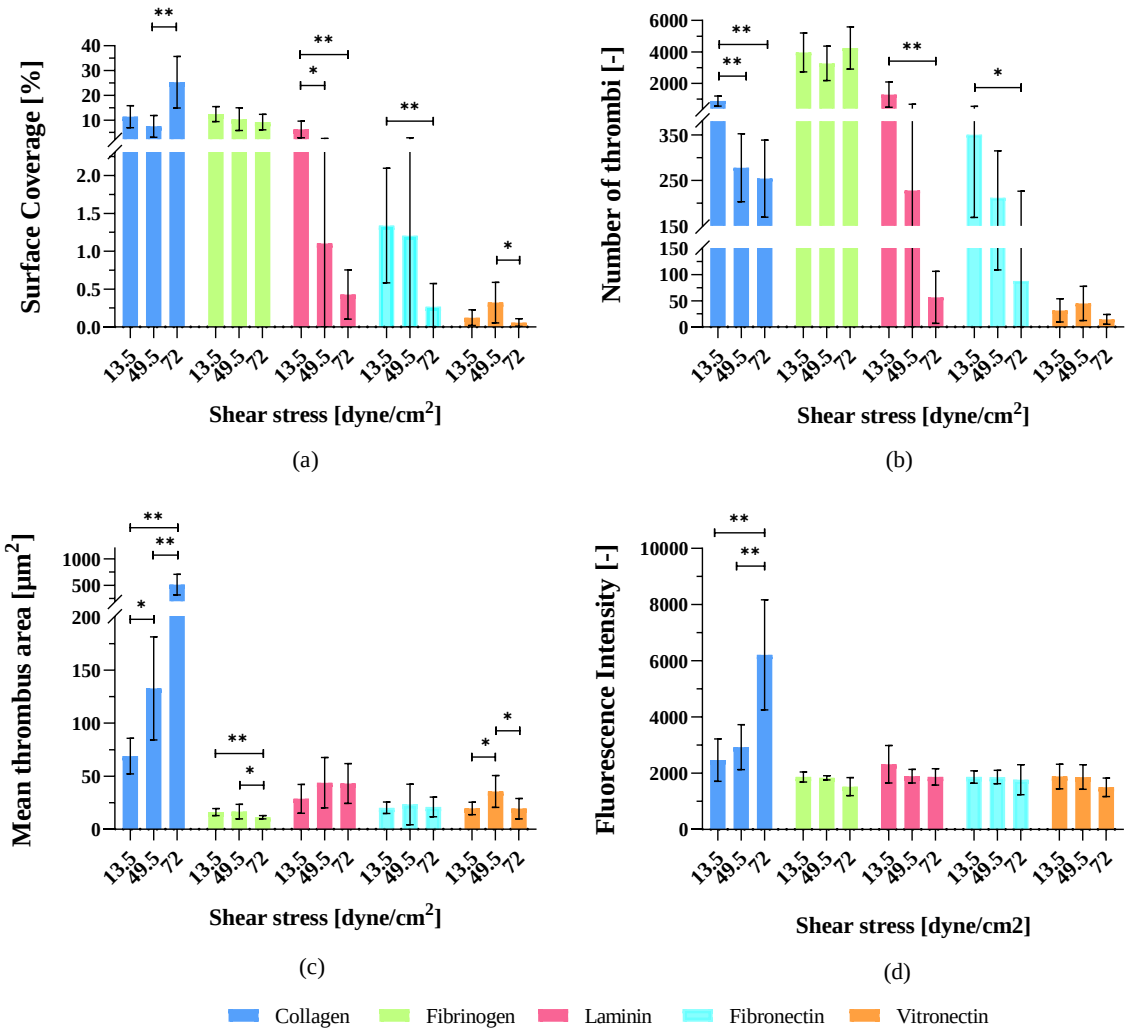

Figure 4.3: *Results of shear induced adhesion and aggregation in whole blood on five different proteins substrates organized by protein: (a) SC, (b) Nth, (c) Ath, (d) FI. Data from 7 donors are shown as mean ± SD. Normally distributed data were analyzed by one-way ANOVA, non-normally distributed data by Kruskal-Wallis test. *p <0.05, **p <0.01, ***p <0.001, ****p<0.0001.*

4.2. Effect of circulating platelet- derived microparticles

In this section, the effect of circulating platelet-derived microparticles on platelet adhesion and aggregation under flow in a microfluidic system will be presented. Prior to the addition of platelet-derived microparticles to whole blood, some trial runs were performed to validate PDMPs activity and their ability to adhere to the collagen substrate. Figure 4.4 shows microparticles (in green) adhering to the collagen substrate at all shear stress levels, proving PDMPs activity.

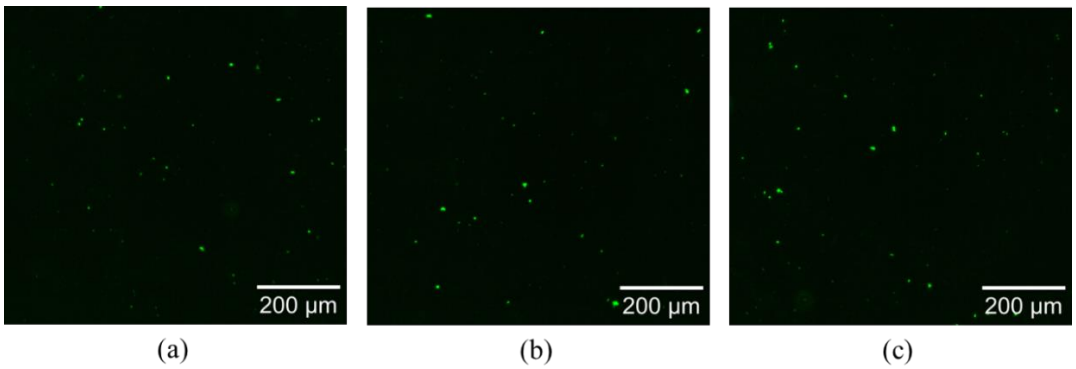

Figure 4.4: *Validation of PDMPs activity under flow: adhesion on collagen substrate at (a) 13.5 dyne/cm², (b) 49.5 dyne/cm², (c) 72 dyne/cm². Images captured by fluorescence microscope with 10X objective. PDMPs labeled with wheat germ agglutinin.*

After this preliminary validation, the actual tests under flow were performed. For each experiment, using blood from a same donor, test with and without microparticles were run at a same shear stress level. A total of three shear stress values (13.5 dyne/cm², 49.5 dyne/cm² and 72 dyne/cm²) were tested. The obtained results are shown in Figure 4.5 as mean ± SD, over a population of 7 donors. The analyzed parameters are surface coverage (Figure 4.5a), thrombus number (Figure 4.5b), mean thrombus area (Figure 4.5c) and fluorescence intensity (Figure 4.5d). Each parameter exhibits the same behavior as shear stress varies, both in presence and absence of PDMPs, as confirmed by statistical analysis: Nth (Figure 4.5b) massively reduces going from low to high shear (Nth: 856 ± 148, 292 ± 103 and 256 ± 81 at 13.5, 49.5 and 72 dyne/cm² respectively, for WB; Nth: 1054 ± 148, 520 ± 234 and 283 ± 86 at 13.5, 49.5 and 72 dyne/cm² respectively, for WB+PDMPs); Ath (Figure 4.5c) and FI (Figure 4.5d) increase at high shear (Ath: 76.57 ± 13.24, 149,71 ± 31.42 and 522 ± 186.12 µm² at 13.5, 49.5 and 72 dyne/cm²

respectively, for WB; Ath: 47.57 ± 11.9, 68.43 ± 19.70 and 195.86 ± 60.30 μm² at 13.5, 49.5 and 72 dyne/cm² respectively, for WB+PDMPs. FI: 2555 ± 738, 2767 ± 798 and 6482 ± 1486 at 13.5, 49.5 and 72 dyne/cm² respectively, for WB; FI: 1961 ± 243, 2017 ± 127 and 3301 ± 888 at 13.5, 49.5 and 72 dyne/cm² respectively, for WB+PDMPs).

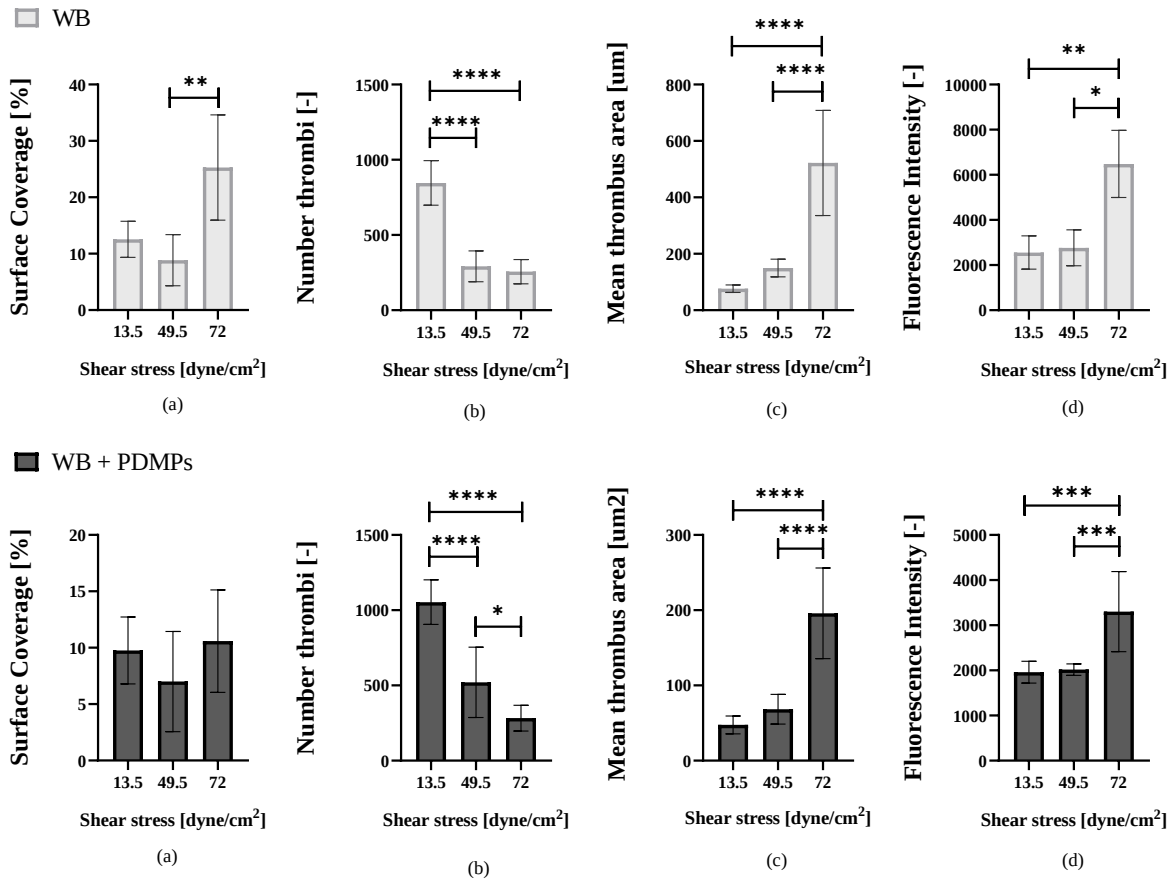

Figure 4.5: *Effect of shear stress on (a) SC, (b) Nth, (c) Ath and (d) FI on a collagen substrate without PDMPs (top) and with PDMPs (bottom). Data from 7 donors are shown as mean ± SD. Normally distributed data were analyzed by one-way ANOVA, non-normally distributed data by Kruskal-Wallis test. *p <0.05, **p <0.01, ***p <0.001, ****p<0.0001.*

Qualitative results of thrombus size and coverage on the collagen substrate are shown in Figure 4.6: Figure 4.6 (left) shows qualitatively surface coverage and thrombi dimension in absence of microparticles; Figure 4.6 (right) qualitatively shows, instead, the effect of the addition of microparticles fraction to whole blood on surface coverage and thrombi dimension. This typical example makes it clear that the addition of microparticles to the blood leads to a reduction in size of the thrombi formed on the substrate.

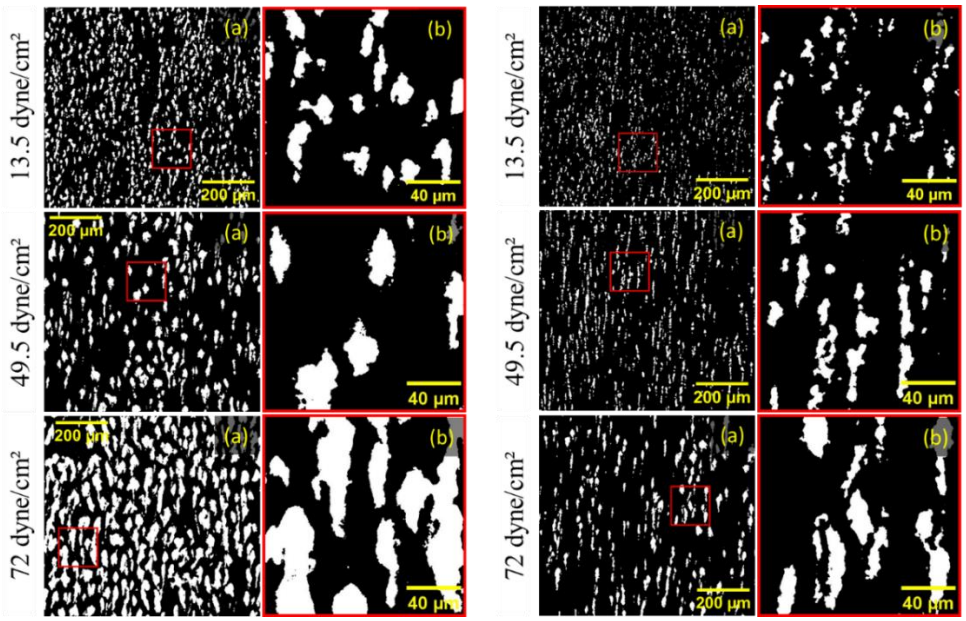

Figure 4.6: *(left) Microscopic images of substrate surface coverage and thrombi on three different level of shear stress: (a) overall coverage of whole blood on collagen; (b) magnified image of thrombi with average size; (right): microscopic images of substrate surface coverage and thrombi on three different level of shear with addition of microparticles: (a) overall coverage of whole blood on collagen; (b) magnified image of thrombi with average size. Images captured by fluorescence microscope with 10X objective.*

These qualitative results are confirmed by data: Figure 4.7 shows the effect of the addition of microparticles fraction on surface coverage (Figure 4.7a), thrombus number (Figure 4.7b), mean thrombus area (Figure 4.7c) and fluorescence intensity (Figure 4.7d) on collagen substrate. Data from 7 donors are shown as mean ± SD. At each shear stress level the presence of circulating microparticles leads to a reduction of SC, also confirmed by statistically significant differences found at the lowest and highest shear stress values (SC [%]: 12.6 ± 3.2 and 9.8 ± 2.96 at shear value 13.5 dyne/cm^2 for WB and WB+PDMPs respectively; 8.8 ± 4.5 and 7.0 ± 4.4 at shear value 49.5 dyne/cm^2 for WB and WB+PDMPs respectively; 25.3 ± 9.3 and 10.6 ± 4.5 at shear value 72 dyne/cm^2 for WB and WB+PDMPs respectively). Moreover, there is an increase in Nth (Figure 4.7b), most evident at 13.5 and 49.5 dyne/cm^2 where statistically relevant differences were found (Nth: 846 ± 148 and 1054 ± 148 at shear value 13.5 dyne/cm^2 for WB and WB+PDMPs respectively; 292 ± 103 and 520 ± 234 at shear value 49.5 dyne/cm^2 for WB and WB+PDMPs respectively; 255 ± 81 and 283 ± 86 at shear value 72 dyne/cm^2 for WB and WB+PDMPs respectively).

Statistical analysis highlights significant differences between the two groups at every shear level both for Ath (Figure 4.7c) and FI (Figure 4.7d) meaning that aggregates on the collagen substrate, in presence of microparticles fraction, are smaller in size, and suggesting that they have a lower height compared to what happens when PDMPs are not added to the blood (Ath: 76.6 ± 13.2 and 47.6 ± 11.9 μm^2 at shear value 13.5 dyne/cm^2 for WB and WB+PDMPs respectively; 149.7 ± 31.4 and 68.4 ± 19.7 μm^2 at shear value 49.5 dyne/cm^2 for WB and WB+PDMPs respectively; 522 ± 186.1 and 195.9 ± 60.3 μm^2 at shear value 72 dyne/cm^2 for WB and WB+PDMPs respectively. FI: 2555 ± 738 and 1961 ± 243 at shear value 13.5 dyne/cm^2 for WB and WB+PDMPs respectively; 2767 ± 798 and 2017 ± 127 at shear value 49.5 dyne/cm^2 for WB and WB+PDMPs respectively; 6482 ± 1486 and 3301 ± 888 at shear value 72 dyne/cm^2 for WB and WB+PDMPs respectively).

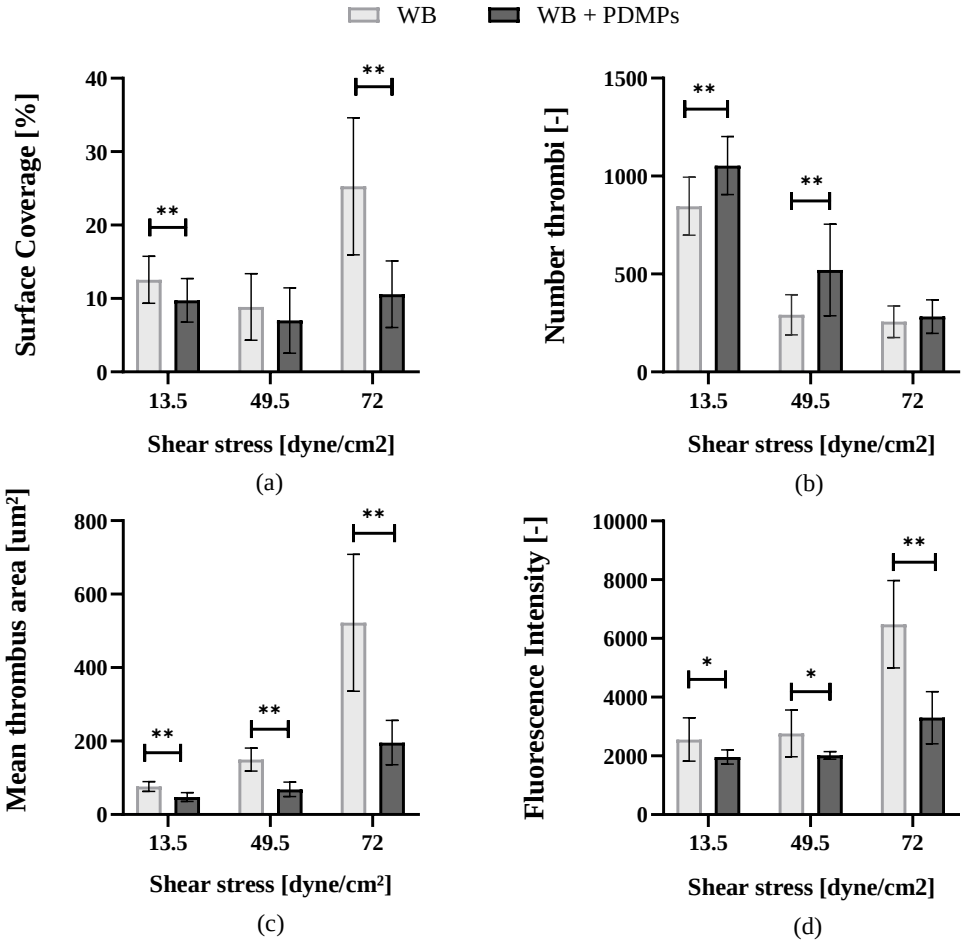

Figure 4.7: *Effect of the addition of microparticles fraction on (a) SC, (b) Nth, (c) Ath and (d) FI on a collagen substrate. Data from 7 donors are shown as mean ± SD. Normally distributed data were analyzed by t-test, non-normally distributed data by Mann-Whitney test. *p <0.05, **p <0.01.*

4.3. Pressure measurements to assess platelet activity

In this section a new approach to evaluate platelet activity, disengaged from the use of microscopy, will be introduced. A change in the microfluidic platform was performed, introducing a pressure sensor. The platform was validated: pressure measurements obtained using the micro pressure sensor will be reported, showing the correlation with platelet aggregation at different collagen concentrations and shear stress levels. The evaluated Δp is caused by minor head losses, hence, it depends on thrombus formation inside the channels. This can be visually seen from Figure 4.8, showing different pressure measurements and the corresponding pictures of the formed thrombi: a higher Δp is obtained when bigger and very fluorescent thrombi form inside the channel.

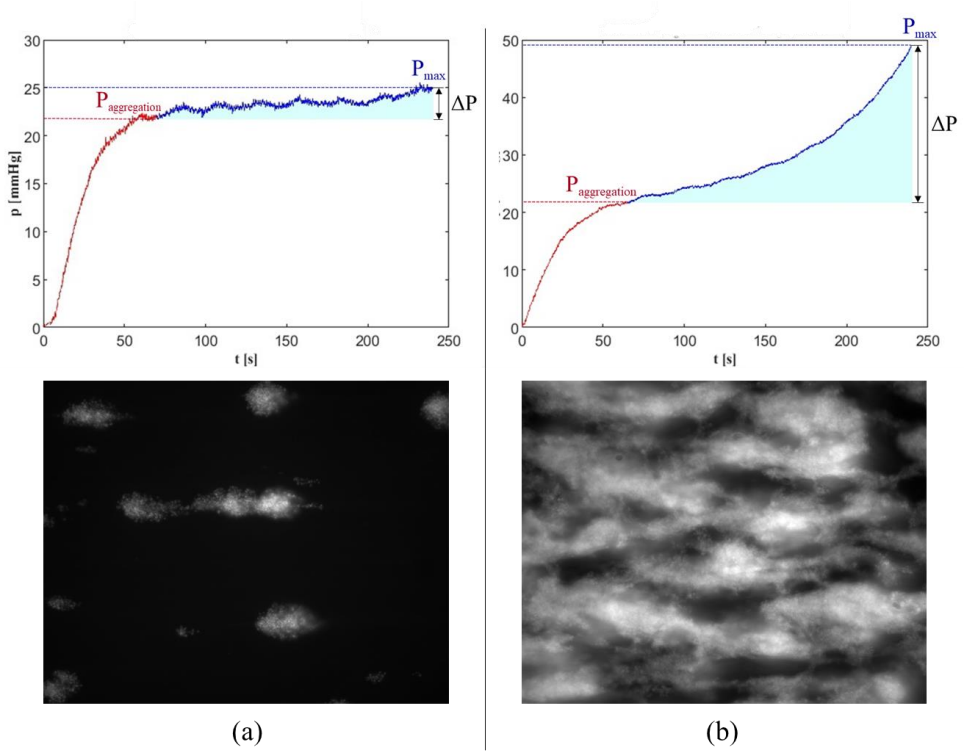

Figure 4.8: *Examples of two different pressure increases correlated to the respective images of the formed thrombi inside the channel.*

Fluorescence intensity, thrombus height and channel occlusion percentage evaluations will be reported. Tests under flow were performed over a population of 13 donors evaluating FI and pressure; for 12 out of 13 experiments, thrombus height and channel occlusion percentage were also evaluated, using confocal microscopy. Then, results

obtained using microscopy will be compared with pressure measurements, showing the correlation between pressure and FI, thrombus height and channel occlusion percentage.

4.3.1. Shear stress and collagen concentration effects on fluorescence intensity

In this paragraph, maximum fluorescence intensity values refer to the "brightest" thrombus, so the highest thrombus, that is supposed to cause local head losses, hence pressure increase, and lead to local channel occlusion. Collagen concentration and shear stress effects on pressure can be appreciated in Figure 4.9. Results are reported as mean ± SD, over a population of 13 donors.

Increasing FI values are noticeable when, at the same shear value, collagen concentration goes from 10 to 100 μg/mL (FI at 42.75 dyne/cm^2 shear stress: 1356 ± 832 and 2386 ± 1084 for low and high collagen concentration respectively. FI at 72 dyne/cm^2 shear stress: 1215 ± 955 and 4393 ± 2638 for low and high collagen concentration respectively). The same noticeable increase happens when, at collagen concentration of 100 μg/mL, shear stress goes from low to high values (FI at 100 μg/mL: 2386 ± 1084 and 4393 ± 2638 for low and high shear stress respectively). Statistical analysis highlights these relevant increments in FI.

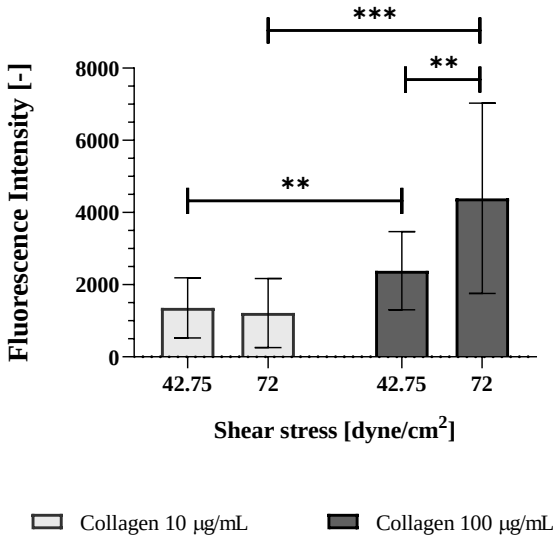

Figure 4.9: *Effect of shear stress and collagen concentration on fluorescence intensity. Data from 13 donors are shown as mean ± SD. Data were analyzed by two-way ANOVA. **p<0.01, ***p<0.001.*

4.3.2. Shear stress and collagen concentration effects on pressure measurements

The effect of varying shear stress and collagen concentration on thrombus formation is shown in Figure 4.10. Data are reported as mean ± SD, over a population of 13 donors. The same statistically significant differences found for the FI measurements can be seen also in pressure results. Statistical analysis shows relevant differences in pressure evaluations as collagen concentration increases (pressure [mmHg] at 42.75 dyne/cm^2: 1.79 ± 0.95 and 3.09 ± 1.75 for low and high collagen concentration, respectively. Pressure [mmHg] at 72 dyne/cm^2: 2.01 ± 1.01 and 9.91 ± 6.12 for low and high collagen concentration respectively); also, statistically relevant differences are present at high collagen concentration moving from 42.75 to 72 dyne/cm^2 shear stress value (pressure [mmHg] at 100 μg/mL: 3.09 ± 1.75 and 9.91 ± 6.12 for low and high shear stress respectively).

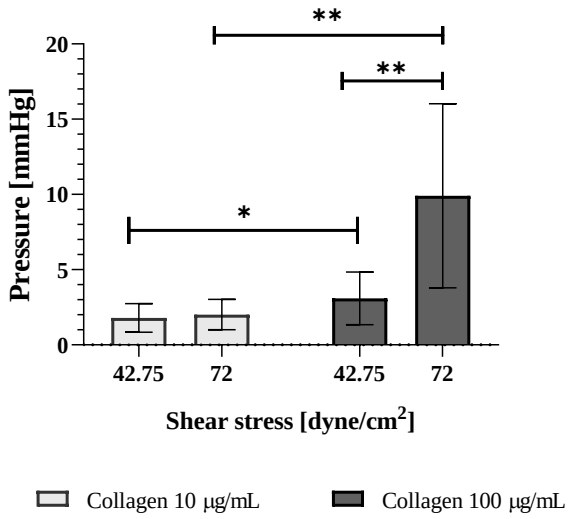

Figure 4.10: *Effect of shear stress and collagen concentration on pressure measurements. Data from 13 donors are shown as mean ± SD. Data were analyzed by two-way ANOVA. *p<0.05, **p<0.01.*

4.3.3. Shear stress and collagen concentration effects on thrombus height

The maximum thrombus height was evaluated by confocal imaging. It refers to the height of the highest thrombus formed inside the channel, that should cause the partial channel occlusion and so minor head losses. Thrombus height was not evaluated at the shear

stress value of 72 [dyne/cm^2] with 100 μg/mL collagen concentration because the confocal microscope used to capture the images does not provide reliable information when the object is higher than 80 μm. Platelet aggregation on 100 μg/mL collagen concentration at high shear stress, in most cases, leads to the formation of thrombi higher than this threshold; therefore, this test condition was not considered for height measurements, as this could have led to wrong evaluations.

Results are shown in Figure 4.11 as mean ± SD, over a population of 12 donors. As for pressure measurements, also the height increases with the shear stress value and the collagen concentration. Statistical analysis, in particular, shows relevant differences as collagen concentration increases for a fixed shear stress (height [μm]: 41.42 ± 14.57 and 52.71 ± 17.83 at 42.75 dyne/cm^2 for low and high collagen concentration, respectively).

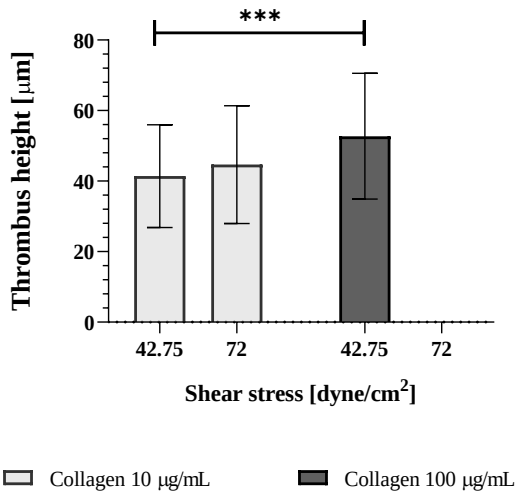

Figure 4.11: *Thrombus height for varying shear stress and collagen concentration. Data from 12 donors are shown as mean ± SD. Normally distributed data were analyzed by t-test, non-normally distributed data by Mann-Whitney test, ***p<0.001.*

4.3.4. Shear stress and collagen concentration effects on channel occlusion percentage

Channel occlusion has been evaluated starting from thrombi volume measurements, obtained analyzing image stacks of the channel captured using the confocal microscope after each experiment. The effects of shear stress and collagen concentration are shown in Figure 4.12 as mean ± SD, over a population of 12 donors. The same confocal microscope used for height evaluations was also used for volume measurements, hence

also channel occlusion percentage was not evaluated for the condition characterized by 100 μg/mL collagen concentration and 72 dyne/cm^2 shear stress, as the thrombi formed at this test condition would have been too high to be properly measured.
Channel occlusion percentage doubles as collagen concentration increases; a statistically significant difference, in fact, was found (channel occlusion [%] at 42.75 dyne/cm^2: 1.32 ± 1.36 and 2.64 ± 2.12 for low and high collagen concentration respectively.

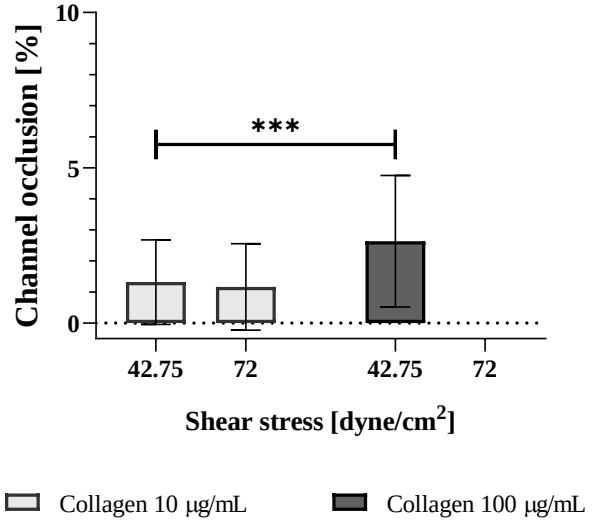

Figure 4.12*: Effect of shear stress and collagen concentration on channel occlusion percentage. Data from 12 donors are shown as mean ± SD. Normally distributed data were analyzed by t-test, non-normally distributed data by Mann-Whitney test, ***p<0.001.*

4.3.5. Pressure-platelet activity correlation

In this paragraph correlation between pressure and FI, pressure and thrombus height and pressure and channel occlusion percentage will be reported.

Pressure-FI correlation

Pressure measurements, obtained using the micro pressure sensor during tests under flow, turned out to be dependent on thrombus fluorescence intensity, as expected; the correlation is shown in Figure 4.13. The pressure-fluorescence intensity dependence is characterized by a linear trend line (R^2 = 0.771) and showed a correlation coefficient (CC) equal to 0.88.

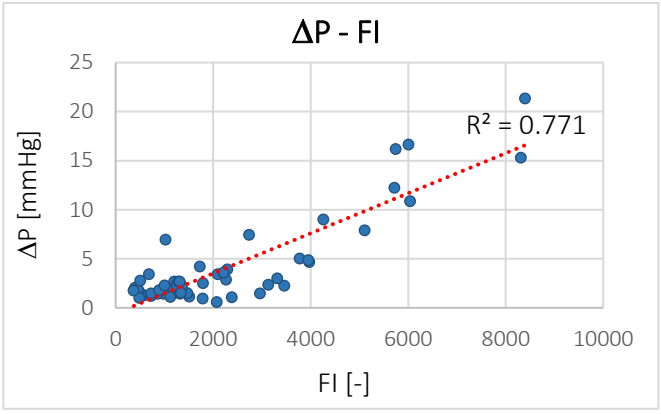

Figure 4.13: *Pressure-fluorescence intensity correlation plot, n=13.*

Pressure-thrombus height correlation

Figure 4.14 shows the pressure-thrombus height correlation. Thrombus height is directly related to channel cross section reduction due to platelet aggregation, but the correlation between pressure and thrombus height did not (CC= 0.41).

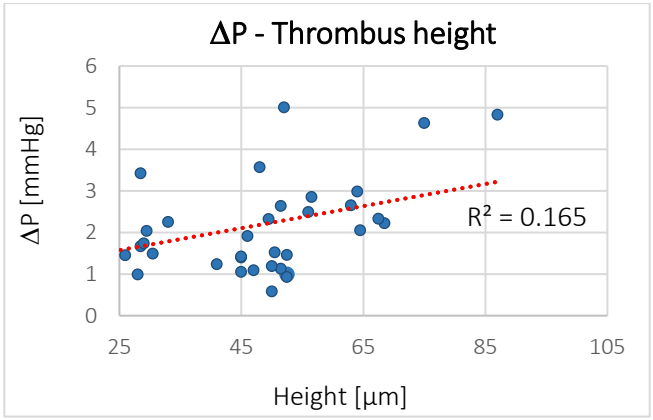

Figure 4.14: *Pressure-thrombus height correlation plot, n=12.*

Pressure-channel occlusion

Figure 4.15 shows the pressure-channel occlusion correlation. The channel occlusion percentage does not show a good correlation with pressure measurements (R^2= 0.168 and CC= 0.41).

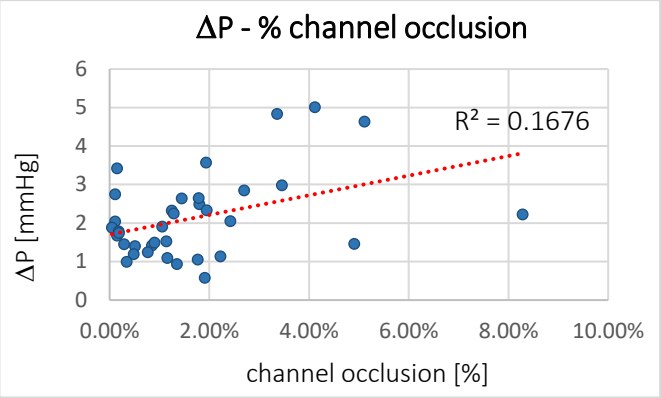

Figure 4.15: *Pressure-channel occlusion percentage correlation plot, n=12.*

4.3.6. Healthy subjects vs covid patients platelet activity

Covid patients and healthy donors are reported to have different platelet activity in adhesion tests under flow, especially at low shear stress levels. For this reason, even if the above-mentioned tests were performed at higher shear stresses, the same results are also reported and analyzed making a distinction between donors: covid patients and healthy subjects. Data are divided into these two groups to evaluate possible statistical differences. Figure 4.16 shows the different platelet aggregation (in green) between healthy subjects (a) and covid patients (b).

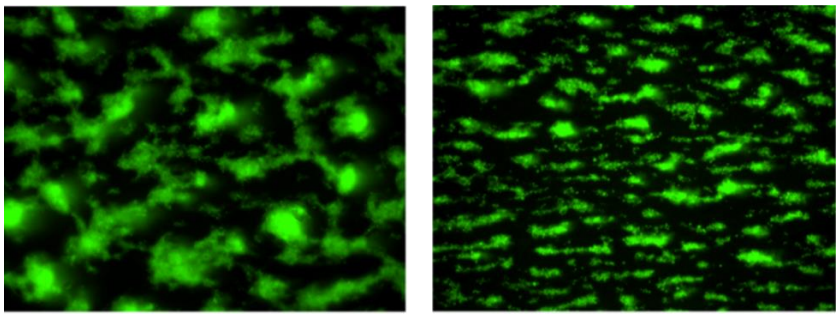

Figure 4.16: *Thrombus formation after 4 minutes on collagen 100 μg/mL at 49.5 dyne/cm: (a) healthy subject; (b) covid patient. Images captured by fluorescence microscope with 40X objective.*

Differences in the results concerning FI, pressure, channel occlusion percentage and thrombus height, between these two groups, are shown.

Fluorescence intensity values evaluated by image postprocessing are reported in Figure 4.17 as mean ± SD, over a population of 7 healthy donors and 6 covid patients. Statistical

differences (p=0.035) were only found at low shear stress and low collagen concentration. However, for the covid patients group, the test condition characterized by high collagen concentration and high shear stress, presents the highest dispersion of data (FI ± SD: 5703 ± 2221 and 2864 ± 2360 at collagen concentration 100μg/mL and shear stress 72 dyne/cm^2 for healthy subjects and covid patients, respectively).

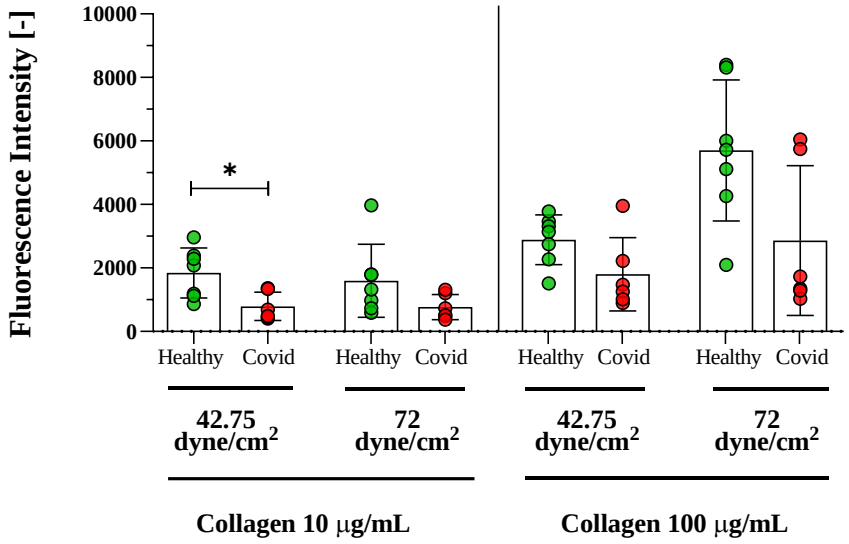

Figure 4.17: *FI at each collagen concentration and shear stress value for healthy subjects and covid patients. Data from 7 healthy subjects and 6 covid patients are shown as mean ± SD. Normally distributed data were analyzed by t-test, non-normally distributed data by Mann-Whitney test. *p <0.05.*

As for the FI evaluations, pressure measurements, obtained using the pressure sensor, will be reported for healthy subjects and covid patients, for all collagen concentrations and shear rate values. Results over a population of 7 healthy subjects and 6 covid patients are shown in Figure 4.18 as dot plot, with mean ± SD. Statistical analysis does not highlight any differences between the two groups in any of the tested conditions (p> 0.05). However, as for FI data, pressure evaluated at high collagen concentration and high shear stress, for covid patients, shows the highest data dispersion (Pressure [mmHg] ± SD, for 100 μg/mL collagen concentration and 72 dyne/cm^2 shear stress: 12.25 ± 6.04 and 7.18 ± 5.44 for healthy subjects and covid patients, respectively).

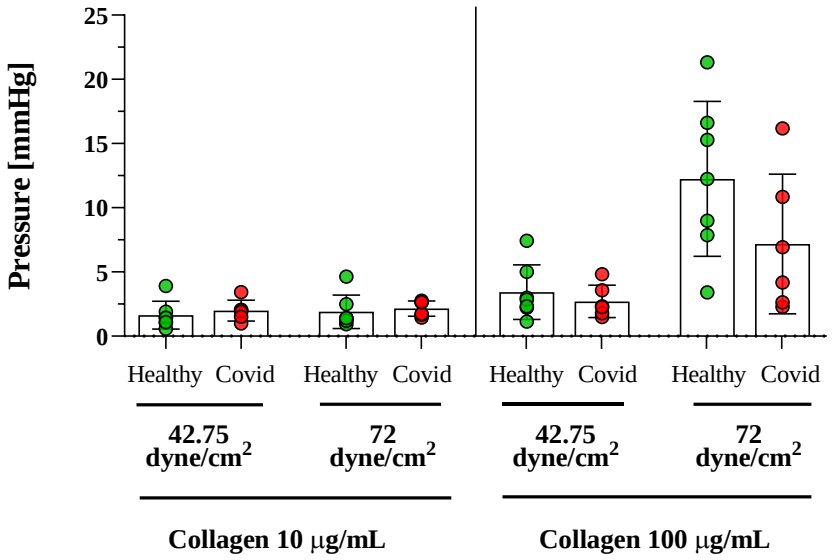

Figure 4.18: *Pressure results for each collagen concentration value and shear stress value for healthy subjects and covid patients. Data from 7 healthy subjects and 6 covid patients are shown as mean ± SD. Normally distributed data were analyzed by t-test, non-normally distributed data by Mann-Whitney test.*

Also for the thrombus height computed by confocal microscopy, results are divided into the healthy subject and covid patient groups. Results over a population of 6 healthy subjects and 6 covid patients are shown in Figure 4.19 as a dot plot, with mean ± SD. No statistically significant differences were found between the two groups in any of the tested conditions ($p > 0.05$), but the covid group presents, at all shear stress levels, a higher data dispersion with respect to the healthy subject group (thrombus height [μm] ± SD for healthy subjects: 47.6 ± 3.0 at low collagen concentration and low shear; 53.3 ± 11.9 at low collagen concentration and high shear; 60 ± 7.7 at low shear and high collagen. Thrombus height [μm] ± SD for covid patients: 35.2 ± 19.1 at low collagen concentration and low shear; 36.1 ± 17.2 at low collagen concentration and high shear; 45.4 ± 22.7 at low shear and high collagen concentration).

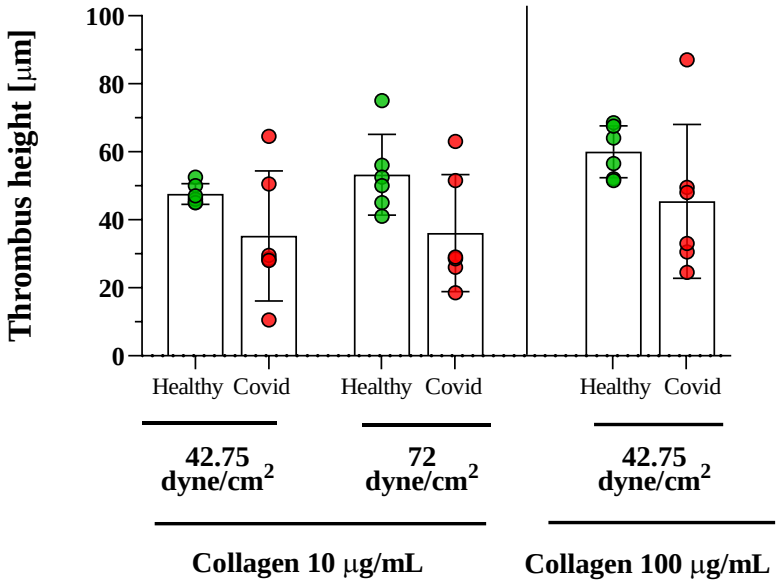

Figure 4.19: *Thrombus height results for each collagen concentration value and shear stress value for healthy subjects and covid patients. Data from 6 healthy subjects and 6 covid patients are shown as mean ± SD. Normally distributed data were analyzed by t-test, non-normally distributed data by Mann-Whitney test.*

Channel occlusion percentages are reported for all the tested shear stress levels and collagen concentration, and results are divided into the two groups. Results over a population of 6 healthy subjects and 6 covid patients are shown in Figure 4.20 as a dot plot, with mean ± SD. No statistically relevant differences were found between the two groups in any of the tested conditions ($p > 0.05$). Also in this case, a high data dispersion is present, for both groups, at high collagen concentration (Channel occlusion [%] ± SD, for 100 [μg/mL] collagen concentration and 42.75 [dyne/cm^2] shear stress: 3.79 ± 2.34 and 1.48 ± 1.08 for healthy subjects and covid patients respectively).

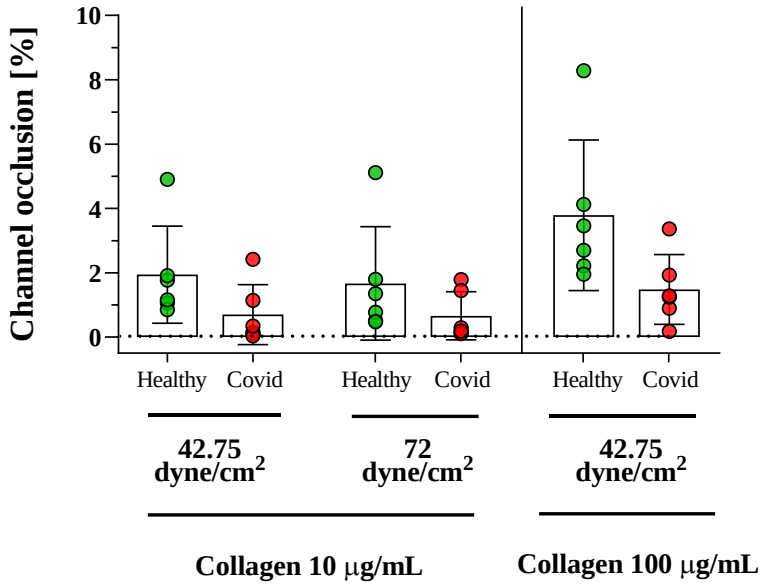

Figure 4.20: *Channel occlusion percentages for each collagen concentration value and shear stress value for healthy subjects and covid patients. Data from 6 healthy subjects and 6 covid patients are shown as mean ± SD. Normally distributed data were analyzed by t-test, non-normally distributed data by Mann-Whitney test.*

All results are fairly consistent, and a statistical difference (p=0.035) was only found in the FI results at 42.75 dyne/cm^2 shear stress and low collagen concentration, suggesting that, especially at the highest shear value, the distinction between the two groups does not lead to relevant differences.

5 Discussion

5.1. Effect of immobilized adhesion proteins

The effect of different protein substrates on shear mediated platelet adhesion and subsequent spreading was evaluated by measuring four parameters: SC, Nth, Ath and FI. At each shear stress level, platelet adhesion and aggregation on all the different ECM protein substrates was evaluated and compared. To assess the shear dependent platelet activity, per each substrate, thrombus formation results at all shear stress values were also compared.

Collagen substrate is the only one allowing good platelet adhesion and aggregation at all the shear stress values. As confirmed by SC data (Figure 4.3a), collagen is a good adhesive substrate, in fact, good platelet adhesion is present at all shear stress levels, especially the highest one (mean SC [%] ± SD: 11.4 ± 4.5, 7.5 ± 4.4 and 25.3 ± 10.4 at shear stress values of 13.5, 49.5 and 72 dyne/cm^2, respectively); platelet aggregation, expressed by Ath and FI (Figure 4.3c and Figure 4.3d) values, increases at increasing shear stress, confirming the platelet activator power of collagen that promotes platelet-to-platelet adhesion (aggregation) [126], hence thrombus growth both horizontally (thrombus area) and vertically (thrombus height) with respect to the channel bottom.
In fact, when exposed to blood flow, this ECM protein binds vWF in plasma; after the shear-mediated platelet activation, the high affinity between collagen and the platelet receptors GPVI and α2β1, and between vWF and the platelet receptors GPIb-V-IX and αIIbβ3, promotes both platelet adhesion and aggregation [128]. Platelet aggregation at the highest shear stress level is mostly due to the binding of the platelet receptors to the collagen-bound vWF, which allows thrombus formation and growth on collagen also at high shear stresses.

Also fibrinogen elicits high platelet affinity at each shear stress level, as confirmed by the SC values (mean SC [%] ± SD: 12.4 ± 3.1, 10.4 ± 4.6 and 9.3 ± 3.1 at shear stress values of 13.5, 49.5 and 72 dyne/cm^2, respectively), due to the αIIbβ3 mediated platelet adhesion on this protein. Fibrinogen plays a pivotal role in the in vivo fibrin clot formation, however, as confirmed by literature studies [129], its contribution in platelet immobilization into the injured vessel wall is not highly significant. Platelets, in fact, adhere to fibrinogen coated surfaces (SC results, Figure 4.2a, are comparable with the one obtained for the collagen substrate), especially at a venous shear stress, but in the absence of other adhesive proteins, only small thrombi will form [130]. This result is coherent with the high number of thrombi and the small thrombus area found at all shear stress levels (Nth ± SD: 3964 ± 1239, 3268 ± 1094 and 4245 ± 1340 at 13.5, 49.5 and 72 dyne/cm^2, respectively; mean Ath [μm^2] ± SD: 16.3 ± 3.4, 16.7 ± 6.9 and 11.4 ± 1.5 at 13.5, 49.5 and 72 dyne/cm^2, respectively).

Platelet adhesion to laminin depends, among others, on the integrin α6β1 and, at low shear stresses, laminin elicits good platelet adhesion, comparable with the one on collagen and fibrinogen (Figure 4.2a) but the formed aggregates are small (mean Ath [μm^2] ± SD on laminin substrate: 28.7 ± 13.5, 43.9 ± 23.8 and 43.1 ± 1.5 at 13.5, 49.5 and 72 dyne/cm^2, respectively). As shear stress increases, laminin adhesion drastically reduces (mean SC [%] ± SD: 6.3 ± 3.3 and 0.4 ± 0.4 at 13.5 and 72 dyne/cm^2, respectively); a significant statistical difference ($p<0.05$), in fact, is present between SC obtained on the collagen substrate and the laminin one at 72 dyne/cm^2 (Figure 4.2). Shear stress, in fact, promotes platelet activation, but platelet adhesion to adhesive ligands only occurs if the receptor-ligand association rate is faster than the relative velocity of the molecules in the blood flow. As the shear stress increases, in fact, also the relative velocity of platelets increases, limiting the time of contact between platelet receptors and the adhesive ligands; depending on the protein in question, this mechanism may lead to lower adhesion [130]. Shear stress may influence platelet aggregation and may also result in a detachment of the adherent cells [131].

Fibronectin is an adhesive substrate that binds two main receptors: α5β1 and αIIbβ3 integrins. As for platelet adhesion on the fibronectin substrate, lower (if compared to collagen, laminin and fibrinogen, Figure 4.2a) but still appreciable adhesion can be observed at both venous and arterial shear stress. At the highest shear stress level, as for

the laminin substrate, platelet adhesion drastically reduces (mean SC [%] ± SD on the fibronectin substrate: 1.3 ± 0.8, 1.2 ± 1.7 and 0.3 ± 0.3 at 13.5, 49.5 and 72 dyne/cm^2, respectively). Moreover, as for fibrinogen and laminin, thrombi formed on the fibronectin substrate are small, especially if compared to the area of the thrombi formed on the collagen substrate (Figure 4.2c). In vivo studies in mice [132] suggest that the insoluble fibronectin of the subendothelial matrix, in presence of fibrinogen and vWF, supports platelet-to-platelet adhesion and contributes to thrombus stability; however, soluble plasma fibronectin appears to reduce the platelet aggregation promoted by the synergetic effect of fibronectin, fibrinogen and vWF and to inhibit the adhesive functions of the αIIbβ3 ligands. In the work, fibronectin from human plasma was used, which can explain the general low adhesion; moreover, as for laminin, the high shear stress, hence the low time of contact between receptors and ligands, may be the reason for the reduced adhesion at 72 dyne/cm^2.

Lastly, results show that, at each shear stress level, platelet adhesion on vitronectin is almost absent (mean SC [%] ± SD on the fibronectin substrate: 0.12 ± 0.1, 0.32 ± 0.3 and 0.06 ± 0.05 at 13.5, 49.5 and 72 dyne/cm^2, respectively), especially if compared to the SC results obtained on the collagen substrate (Figure 4.2Figure 4.3a). Vitronectin binds both to αIIbβ3 and αvβ3 integrins, but its role in thrombus formation is controversial: both supportive and inhibitory properties have been reported for vitronectin [133] [134]. The main hypothesis, deriving from in vivo studies conducted in mice [135], states that platelet-released vitronectin contributes to platelet aggregation and thrombus stability, while plasma vitronectin exhibits platelet adhesion inhibitory functions. Thus, in combination with other proteins, vitronectin could contribute to the thrombus growth, but, alone, it allows almost no adhesion at all.

A factor common to all the tested proteins is the donor dependence of the results. The highest standard deviation is present in the results for the laminin substrate. Despite the high standard deviation, present for all the tested substrates and for each parameter, the prominent effect of shear stress on platelet activity is still highly visible from the results (Figure 4.3), hence the shear-induced platelet activation can be properly studied.

Moreover, this highlights that platelets from different donors respond differently to the stimulation provided by the different protein substrates. Thus, due to its ability in

capturing patients' different platelet activity, this platform has the potential for the development of tailored antiplatelet therapies.

The proposed microfluidic platform is meant to be a PFT method to evaluate platelet activity under in vivo-like conditions. The performed tests assess platelet affinity with the different immobilized adhesion proteins, trying to determine the contribution of each protein alone on thrombus formation, but combinations of diverse proteins may be considered as well.

5.2. Effect of circulating platelet-derived microparticles

Collagen substrate, at the employed collagen concentrations, allows platelet adhesion and aggregation without completely obstructing the blood flow, at each shear stress condition. Hence, keeping the collagen concentration constant, collagen-coated channels were used to assess the effect of high PDMP levels in blood on platelet activity, as, at these test conditions, changes in platelet adhesion and aggregation caused by PDMPs would be appreciable. High PDMP levels are a marker of cardiovascular diseases or, more in general, of disorders associated with a pathological and increased platelet activity (such as Covid-19) that leads then to a greater PDMP formation. High shear stresses also lead to further PDMP generation [136].

Experiments were performed at three shear stress levels (13.5, 49.5 and 72 dyne/cm^2), and what is important to point out is that each of the evaluated parameters (SC, Nth, Ath and FI) exhibits the same trend, as shear stress increases, both when PDMPs are added to the blood and when they are not (Figure 4.5). Nevertheless, the presence of microparticles attenuates the overall adhesion to the protein substrate and platelet-to-platelet adhesion: comparing the two sets of results (WB and WB+PDMPs), in fact, a reduction of the SC, hence platelet adhesion (Figure 4.7a), and a reduction of Ath and FI, hence platelet aggregation (Figure 4.7c and d), is noticeable when PDMPs are added. This behavior is much more visible at a high shear stress (SC [%] ± SD: 25.3 ± 9.3 and 10.6 ± 4.5 at 72 dyne/cm^2 for WB and WB+PDMPs, respectively; Ath [μm^2] ± SD: 522 ± 186.1 and 195.9 ± 60.3 at 72 dyne/cm^2 for WB and WB+PDMPs, respectively; FI ± SD: 6482 ± 1486 and 3301 ± 888 at 72 dyne/cm^2 for WB and WB+PDMPs, respectively).

What can be appreciated both qualitatively, by looking at the images of the thrombi formed on the collagen-coated channel (Figure 4.6), and quantitatively, from the statistically significant differences present between the results of the two groups (Figure 4.7), is that the addition of PDMPs causes the formation of a higher number of thrombi of reduced dimensions. This may suggest a reduction in platelet aggregation capabilities. What must be underlined is that platelet adhesion and platelet aggregation are two strictly correlated concepts: aggregation in fact contributes to platelet aggregate spreading, which also results in a further adhesion. So, the increased number of thrombi obtained adding PDMPs (Nth: 846 ± 148 and 1054 ± 148 at 13.5 dyne/cm^2 for WB and WB+PDMPs, respectively; 292 ± 103 and 520 ± 234 at 49.5 dyne/cm^2 for WB and WB+PDMPs, respectively; 255 ± 81 and 283 ± 86 at 72 dyne/cm^2 for WB and WB+PDMPs, respectively) may suggest the presence of a higher number of focal adhesion points on the collagen substrate, implying that PDMPs still enhance the initial platelet adhesion (in accordance with literature studies [137]), but, due to the reduced aggregation (platelet-to-platelet adhesion), platelets are less willing to adhere to immobilized platelets, so platelet spreading on the collagen substrate is reduced. This subsequently leads to lower Ath, FI and also SC values.

Studies conducted on PDMPs added to PRP showed how microparticles inhibit collagen-induced platelet aggregation [138], which is in accordance with the presented results: PDMPs apparently seam to reduce thrombus formation on the collagen substrate. A hypothetical interpretation of the presented results could be the following: platelet stimulation and aggregation promoted by PDMPs is higher than collagen-induced stimulation and aggregation; due to their high affinity, platelets in blood adhere to circulating microparticles, generating flowing aggregates, rather than forming immobilized aggregates by adhering to other platelets on the collagen substrate. Due to the adhesion receptors expressed on the surface of PDMPs, in fact, platelets may be more willing to adhere to microparticles than to the collagen substrate, causing then the presence of a huge amount of activated aggregates and microaggregates that flows in the bloodstream, and that can reach microvessels, causing microthrombosis, or can accumulate in organs, leading, in most severe cases, to organ failure and ultimately to death.

This hypothesis is actually in accordance with findings on platelet activity in Covid-19 patients: Covid-19 is associated with increased numbers of PDMPs, and many patients were reported to have increased levels of circulating activated platelets, with high surface levels of P-selectin [139].
Furthermore, both in vivo and in vitro studies show how PDMPs increase thrombin levels and are highly activated and stimulated by thrombin, leading to increased PDMP and platelet activity [140] [141]. However, in this work hirudin-anticoagulated WB was used, so thrombin formation was inhibited by hirudin, hence neither the thrombin-induced PDMP stimulation nor the resulting platelet behavior were assessed.

The effect of the presence of PDMPs in hirudin-anticoagulated WB was assessed leading to the main hypothesis of PDMPs triggering the generation of new platelet-derived microparticles at high shear stress and circulating thrombi or microthrombi (due to adhesion of platelets to PDMPs in the bloodstream).

5.3. Pressure measurements to assess platelet activity

The pressure sensor was added to the microfluidic platform to perform some preliminary studies to determine a correlation between thrombus formation and pressure increase. The final aim is the development and design of a bedside POC device that evaluates platelet activity only from pressure measurements. Thrombus formation causes a pressure drop inside the microchannel: in particular, the generation of thrombi creates minor head losses, and the resulting pressure increase inside the channel is recorded and measured by the sensor placed at the channel outlet.

The tested shear stresses are 42.75 and 72 dyne/cm^2; the venous shear stress employed for the ECM adhesion experiments was not tested here, because the pressure increase obtained at low shear stress is too small to be appreciated by the used pressure sensor.
At first, the effect of shear stress and collagen concentration on all the parameters was evaluated. FI results reflect literature studies [127]: FI increases for increasing shear stress and for increasing collagen concentration, hence it assesses very well platelet aggregation and thrombus formation. Also the other parameters (pressure, channel

occlusion percentage and thrombus height) exhibit a similar trend, at each shear stress level.

The relationship between pressure and FI was taken into account, to confirm that also pressure is actually related to thrombus formation; the good correlation found proves it. A correlation between pressure and the maximum thrombus height was also investigated. The maximum height refers to the height of the highest thrombus, that should be the one causing the highest cross section reduction, hence the highest local pressure drop, but results show a very bad correlation. This suggests that the highest thrombus is not the main and only contributor to minor head losses which are the one causing local pressure drops, and that other thrombi formed inside the channel give non-negligible contribution to the pressure drop.

For this reason, finally, the presence of a correlation between pressure increase and channel occlusion rate was investigated. The channel occlusion percentage was evaluated from thrombus volume measurements by confocal microscopy. The correlation found was not good as expected. A reason for this bad correlation is the poor resolution of the images captured with the confocal microscope, which did not allow precise volume measurements. Moreover, due to the upper limit in the thrombus height imposed by the confocal microscope, both thrombus volume and height could not be measured at 100 μg/mL collagen concentration and 72 dyne/cm^2 shear stress, as the thrombi formed at this test condition are usually higher than this threshold. Therefore, not a very high number of points were taken into account to determine the pressure-channel occlusion correlation, and this may have contributed to such a bad correlation. Another explanation could be sought in the channel washing operation: the flow rate used to rinse the channels with PBS after the test, before looking at the channel under the confocal microscope, was 30 μL/min and may have caused the breakdown or the detachment of some thrombi, resulting in misleading volume evaluations. As consequence, in some cases, the resulting volume may be lower than the real one.

COVID-19 and platelet activity

For this part of the work, the analyzed blood samples were withdrawn from healthy subjects and covid patients; both clinical and laboratory studies report different platelet

activity, especially at low shear stress, in Covid-19 patients [142] [143] [144]. For this reason, results were also divided in these two groups (healthy subjects and covid patients), to evaluate the presence of any difference.

The distinction between results from the two donor groups (from healthy subjects and covid patients), at high shear stress, does not lead to relevant differences. The only statistically relevant difference ($p<0.05$) was found for the FI at low collagen concentration at 42.75 dyne/cm^2 shear stress. According to literature studies, significant differences should be instead evident at venous shear stress, but that shear stress value was not tested as it results in too small pressure variations to be detected by the pressure sensor.

It must also be considered that the number of experiments performed for each group is small (n=6 per group), and this may be the reason why no statistical difference was found ($0.06<p<0.188$) even though, from Figure 4.17,Figure 4.18, Figure 4.19 and Figure 4.20, it is visible that the parameters mean values between the two groups differ. Therefore, more experiments should be performed to confirm the absence or presence of any statistically significant difference.

The first step in the design of the POC device consisted in validating the pressure-channel readings. Better volume measurements are needed to be able to correlate pressure and channel occlusion rate and proceed with the device development, but the results achieved so far have the potential to build an easy-to-use, inexpensive, user-friendly device for the assessment of platelet function.

6 Conclusion and future developments

Platelet adhesion and aggregation mechanisms on five ECM proteins were explored. Data confirmed literature studies, suggesting that collagen, among the tested adhesive protein substrates, is the only one promoting not only platelet adhesion but also platelet aggregation and thrombus formation. Meaning that, in vivo, upon a vessel injury, all the tested adhesive proteins act synergically to induce platelet activation, platelet-to-platelet adhesion and contribute to thrombus stability, but collagen plays a pivotal role, as it is able to promote both platelet adhesion and aggregation. However, also other tested substrates elicit good platelet adhesion at different shear stress levels.
The platform used allows to determine the platelet adhesion and aggregation rate that characterizes each protein substrate, at each shear stress level. This leads to an important result: the effects of different events on platelet activity can be tested on the most suitable substrates for the phenomena that needs to be investigated.

High PDMP levels represent pathological conditions, so the effect of these high levels was assessed by generating and introducing a controlled quantity of PDMPs in hirudin-anticoagulated WB. The obtained effect is a change in platelet activity, resulting in the reduction of platelet aggregation on the collagen substrate. A hypothesis was made: flowing platelets adhere to circulating microparticles, determining the presence of circulating activated microaggregates that, in vivo, could reach microvessels causing microthrombosis or accumulate in organs causing organ failure.
What was not assessed is the effect of thrombin on PDMP activity; as a next step, experiments could be performed using a different kind of anticoagulant that does not inhibit thrombin formation. As a further step, the tested blood could be collected and analyzed using flow cytometry, to investigate the presence of the PDMP-generated microaggregates, to understand if this hypothesis is verified or if PDMPs just alter platelet activity reducing platelet aggregation.

Moreover, for a better understanding of the effect of high PDMP levels on platelet activity, experiments could be also conducted using the other protein substrates, to verify if the results are coherent with the one found with the collagen coated channels.

The proposed method to assess platelet activity, however, is highly operator dependent, time consuming, and involves the use of a fluorescent microscope, which is expensive and is only found in specialized laboratories. An effort should be made in trying to reduce the operator dependent operations, such as the image postprocessing. A change in the MATLAB code could be made to avoid the manual thresholding of the images. Also the microfluidic chip fabrication process could be automatized, by using 3D printing techniques that allow obtaining a device with the required features, such as micro-stereolithography (μSLA) or two-photon polymerization (TPP).

The preliminary tests for the designing of a bedside POC device for the assessment of platelet activity were presented. Overall, the results achieved so far have a good potential in the POC designing process, but further steps need to be taken.
The first aim was proving the ultimate correlation between the pressure increase inside the microchannels and the channel occlusion caused by thrombus formation. The found correlation could be definitely improved by using a higher quality confocal microscope, that would allow more precise evaluations of the thrombi volume, even of big thrombi (without the limit on the maximum admissible thrombus height), enabling, hence, more precise measurements of the channel occlusion percentage. The potential issue of the too high flow rate to rinse the channels after the test can be easily overcome by reducing the flow rate, to avoid the thrombi in the channel to be washed away.
Moreover, it would also be useful to perform experiments at venous shear stress. The 13.5 dyne/cm^2 shear stress was not tested as it generates small pressure variations that are not detected by the pressure sensor; as a further step, to obtain information about pressure increase also at low shear stress, a different pressure sensor, that can capture even little pressure variations, need to be used (as the Amphenol ELV series pressure sensor (Amphenol, Wallingford, CT, USA)).
Concerning the assessment of the different platelet activity between healthy subjects and covid patients, the low number of tests performed for each donor group may be the reason why no difference was highlighted by statistical analysis; therefore, as a next step,

more experiments should be performed, to further investigate the different platelet activity caused by Covid-19 and the relative pressure measurements. Moreover, it has been showed that most relevant changes in platelet activity occur at a venous shear stress, so, as previously mentioned, by changing the pressure sensor with a higher resolution one, changes in pressure measurements caused by Covid-19 could also be assessed at low shear stress.

The presented work had a twofold aim: characterizing the platform, and moving towards an easy-to-use, label-free system, with a small footprint, to evaluate platelet activity from pressure measurements.

A protocol was defined to assess the effects of shear stresses and protein substrates on platelet activation.

This microfluidic platform, in combination with different test variables (i.e. shear stress and protein substrate) is a tool that was used to investigate the underlying mechanisms of microthrombosis: PDMPs were introduced to the blood, allowing to take a closer look to one of the aspects of cardiovascular diseases, platelet disorders, inflammations, the implantation of biomedical devices.

Also, the effect of Covid-19 on platelet adhesion and aggregation was investigated, by comparing results obtained from healthy subjects and covid patients.

The use of a pressure transducer allowed to perform the preliminary tests for the development of a POC device that evaluates platelet function from pressure measurements. The achieved results are the starting point for the development of an inexpensive, user-friendly device for the assessment of platelet activity.

Bibliography

[1] "World Health Organization," [Online]. Available: https://www.who.int/news-room/fact-sheets/detail/cardiovascular-diseases-(cvds).

[2] D. Bluestein, K. B. Chandran, and K. B. Manning, "Towards Non-thrombogenic Performance of Blood Recirculating Devices," Ann Biomed Eng. 2010 Mar;38(3):1236-56. doi: 10.1007/s10439-010-9905-9..

[3] D. J. Angiolillo, L. A. Guzman, T. A. Bass, "Current antiplatelet therapies: Benefits and limitations," *American Heart Journal,* 2008.

[4] R. E. Rumbaut, P. Thiagarajan, "Chapter 1 - Introduction," in *Platelet-Vessel Wall Interactions in Hemostasis and Thrombosis*, 2010.

[5] M. A. D., Platelets-Second Edition, Academic press, 2007.

[6] R. E. Rumbaut, P. Thiagarajan, "Chapter 2: General Characteristics of Platelets," in *Platelet-Vessel Wall Interactions in Hemostasis and Thrombosis*, 2010; PMID: 21452436; DOI: 10.4199/C00007ED1V01Y201002ISP004.

[7] M.H. Periayah, A.S. Halim, A.Z. Mat Saad, "Mechanism Action of Platelets and Crucial Blood Coagulation Pathways in Hemostasis," *International Journal of Hematology-Oncology and Stem Cell Research,* vol. 11, no. 4, 1 October 2017; PMID: 29340130; PMCID: PMC5767294..

[8] A. J. Gale, "Current Understanding of Hemostasis," Toxicol Pathol. 2011 Jan;39(1):273-80. doi: 10.1177/0192623310389474. PMID: 21119054..

[9] R. E. Rumbaut, P. Thiagarajan, "Chapter 3: Platelet Adhesion to Vascular Walls," in *Platelet-Vessel Wall Interactions in Hemostasis and Thrombosis*, PMID: 21452436; Bookshelf ID: NBK53450; DOI: 10.4199/C00007ED1V01Y201002ISP004.

[10] Allison P. Wheeler, David Gailani, "The Intrinsic Pathway of Coagulation as a Target for Antithrombotic Therapy," *Hematol Oncol Clin North Am. ,* vol. 30, no. 5, pp. 1099-1114, 2016 Oct; doi: 10.1016/j.hoc.2016.05.007. PMID: 27637310;.

[11] R. E. Rumbaut, P. Thiagarajan, "Chapter 6: Arterial, Venous, and Microvascular Hemostasis/Thrombosis," in *Platelet-Vessel Wall Interactions in Hemostasis and Thrombosis*, 2010.

[12] P. Prandoni, "Venous and arterial thrombosis: Two aspects of the same disease?," *Clin Epidemiol,* vol. 1, 2009; doi: 10.2147/clep.s4780.

[13] A. Delluc, K. Lacut, M. A. Rodger, "Arterial and venous thrombosis: What's the link? A narrative review," *Thrombosis Research,* vol. 191, pp. 97-201, July 2020; https://doi.org/10.1016/j.thromres.2020.04.035.

[14] M. Weber, H. Steinle, S. Golombek, L. Hann, C. Schlensak,, "Blood-Contacting Biomaterials: In Vitro Evaluation of the Hemocompatibility," *Frontiers in Bioengineering and Biotechnology,* vol. 6, 16 July 2018; doi: 10.3389/fbioe.2018.00099.

[15] M. N. D. Di Minno, A. Guida, M. Camera, S. Colli, G. Di Minno, E. Tremoli, "Overcoming limitations of current antiplatelet drugs: A concerted effort for more profi table strategies of intervention," *Annals of Medicine, 2011; 43: 531–544 DOI: 10.3109/07853890.2011.582137.*

[16] Bray MA, Sartain SE, Gollamudi J, Rumbaut RE., "Microvascular thrombosis: experimental and clinical implications," *Transitional Research,* 2020; https://doi.org/10.1016/j.trsl.2020.05.006.

[17] Puhr-Westerheide D., Schink S.J., Fabritius M., Mittmann, Hessenauer M.E.T., Pircher J., Zuchtriegel G., Uhl B., Holzer M., Massberg S., Krombach F. ,Reichel C.A., "Neutrophils promote venular thrombosis by shaping the rheological environment for platelet aggregation," *Scientific Reports,* 2019.

[18] T. Manon-Jensen, N.G. Kjeld, M.A. Karsda, "Collagen-mediated hemostasis," *Journal of Thrombosis and Haemostasis,* vol. 14, pp. 438-488, 2016.

[19] W. Bergmeier, R. O. Hynes, "Extracellular Matrix Proteins in Hemostasis and Thrombosis," *Cold Spring Harbor Perspectives Biology,* vol. 4, no. 2, 2012; doi: 10.1101/cshperspect.a005132.

[20] A. J. Zollinger, M. L. Smith, "Fibronectin, the extracellular glue," *Matrix Biology,* 2017; https://doi.org/10.1016/j.matbio.2016.07.011.

[21] Wing S To, Kim S Midwood, "Plasma and cellular fibronectin: distinct and independent functions during tissue repair," *Fibrogenesis and Tissue Repair,* vol. 4, 2011; https://doi.org/10.1186/1755-1536-4-21.

[22] S. Beurner, H. F.G. Heijnen, M. J.W. IJsseldijk, E. Orlando, P. G. de Groot, J. J. Sixrna, "latelet Adhesion to Fibronectin in Flow: The Importance of von Willebrand Factor and Glycoprotein Ib," *The American Society of Hematology,* 1995; https://doi.org/10.1182/blood.V86.9.3452.bloodjournal8693452.

[23] R. Hallmann, N. Horn, M. Selg, O. Wendler, F. Pausch, L. M. Sorokin, "Expression and function of laminins in the embryonic and mature vasculature," *Physiological reviews,* 2005; https://doi.org/10.1152/physrev.00014.2004.

[24] Aumailley M, Smyth N., "The role of laminins in basement membrane function," *Journal of anatomy,* 1998; doi: 10.1046/j.1469-7580.1998.19310001.x.

[25] O. Inoue, K. Suzuki-Inoue, O. J. T. McCarty, M. Moroi, Z. M. Ruggeri, T. J. Kunicki, Y. Ozaki, S. P. Watson, "Laminin stimulates spreading of platelets through integrin α6β1–dependent activation of GPVI," *Hemostasis, thrombosis and vascular biology,* 2006; https://doi.org/10.1182/blood-2005-06-2406.

[26] D. Tousoulis, N. Papageorgiou, E. Androulakis, A. Briasoulis, C. Antoniades, C. Stefanadis, "Fibrinogen and cardiovascular disease: Genetics and biomarkers".

[27] Schvartz I., Seger D., Shaltiel S., "Vitronectin," *The International Journal of Biochemistry & Cell Biology,* vol. 31, no. 5, pp. 539-544, https://doi.org/10.1016/S1357-2725(99)00005-9.

[28] D. Varga-Szabo, I. Pleines, B. Nieswandt, "Cell Adhesion Mechanisms in Platelets," *Arteriosclerosis, Thrombosis, and Vascular Biology,* vol. 38, no. 3, 2008; https://doi.org/10.1161/ATVBAHA.107.150474.

[29] P. R. M. Siljander, "Platelet-derived microparticles - an updated perspective," *Thrombosis research,* 2011; DOI: 10.1016/S0049-3848(10)70152-3.

[30] J. Kailashiya, "Platelet-derived microparticles analysis: Techniques, challenges and recommendations," *Analytical Biochemistry,* vol. 546, pp. 78-85, 2018; https://doi.org/10.1016/j.ab.2018.01.030.

[31] Zhi-Ting Wang, Zi Wang, Yan-Wei Hu, "Possible roles of platelet-derived microparticles in atherosclerosis," *Atherosclerosis,* vol. 248, pp. 10-16, 2016; https://doi.org/10.1016/j.atherosclerosis.2016.03.004.

[32] X Dai, X Cao, Q Jiang, B Wu, T Lou, Y Shao, Y Hu, Q Lan, "Neurological complications of COVID-19," *QJM: An International Journal of Medicine,* 2022; https://doi.org/10.1093/qjmed/hcac272.

[33] Mui LW, Lau JF, Lee HK., "Thromboembolic complications of COVID-19," *Emergency Radiology,* 2021; doi: 10.1007/s10140-020-01868-0.

[34] Malas MB, Naazie IN, Elsayed N, Mathlouthi A, Marmor R, Clary B., "Thromboembolism risk of COVID-19 is high and associated with a higher risk of mortality: A systematic review and meta-analysis," *EClinicalMedicine,* 2020; doi: 10.1016/j.eclinm.2020.100639.

[35] McFadyen J.D., Stevens H., Peter K., "The Emerging Threat of (Micro)Thrombosis in COVID-19 and Its Therapeutic Implications," *Circulation Research ,* 2020; https://doi.org/10.1161/CIRCRESAHA.120.317447.

[36] Sastry S, Cuomo F, Muthusamy J., "COVID-19 and thrombosis: The role of hemodynamics," *Thrombosis research,* 2022; doi: 10.1016/j.thromres.2022.02.016.

[37] Hernandez Acosta RA, Esquer Garrigos Z, Marcelin JR, Vijayvargiya P., "COVID-19 Pathogenesis and Clinical Manifestations," *Infectious disease clinics of North America,* 2022;doi: 10.1016/j.idc.2022.01.003.

[38] J. A. Páramo, "Microvascular thrombosis and clinical implications," *Medicina Clínica,* 2021; https://doi.org/10.1016/j.medcle.2020.12.025.

[39] Choi J.L., Li S., Han J.Y., "Platelet Function Tests: A Review of Progresses in Clinical Application," *BioMed Research International,* 2014; doi: 10.1155/2014/456569.

[40] Van Werkum JW, Hackeng CM, de Korte FI, Verheugt FW, Ten Berg JM., "Point-of-care platelet function testing in patients undergoing PCI: between a rock and a hard place," *Netherlands Heart Journal,* vol. 15, no. 9, pp. 299-305, 2007; DOI: 10.1007/bf03086004 .

[41] Paniccia R., Priora R., Liotta A.A., Abbate R., "Platelet function tests: a comparative review," *Vascular Health and risk management,* 2015; doi: 10.2147/VHRM.S44469.

[42] Andrew P. Russeau; Hacen Vall; Biagio Manna., "Bleeding Time," in *StatPearls Publishing*.

[43] Peterson P, Hayes TE, Arkin CF, Bovill EG, Fairweather RB, Rock WA Jr, Triplett DA, Brandt JT. , "The preoperative bleeding time test lacks clinical benefit: College of American Pathologists' and American Society of Clinical Pathologists' position article," *Archives of Surgery ,* 1998; doi: 10.1001/archsurg.133.2.134..

[44] Rodgers RP, Levin J., "A critical reappraisal of the bleeding time.," *Seminars in Thrombosis and Hemostasis,* 1990; doi: 10.1055/s-2007-1002658..

[45] A. Cuker, "Light Transmission Aggregometry," *The Hematologist,* 2014; https://doi.org/10.1182/hem.V11.2.2555.

[46] "Platelet Function Testing-Light Transmission Aggregometry [LTA]," [Online]. Available: Practical-Haemostasis.com.

[47] Alessi MC, Sié P, Payrastre B., "Strengths and Weaknesses of Light Transmission Aggregometry in Diagnosing Hereditary Platelet Function Disorders," *J Clin Med,* 2020; doi: 10.3390/jcm9030763..

[48] Le Blanc J, Mullier F, Vayne C, Lordkipanidzé M., "Advances in Platelet Function Testing-Light Transmission Aggregometry and Beyond," *Journal of clinical medicine,* 2020; DOI: 10.3390/jcm9082636.

[49] "Platelet Function Testing:Impedance Platelet Aggregometry," [Online]. Available: Practical-Haemostasis.com.

[50] Davies GR, Mills GM, Lawrence M, Battle C, Morris K, Hawkins K, Williams PR, Davidson S, Thomas D, Evans PA., "The Role of Whole Blood Impedance Aggregometry and Its Utilisation in the Diagnosis and Prognosis of Patients with Systemic Inflammatory Response Syndrome and Sepsis in Acute Critical Illness," *PLoS One,* 2014; doi: 10.1371/journal.pone.0108589..

[51] Adamzik M., Görlinger K., Peters J., Hartmann M., "Whole blood impedance aggregometry as a biomarker for the diagnosis and prognosis of severe sepsis," *Critical Care,* 2012.

[52] G. A. Fritsma, "Platelet function testing: aggregometry and lumiaggregometry," *Clinical Laboratory Science,* 2007.

[53] R. Knoefler, G. Siegert, E. Kuhlisch & G. Weissbach , "Diagnostics of Platelet Function Disorders by Lumi-Aggregometry — Results and Comparison of Methods," *Hemophilia Symposium,* 2005.

[54] Trampuš-Bakija A, Jazbec J, Faganel-Kotnik B., "Platelet lumiaggregation testing: Reference intervals and the effect of acetylsalicylic acid in healthy adults," *Journal of Medical Biochemistry,* 2020; doi: 10.5937/jomb0-24690.

[55] "Helena Laboratories - Plateletworks: Rapid Platelet Function Screening," [Online].

[56] Breet NJ, van Werkum JW, Bouman HJ, Kelder JC, Ruven HJ, Bal ET, Deneer VH, Harmsze AM, van der Heyden JA, Rensing BJ, Suttorp MJ, Hackeng CM, ten Berg JM. , "Comparison of platelet function tests in predicting clinical outcome in patients undergoing coronary stent implantation," *JAMA,* 2010; doi: 10.1001/jama.2010.181. .

[57] "A PRACTICAL GUIDE TO HAEMOSTASIS: 1. Thromboelastography - TEG® 2. Rotational Thromboelastometry - ROTEM®," [Online]. Available: Practical-Haemostasis.com.

[58] Whiting D., DiNardo J. A., "TEG and ROTEM: Technology and clinical applications," *American Journal of Hematology,* 2013; https://doi.org/10.1002/ajh.23599Citations: 381.

[59] Sankarankutty A., Nascimento B., Teodoro da Luz L., Rizoli S., "TEG and ROTEM in trauma: similar test but different results?," *World Journal of Emergency Surgery,* 2012; .

[60] Wikkelsoe AJ, Afshari A, Wetterslev J, Brok J, Moeller AM. , "Monitoring patients at risk of massive transfusion with Thrombelastography or Thromboelastometry: a systematic review," *Acta Anaesthesiologica Scandinavica,* 2011; doi: 10.1111/j.1399-6576.2011.02534.x. .

[61] Cannata, G.; Mariotti Zani, E.; Argentiero, A.; Caminiti, C.; Perrone, S.; Esposito, S. , "TEG® and ROTEM® Traces: Clinical Applications of Viscoelastic Coagulation Monitoring in Neonatal Intensive Care Unit," *Diagnostics,* 2021; https://doi.org/10.3390/diagnostics11091642.

[62] Korpallová B, Samoš M, Bolek T, Škorňová I, Kovář F, Kubisz P, Staško J, Mokáň M. , "Role of Thromboelastography and Rotational Thromboelastometry in the Management of Cardiovascular Diseases," *Clinical and Applied Thrombosis/Hemostasis,* 2018; doi: 10.1177/1076029618790092.

[63] D. A. Gorog, Y. H. Jeong, "Platelet Function Tests: Why They Fail to Guide Personalized Antithrombotic Medication," *Journal of the American Heart Association,* 2015; https://doi.org/10.1161/JAHA.115.002094.

[64] M. Franchini, "The platelet-function analyzer (PFA-100w) for evaluating primary hemostasis," *Hematology,* 2013; https://doi.org/10.1080/10245330400026097..

[65] E. J. Favaloro, "The utility of the PFA-100 in the identification of von Willebrand disease: a concise review," *Seminars in thrombosis and hemostasis,* 2006; DOI: 10.1055/s-2006-947869..

[66] Hayward CP, Harrison P, Cattaneo M, Ortel TL, Rao AK; Platelet Physiology Subcommittee of the Scientific and Standardization Committee of the International Society on Thrombosis and Haemostasis, "Platelet function analyzer (PFA)-100® closure time in the evaluation of platelet disorders and platelet function," *Journal of Thrombosis and Haemostasis.,* 2006; https://doi.org/10.1111/j.1538-7836.2006.01771.x.

[67] Savion N, Varon D., "Impact--the cone and plate(let) analyzer: testing platelet function and anti-platelet drug response.," *Pathophysiology of haemostasis and thrombosis,* 2006; DOI: 10.1159/000093548.

[68] Kenet, Lubetsky, Shenkman, Tamarin, Dardik, Rechavi, Barzilai, Martinowitz, Savion, Varon, "Cone and platelet analyser (CPA): a new test for the prediction of bleeding among thrombocytopenic patients," *British Journal of Haematology,* 2001; https://doi.org/10.1046/j.1365-2141.1998.00690.x.

[69] Spectre G., Brill A., Gural A., Shenkman B., Turetzky N., Savion N., Varon D., "Application of the Cone and Plate(let) Analyzer as a Point-of-Care Method for Monitoring Anti-Platelet Therapy," *Blood,* 2004; http://doi.org/10.1182/blood.V104.11.4071.4071.

[70] Yamamoto J, Inoue N, Otsui K, Ikarugi H, Shimizu M, Yamamoto S, Murakami M, Ijiri Y, Sakariassen KS. , "A point-of-care global thrombosis test measuring occlusion time and endogenous lysis time may indicate thrombotic status," *Future Science OA,* 2019; doi: 10.2144/fsoa-2019-0052.

[71] M. Murakami, K. Otsui, Y. Ijiri, M. Shimizu, H. Ikarugi, W. Shioyama, J. Yamamoto , K. S. Sakariassen, "Global thrombosis test for assessing thrombotic status and efficacy of antithrombotic diet and other conditions," *Future Science OA,* 2022; https://doi.org/10.2144/fsoa-2021-0086.

[72] "t-tas.info," [Online]. Available: https://www.t-tas.info/index.html.

[73] M. K.M., "Flow Cytometry: An Overview," *Curr Protoc Immunol.,* 2018; doi: 10.1002/cpim.40.

[74] M. D. Linden, "Platelet Flow Cytometry," in *Methods in Molecular Biology* , 2013.

[75] "Platelet Function Testing: Flow Cytometry," [Online]. Available: Practical-Haemostasis.com.

[76] Rondina MT, Grissom CK, Men S, Harris ES, Schwertz H, Zimmerman GA, Weyrich AS. , "Whole Blood Flow Cytometry Measurements of In Vivo Platelet Activation in Critically-Ill Patients are Influenced by Variability in Blood Sampling Techniques," *Thrombosis Research,* 2012; doi: 10.1016/j.thromres.2011.11.031.

[77] M. A., "Platelet function tests and flow cytometry to monitor antiplatelet therapy," *Seminars in Thrombosis and Hemostasis ,* 2005; doi: 10.1055/s-2005-916672. .

[78] J. Pihl, J. Sinclair, M. Karlsson, O. Orwar, "Microfluidics for cell-based assays," *Materials Today,* 2005; https://doi.org/10.1016/S1369-7021(05)71224-4.

[79] D. D. Nalayanda, M. Kalukanimuttam, D. W. Schmidtke, "Micropatterned surfaces for controlling cell adhesion and rolling under flow," *Biomedical Microdevices ,* 2007; https://doi.org/10.1007/s10544-006-9022-6.

[80] J. J. Sixma, K. S. Sakariassen, N. H. Beeser-Visser, M. Ottenhof-Rovers, P. A. Bolhuis, "Adhesion of Platelets to Human Artery Subendothelium: Effect of Factor VIII–von Willebrand Factor of Various Multimeric Composition," *Blood,* 1984; https://doi.org/10.1182/blood.V63.1.128.128.

[81] J. Mustard, "The Gordon Wilson lecture: function of blood platelets and their role in thrombosis.," *rans Am Clin Climatol Assoc.,* 1976;87:104-27. PMID: 785767; .

[82] S. A. Santoro, L. W. Cunningham, "Fibronectin and the multiple interaction model for platelet-collagen adhesion.," *Proc Natl Acad Sci U S A. ,* 1979; doi: 10.1073/pnas.76.6.2644.

[83] J. D. Hellums, D. M. Peterson, N. A. Stathopoulos, J. L. Moake & T. D. Giorgio , "Studies on the Mechanisms of Shear-Induced Platelet Activation," *Cerebral Ischemia and Hemorheology ,* 1987; https://doi.org/10.1007/978-3-642-71787-1_8.

[84] Kita A, Sakurai Y, Myers DR, Rounsevell R, Huang JN, Seok TJ, Yu K, Wu MC, Fletcher DA, Lam WA., "Microenvironmental Geometry Guides Platelet Adhesion and Spreading: A Quantitative Analysis at the Single Cell Level," *PLoS One.,* 2011; doi: 10.1371/journal.pone.0026437.

[85] Ciciliano JC, Tran R, Sakurai Y, Lam WA. , "The Platelet and the Biophysical Microenvironment: Lessons from Cellular Mechanics," *Thrombosis research ,* 2014; doi: 10.1016/j.thromres.2013.12.037.

[86] R. R. Hansen, A. R. Wufsus, S. T. Barton, A. A. Onasoga, R. M. Johnson-Paben, K. B. Neeves, "High content evaluation of shear dependent platelet function in a microfluidic flow assay," *National Institute of Health,* 2013; doi:10.1007/s10439-012-0658-5..

[87] Herbig BA, Yu X, Diamond SL., "Using microfluidic devices to study thrombosis in pathological blood flows," *Biomicrofluidics,* 2018; doi: 10.1063/1.5021769.

[88] Maloney SF, Brass LF, Diamond SL., "P2Y12 or P2Y1 inhibitors reduce platelet deposition in a microfluidic model of thrombosis while apyrase lacks efficacy under flow conditions," *Integrative Biology (Camb).,* 2010; doi: 10.1039/b919728a.

[89] F. Akther, J. Zhang, H. Tran, H. Fallahi, H. Adelnia, H.P. Phan, N.T. Nguyen, H.T. Ta, "Atherothrombosis-on-Chip: A Site-Specific Microfluidic Model for Thrombus Formation and Drug Discovery," *Advanced Biology,* 2022; https://doi.org/10.1002/adbi.202101316.

[90] E. Gutierrez, B. G. Petrich, S. J. Shattil, M. H. Ginsberg, A. Groisman, A. Kasirer-Friede, "Microfluidic devices for studies of shear-dependent platelet adhesion," *Lab on a Chip,* 2008; doi: 10.1039/b804795b..

[91] Neeves KB, Onasoga AA, Hansen RR, Lilly JJ, Venckunaite D, Sumner MB, Irish AT, Brodsky G, Manco-Johnson MJ, Di Paola JA, "Sources of variability in platelet

accumulation on type 1 fibrillar collagen in microfluidic flow assays," *PLoS ONE 8(1): e54680. doi:10.1371/journal.pone.0054680,* 2013.

[92] Tunströmer K, Faxälv L, Boknäs N, Lindahl TL., "Quantification of Platelet Contractile Movements during Thrombus Formation," *Thrombosis and Haemostasis,* 2018; doi: 10.1055/s-0038-1668151.

[93] Montague S. J., Lim Y.J., Lee W. M., Gardiner E. E., "Imaging Platelet Processes and Function—Current and Emerging Approaches for Imaging in vitro and in vivo," *Frontiers in Immunology,* 2020; https://doi.org/10.3389/fimmu.2020.00078.

[94] de Witt SM, Swieringa F, Cavill R, Lamers MM, van Kruchten R, Mastenbroek T, Baaten C, Coort S, Pugh N, Schulz A, Scharrer I, Jurk K, Zieger B, Clemetson KJ, Farndale RW, Heemskerk JW, Cosemans JM. , "Identification of platelet function defects by multi-parameter assessment of thrombus formation," *Nature Communications,* 2014; doi: 10.1038/ncomms5257.

[95] K. Hosokawa, T. Ohnishi, T. Kondo, M. Fukasawa, T. Koide, I. Maruyama, K. A. Tanaka, "A novel automated microchip flow-chamber system to quantitatively evaluate thrombus formation and antithrombotic agents under blood flow conditions," *Journal of Thrombosis and Haemostasis,* 2011; https://doi.org/10.1111/j.1538-7836.2011.04464.x.

[96] Roest M, Reininger A, Zwaginga JJ, King MR, Heemskerk JW; Biorheology Subcommittee of the SSC of the ISTH, "Flow chamber-based assays to measure thrombus formation in vitro: requirements for standardization," *Journal of Thrombosis and haemostasis,* 2011; https://doi.org/10.1111/j.1538-7836.2011.04492.x.

[97] "Point of care testing (POCT) devices," Ibsen Photonics, [Online]. Available: https://ibsen.com/industries/healthcare/point-of-care-testing-devices/.

[98] T. Mistral, Y. Boué, J.L. Bosson, P. Manhes, J. Greze, J. Brun, P. Albaladejo, J.F. Payen, P. Bouzat, "Performance of point-of-care international normalized ratio measurement to diagnose trauma-induced coagulopathy," *Scandinavian Journal of Trauma, Resuscitation and Emergency Medicine,* 2017; DOI 10.1186/s13049-017-0404-y.

[99] A. H. A. M. E. J. Frenkel, "ELECTROCHEMICAL SYSTEM FOR DETERMINING BLOOD COAGULATION TIME". US Patent USOO635263OB1, 5 March 2002.

[100] "Coag-Sense," [Online].

[101] Arline K., Rodriguez C., Sanchez K., "Reliability of Point-of-Care International Normalized Ratio Measurements in Various Patient Populations," *Point of Care: The Journal of Near-Patient Testing & Technology ,* 2020; DOI: 10.1097/POC.0000000000000197.

[102] M. Siman-Tov, "Novel Device May Provide Rapid POC Assessment of Clot Ability," LabMedica, 2016.

[103] Italiano JE Jr, Mairuhu AT, Flaumenhaft R. , "Clinical Relevance of Microparticles from Platelets and Megakaryocytes," *Curr Opin Hematol,* 2010; doi: 10.1097/MOH.0b013e32833e77ee.

[104] F. Chen, Z. Liao, D. Peng, L. Han, "Role of Platelet Microparticles in Blood Diseases: Future Clinical Perspectives," *Annals of Clinical & Laboratory Science,* 2019.

[105] Michelsen AE, Wergeland R, Stokke O, Brosstad F., "Development of a time-resolved immunofluorometric assay for quantifying platelet-derived microparticles in human plasma," *Thromb Res.,* 2006; doi: 10.1016/j.thromres.2005.05.024.

[106] H.S. LEONG, T.J. PODOR, B. MANOCHA, J.D. LEWIS, "Validation of flow cytometric detection of platelet microparticles and liposomes by atomic force microscopy," *Journal of Thrombosis and Haemostasis,* 2011; https://doi.org/10.1111/j.1538-7836.2011.04528.x.

[107] Sabrkhany S, Kuijpers MJE, Knol JC, Olde Damink SWM, Dingemans AC, Verheul HM, Piersma SR, Pham TV, Griffioen AW, Oude Egbrink MGA, Jimenez CR., "Exploration of the platelet proteome in patients with early-stage cancer," *Journal of Proteomics,* 2018; doi: 10.1016/j.jprot.2018.02.011.

[108] Michelsen AE, Brodin E, Brosstad F, Hansen JB., "Increased level of platelet microparticles in survivors of myocardial infarction," *Lab Invest.,* 2008; doi: 10.1080/00365510701794957.

[109] Boulanger C. M., Amabile N., Tedgui A., "Circulating Microparticles-A Potential Prognostic Marker for Atherosclerotic Vascular Disease," *Hypertension,* 2006; https://doi.org/10.1161/01.HYP.0000231507.00962.b5.

[110] Ohtsuka M, Sasaki K, Ueno T, Seki R, Nakayoshi T, Koiwaya H, Toyama Y, Yokoyama S, Mitsutake Y, Chibana H, Itaya N, Okamura T, Imaizumi T., "Platelet-derived microparticles augment the adhesion and neovascularization capacities of circulating angiogenic cells obtained from atherosclerotic patients," *Atherosclerosis,* 2013; doi: 10.1016/j.atherosclerosis.2013.01.040.

[111] Nazari M, Javandoost E, Talebi M, Movassaghpour A, Soleimani M. , "Platelet Microparticle Controversial Role in Cancer," *Adv Pharm Bull.,* 2021; doi: 10.34172/apb.2021.005.

[112] Burnouf T., Goubran H. A., Chou M.L., Devos D., Radosevic M., "Platelet microparticles: Detection and assessment of their paradoxical functional roles in disease and regenerative medicine," *Blood Reviews,* 2014; https://doi.org/10.1016/j.blre.2014.04.002.

[113] Mause SF, Ritzel E, Liehn EA, Hristov M, Bidzhekov K, Müller-Newen G, Soehnlein O, Weber C., "Platelet microparticles enhance the vasoregenerative potential of angiogenic early outgrowth cells after vascular injury," *Circulation,* 2010; DOI: 10.1161/CIRCULATIONAHA.109.909473.

[114] Iba T, Levy JH, Levi M, Thachil J., "Coagulopathy in COVID-19," *Journal of Thrombosis and Haemostasis,* 2020; doi: 10.1111/jth.14975.

[115] Ercan H., Schrottmaier W. C., Pirabe A., Schmuckenschlager A., Pereyra D., Santol J., Pawelka E., Traugott M. T., Schörgenhofer C., Seitz T., Karolyi M., Yang J.W., Jilma B., Zoufaly A., Assinger A., Zellner M., "Platelet Phenotype Analysis of COVID-19 Patients Reveals Progressive Changes in the Activation of Integrin αIIbβ3, F13A1, the SARS-CoV-2 Target EIF4A1 and Annexin A5," *Frontiers in Cardiovascular Medicine,* 2021; https://doi.org/10.3389/fcvm.2021.779073.

[116] Schrottmaier WC, Pirabe A, Pereyra D, Heber S, Hackl H, Schmuckenschlager A, Brunnthaler L, Santol J, Kammerer K, Oosterlee J, Pawelka E, Treiber SM, Khan AO, Pugh M, Traugott MT, Schörgenhofer C, Seitz T, Karolyi M, Jilma B, Rayes J, Zoufaly A, Assinger , "Platelets and Antiplatelet Medication in COVID-19-Related Thrombotic Complications," *Frontiers in Cardiovascular Medicine,* 2022; https://doi.org/10.3389/fcvm.2021.802566.

[117] Schrottmaier WC, Pirabe A, Pereyra D, Heber S, Hackl H, Schmuckenschlager A, Brunnthaler L, Santol J, Kammerer K, Oosterlee J, Pawelka E, Treiber SM, Khan AO, Pugh M, Traugott MT, Schörgenhofer C, Seitz T, Karolyi M, Jilma B, Rayes J, Zoufaly

A, Assinger , "Adverse Outcome in COVID-19 Is Associated With an Aggravating Hypo-Responsive Platelet Phenotype.," *Frontiers in Cardiovascular Medicine,* 2021; https://doi.org/10.3389/fcvm.2021.795624.

[118] Branchford BR, Ng CJ, Neeves KB, Di Paola J., "Microfluidic technology as an emerging clinical tool to evaluate thrombosis and hemostasis," *Thromb Res. 136(1):13-9. doi: 10.1016/j.thromres.2015.05.012. PMID: 26014643; PMCID: PMC4910695.,* 2015 Jul.

[119] De Witt SM, Swieringa F, Cavill R, Lamers MM, van Kruchten R, Mastenbroek T, Baaten C, Coort S, Pugh N, Schulz A, Scharrer I, Jurk K, Zieger B, Clemetson KJ, Farndale RW, Heemskerk JW, Cosemans JM, "Identification of platelet function defects by multi-parameter assessment of thrombus formation," *Nat Commun 5:4257. doi: 10.1038/ncomms5257. PMID: 25027852; PMCID: PMC4109023,* 2014 Jul 16.

[120] Farndale RW, Sixma JJ, Barnes MJ, de Groot PG, "The role of collagen in thrombosis and hemostasis," *Journal of Thrombosis and Haemostasis, 2:561–73,* 2004.

[121] Heemskerk JWM, Sakariassen KS, Zwaginga JJ, Brass LF, Jackson SP, Farndale RW, Biorheology Subcommittee of the SSC of theISTH, "Collagen surfaces to measure thrombus formation under flow: possibilities for standardization," *Journal of Thrombosis and Haemostasis,9: 856–858,* 2011.

[122] Colace TV, Tormoen GW, McCarty OJ, Diamond SL. Microfluidics and coagulation biology, "Microfluidics and Coagulation Biology," *Annu Rev Biomed Eng. 15: 283–303. doi:10.1146/annurev-bioeng-071812-152406.,* 2013.

[123] "PendoTECH," [Online]. Available: https://www.pendotech.com/.

[124] Red Pitaya Company, [Online]. Available: https://redpitaya.com/.

[125] J. W.M. Heemskerk, M. J.E. Kuijpers, I. C.A. Munnix, P. R.M. Siljander, "Platelet Collagen Receptors and Coagulation. A Characteristic Platelet Response as Possible Target for Antithrombotic Treatment," in *Trends in Cardiovascular Medicine*, 2005; https://doi.org/10.1016/j.tcm.2005.03.003, pp. Volume 15, Issue 3, Pages 86-92.

[126] Kee MF, Myers DR, Sakurai Y, Lam WA, Qiu Y., "Platelet Mechanosensing of Collagen Matrices," *PLOSONE DOI:10.1371/journal.pone.0126624,* April 27,2015.

[127] M. Scavone, S. Bozzi, T. Mencarini, G. Podda, M. Cattaneo, A. Redaelli, "Platelet Adhesion and Thrombus Formation in Microchannels: The Effect of Assay-Dependent Variables," *International Journal of Article Molecular Sciences,* vol. doi:10.3390/ijms21030750, January 2020.

[128] Moroi M, Jung SM, Shinmyozu K, Tomiyama Y, Ordinas A, Diaz-Ricart M., "Analysis of platelet adhesion to a collagen-coated surface under flow conditions: the involvement of glycoprotein VI in the platelet adhesion," *Blood,* 1996.

[129] Savage B, Saldívar E, Ruggeri ZM. , "Initiation of platelet adhesion by arrest onto fibrinogen or translocation on von Willebrand factor," *Cell,* 1996; doi: 10.1016/s0092-8674(00)80983-6..

[130] R. Z.M., "Platelet Adhesion under Flow," *Microcirculation,* 2011; doi: 10.1080/10739680802651477.

[131] Chen S, Springer TA. , "Selectin receptor-ligand bonds: Formation limited by shear rate and dissociation governed by the Bell model," *PNAS ,* 2001; doi: 10.1073/pnas.98.3.950. .

[132] Reheman A, Yang H, Zhu G, Jin W, He F, Spring CM, Bai X, Gross PL, Freedman J, Ni H., "Plasma fibronectin depletion enhances platelet aggregation and thrombus formation in mice lacking fibrinogen and von Willebrand factor," *Blood,* 2009; doi: 10.1182/blood-2008-04-148361.

[133] Reheman A, Gross P, Yang H, Chen P, Allen D, Leytin V, Freedman J, Ni H. , "Vitronectin stabilizes thrombi and vessel occlusion but plays a dual role in platelet aggregation," *Journal of Thrombosis and Haemostasis,* 2005; doi: 10.1111/j.1538-7836.2005.01217.x. .

[134] Fay WP, Parker AC, Ansari MN, Zheng X, Ginsburg D. , "Vitronectin Inhibits the Thrombotic Response to Arterial Injury in Mice," *Blood,* 1999; PMID: 10068653.

[135] Konstantinides S, Schäfer K, Thinnes T, Loskutoff DJ., "Plasminogen activator inhibitor-1 and its cofactor vitronectin stabilize arterial thrombi after vascular injury in mice," *Circulation,* 2001; doi: 10.1161/01.cir.103.4.576. .

[136] J.M. Herring, M.A. McMichael, S.A. Smith, "Microparticles in Health and Disease," *Journal of Veterinary Internal Medicine,* 2013; https://doi.org/10.1111/jvim.12128.

[137] Merten M, Pakala R, Thiagarajan P, Benedict CR., "Platelet Microparticles Promote Platelet Interaction With Subendothelial Matrix in a Glycoprotein IIb/IIIa–Dependent Mechanism," *Circulation logo,* 1999; doi: 10.1161/01.cir.99.19.2577.

[138] Roka-Moiia Y., Ammann K., Miller-Gutierrez S., Sheriff J., Bluestein D., Italiano J.E., Flaumenhaft R.C., Slepian M.J., "Shear-Mediated Platelet Microparticles Demonstrate Phenotypic Heterogeneity as to Morphology, Receptor Distribution, and Hemostatic Function," *BioRxiv,* https://doi.org/10.1101/2023.02.08.527675.

[139] Wool GD, Miller JL., "The Impact of COVID-19 Disease on Platelets and Coagulation," *Pathobiology,* 2021; doi: 10.1159/000512007.

[140] Bonora M., Gianiorio T., "Analysis of platelet-derived Microparticles and their role in platelet activation and stimulation under static and dynamic conditions," Master thesis, Politecnico di Milano, 2020.

[141] M.M. ALEMAN, C. GARDINER, P. HARRISON, A.S. WOLBERG, "Differential contributions of monocyte- and platelet-derived microparticles towards thrombin generation and fibrin formation and stability," *Journal of Thrombosis and Haemostasis,* 2011; https://doi.org/10.1111/j.1538-7836.2011.04488.x.

[142] Jevtic S.D., Nazy I., "The COVID Complex: A Review of Platelet Activation and Immune Complexes in COVID-19," *Front. Immunol.,* 2022; https://doi.org/10.3389/fimmu.2022.807934.

[143] Lundström A., Sandén P., Mitroulis I., Van der Meijden P.E.J., "Editorial: Platelet Function in COVID-19," *Frontiers in Cardiovascular Medicine,* 2022; doi: 10.3389/fcvm.2022.912472. .

[144] Longchamp G, Manzocchi-Besson S, Longchamp A, Righini M, Robert-Ebadi H, Blondon M., "Proximal deep vein thrombosis and pulmonary embolism in COVID-19 patients: a systematic review and meta-analysis," *Thrombosis Journal,* 2021; doi: 10.1186/s12959-021-00266-x..

A Fabrication protocol

1. mix PDMS and curing agent (10:1 ratio) in a plastic container and stir for 2 minutes;
2. place the PDMS in the vacuum bell for 15 minutes;
3. pour the PDMS into the molds and place them in the vacuum bell for 15 minutes;
4. place the molds in the oven at 65 °C for two hours or at room temperature overnight;
5. remove the PDMS layers from the molds;
6. cut the chips and punch the inlet and outlet of each channel with a 1.5mm biopsy punch;
7. place the glass coverslip and the PDMS chip, with features facing upwards, on a glass support;
8. put the support inside the Plasma Cleaner and close the door, with the valve in vertical position, pointing downward;
9. switch on the vacuum pump and wait until pressure reaches 200mTorr;
10. move the valve in horizontal position pointing left;
11. wait until pressure reaches 425mTorr, then switch on the Plasma Cleaner machine on “high RF level” for 2 minutes;
12. switch off both the Plasma Cleaner machine and the vacuum pump;
13. move the valve in horizontal position, facing right, to bring back the pressure inside the Plasma Cleaner to the atmospheric one;
14. transfer both the chip and the coverslip under a laminar flow hood;
15. align the PDMS layer and the coverslip and bind them together by applying a gentle pressure around the features (do not press on top of the features) to remove all the air bubbles between the chip and the coverslip;
16. place in the oven at 65 °C for at least 15 minutes to make the bonding permanent.

B Experimental protocol

B.1. Blood preparation

1. collect blood from healthy volunteers;
2. add hirudin (HYPHEN BioMed, Recombinant hirudin, RE120A) to the blood sample for a final concentration of 450 ATU/mL blood;
3. tag the blood sample with fluorescent lipophilic platelet dye DiOC6 (1 µM, Sigma Aldrich) and leave at room temperature for 15 minutes;
4. aliquot the blood in Eppendorf tubes.

B.2. Preparation of microparticles-rich fraction

1. Centrifugate whole blood at 1300 rpm for 15 minutes to get platelet-rich plasma (PRP) and gently collect it with a Pasteur pipette;
2. isolate gel-filtered platelets (GFP) from PRP by gel-chromatography through Sepharose-2B gel-filtration;
3. measure platelet count on the Z1 Particle Counter (Beckman Coulter, Indianapolis, IN);
4. add calcium chloride (2.5 mM CaCl2) to 350 µL of gel-filtrated platelets (GFP, 100000 platelets/µL);
5. PDMP generation sonicating (10s, 50%) 100k GFP
6. centrifuge at 2000rpm for 15 minutes to sediment platelets and obtain PDMP fraction;
7. collect the supernatant containing PDMPs and centrifuge again;

8. collect the supernatant;
9. aliquot the microparticle-rich fraction and freeze at -80°C;
10. add to the blood aliquot (at a ratio blood:PDMPs of 10:1).

Protocol is also shown in Figure B.1.

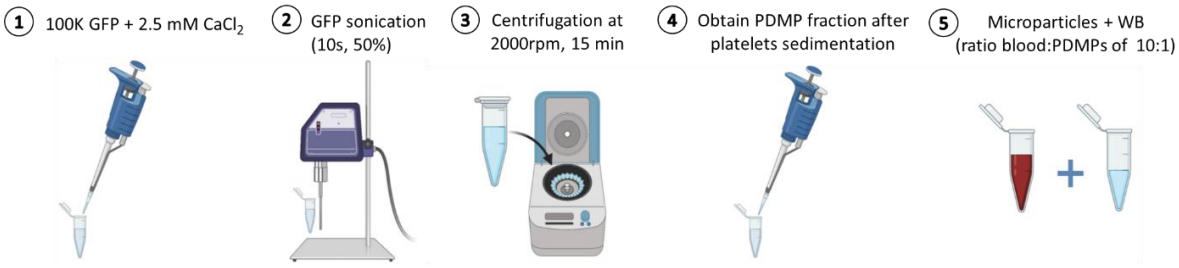

Figure B.1: *PDMPs production protocol.*

B.3. Channel coating with extra cellular matrix proteins

Collagen coating

1. Dilute collagen (Chronolog, product number 385) at the desired concentration with an isotonic glucose solution (ph 2.7);
2. use a pipette to coat 1/3 of the channel introducing 5 µL of collagen from the channel outlet;
3. leave at 4°C overnight;
4. rinse with 50µL of PBS 1x;
5. passivate the channel with BSA diluted in PBS 1x;
6. leave at room temperature for 30 minutes.

Fibrinogen coating

1. Dilute fibrinogen (F3879 Millipore Sigma) at the desired concentration with saline (0.9% NaCl in water);

2. use a pipette to coat 1/3 of the channel introducing 5 µL of fibrinogen from the channel outlet;
3. leave at 4°C overnight;
4. rinse with 50µL of PBS 1x;
5. passivate the channel with BSA diluted in PBS 1x;
6. leave at room temperature for 30 minutes.

Laminin coating

1. Dilute laminin (CC095 Millipore Sigma) at the desired concentration with PBS 1x (ph 7.4);
2. use a pipette to coat 1/3 of the channel introducing 5 µL of vitronectin from the channel outlet;
3. leave at 4°C overnight;
4. rinse with 50µL of PBS 1x;
5. passivate the channel with BSA diluted in PBS 1x;
6. leave at room temperature for 30 minutes.

Fibronectin coating

1. Dilute fibronectin (FIBRP-RO Millipore Sigma) at the desired concentration with PBS 1X (ph 7.4);
2. use a pipette to coat 1/3 of the channel introducing 5 µL of fibronectin from the channel outlet;
3. leave at 4°C overnight;
4. rinse with 50µL of PBS 1x;
5. passivate the channel with BSA diluted in PBS 1x;
6. leave at room temperature for 30 minutes.

Vitronectin coating

1. Dilute vitronectin (CC130 Millipore Sigma) at the desired concentration with PBS 1x (ph 7.4);
2. use a pipette to coat 1/3 of the channel introducing 5 µL of vitronectin from the channel outlet;
3. leave at 4°C overnight;
4. rinse with 50µL of PBS 1x;
5. passivate the channel with BSA diluted in PBS 1x;
6. leave at room temperature for 30 minutes.

Coating protocol is also shown in Figure B.2.

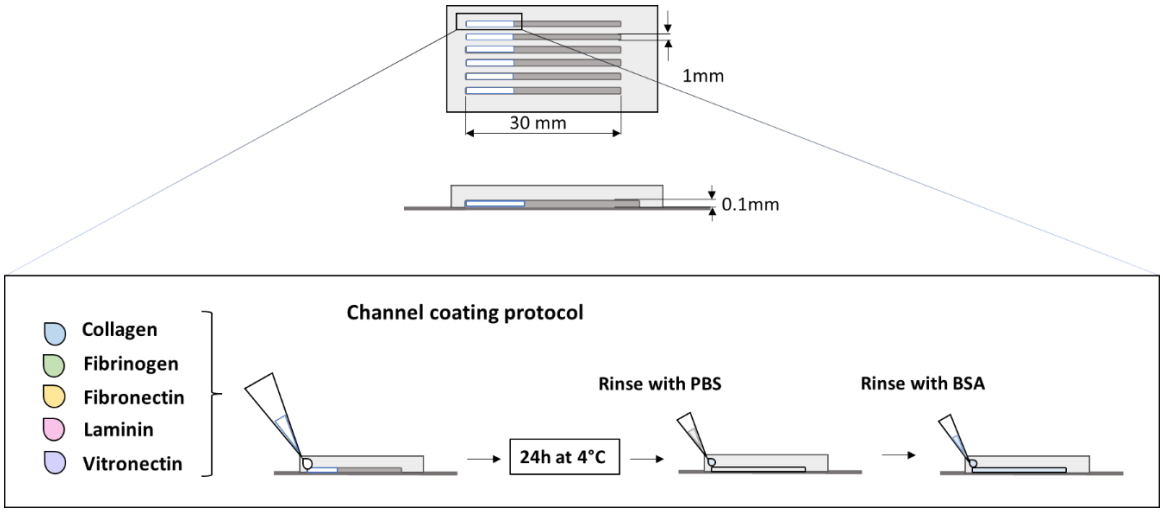

Figure B.2: *Microfluidic device and coating protocol.*

B.4. Experimental protocol for test under flow conditions

1. Connect all the tubes together in the right order to create two circuits: the main one for suction (C1) and the secondary one for PBS washing (C2), as shown in Figure B.3 ;

2. insert a flat needle to the end of both circuits;
3. connect C2 to a Tygon tube, fill it up with PBS and then connect it to the outlet of a channel in the chip, fill the channel up with PBS, insert a second Tygon tubing in the channel inlet and fill it up with PBS, then immerse the end of the tubing in an Eppendorf tube full of PBS;
4. switch the connection of the first Tygon tube from C2 to C1;
5. place the chip and everything that is connected to it under the microscope;
6. set microscope to the correct objective and filter for green fluorescence (FITC);
7. switch the connection of the final Tygon tube from the PBS Eppendorf to the blood Eppendorf;
8. switch off the light and start the test: run blood aspiration and after 4 minutes take pictures of the thrombi formed in the channel;
9. manually stop the pump.

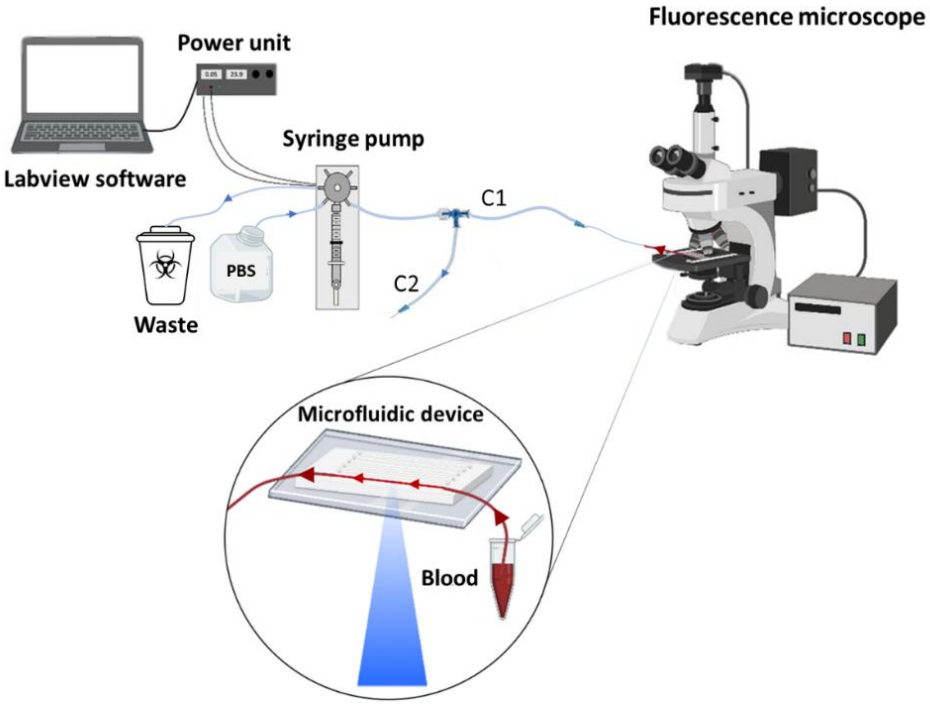

Figure B.3: *Experimental set-up.*

C Matlab code

C.1. Image analysis for thrombus formation under flow

```
function [] = SC_FI_Nth_Ath_Tucson_NO_BG(exp_name)

path = uigetdir;
dirInput = dir(fullfile(path,'*.tif'));
filenames = {dirInput.name}';

for i = 1:length(filenames)
   img = imread([path '\' char(filenames(i,:))]);

   % Crop image
         img = img(0.125*size(img,1) : 0.875*size(img,1), 0.25*size(img,2) :
         0.75*size(img,2));

   % open the modified image
   path2 = uigetdir;
   dirInput2 = dir(fullfile(path2,'*.tif'));
   filenames2 = {dirInput2.name}';

   % crop the modified image
    img_mod = imread([path2 '\' char(filenames2)]);
    img_mod = img_mod(0.125*size(img_mod,1) : 0.875*size(img_mod,1),
    0.25*size(img_mod,2) : 0.75*size(img_mod,2));
   % Convert to binary
   % Otsu method for the modified image
   [level,EM] = graythresh(img_mod);
   imgBW_mod_O = im2bw(img_mod,level);
    imgBW_mod_O = bwareaopen(imgBW_mod_O,37); % Remove pixel clusters smaller
    than platelet area (d=2 um)
```

```
% make image and modified otsu image into matrices of uint16 values
img_int16 = uint16(img);
img_new_mod_0 = img_int16.*uint16(imgBW_mod_0);
img_new_mod_0 = double(img_new_mod_0);
img_new_mod_0(img_new_mod_0==0) = NaN;
% Calculate surface coverage
SC_0(i) = sum(sum(imgBW_mod_0))/size(imgBW_mod_0,1)/size(imgBW_mod_0,2);

% Calculate fluorescence intensity
% evaluate FI of thrombi only NO BACKGROUND
FI_mod = mean(mean(img_new_mod_0,'omitnan'),'omitnan');

% Calculate number of thrombi and mean thrombus area
s_0  = regionprops(imgBW_mod_0, 'Area');
 area_0 = cat(1, s_0.Area);  Nth_0(i) = length(area_0); Ath_0(i) =
 sum(area_0)/Nth_0(i) * 0.0858; % 10x TUCSON

% Plots
% Convert image from gray-scale to greenscale
% Adjust image intensity
grayImage = imadjust(img);
% Convert grayscale to rgb
rgbImage = cat(3, grayImage, grayImage, grayImage);
% Convert rgb to hsv
% Convert rgb to hsv
hsv = rgb2hsv(rgbImage);
% Change hsv value
hsv(:, :, 1) = 0.3;    hsv(:, :, 2) = 1;
% Convert back to rgb
greenImage = uint8(255*hsv2rgb(hsv));

% Plot (Otsu method)
subplot(2,2,1), imshow(grayImage)
subplot(2,2,2), imshow(greenImage), hold on
subplot(2,2,3), imshow(imgBW_mod_0)
subplot(2,2,4), imshow(imgBW_mod_0), hold on
if Nth_0(i) > 0
        s  = regionprops(imgBW_mod_0, 'centroid');
        centroids = cat(1, s.Centroid);
```

```
        plot(centroids(:,1), centroids(:,2),
        'o','MarkerEdgeColor','r','MarkerFaceColor','r','MarkerSize',3);
    end

     sgtitle([exp_name ' - ' num2str(i)],'FontName','Times New
     Roman','FontSize',12,'Fontweight','bold');
    set(gcf,'PaperUnits', 'centimeters');
    set(gcf,'PaperPosition', [0 0 21 14]);
    set(gcf,'PaperSize', [21 14]);
    print(gcf, '-dpng', [path '\' exp_name ' - Otsu - ' num2str(i) '.png']);

    subplot(1,1,1), imshow (imgBW_mod_O)
    sgtitle([exp_name],'FontName','Times New Roman','FontSize',12,'Fontweight','bold');
    set(gcf,'PaperUnits', 'centimeters');
    set(gcf,'PaperPosition', [0 0 14 14]);
    set(gcf,'PaperSize', [14 14]);
    print (gcf, '-dpng', [path '\' exp_name '.png']);
    close all
end

% Save text files with output parameters
fid = fopen([path '\' exp_name ' - Results.txt'],'w');
fprintf(fid,'\n%s\n', exp_name);

fprintf(fid,'\n%s\n', 'Mean FI - NO BACKGROUND [-]');
fprintf(fid,'%4.0f\n', FI_mod);

fprintf(fid,'\n%s\n', 'Surface coverage Otsu [-]');
fprintf(fid,'%4.4f\n', SC_O);

fprintf(fid,'\n%s\n', 'Number of thrombi Otsu [-]');
fprintf(fid,'%4.0f\n', Nth_O);

fprintf(fid,'\n%s\n', 'Mean thrombus area Otsu [um2]');
fprintf(fid,'%4.0f\n', Ath_O);

fclose(fid);
end
```

C.2. Pressure data acquisition

```
%% Define Red Pitaya as TCP/IP object.
clc, clear all
close all

%% Connection to RedPitaya, input IP of your Red Pitaya
IP= '192.168.128.1';
port = 5000;
s=tcpip(IP, port);
% Open connection with your Red Pitaya.
fopen(s);
s.Terminator = 'CR/LF';

%% variables initialization
t = 0;
y = 1;
j = 1;
% array connected to analog port AIN2
VoltageValue(y)=str2num(query(s,'ANALOG:PIN? AIN2'));
% creation of the animated line for measured pressure values over time
h = animatedline(t,VoltageValue(y));
%% create file .txt with info provided by the user
filename = sprintf('Exp%s-coll%s-shear-%s.txt',input ('Exp numero: ', 's'),input ('coll: ',
's'), input ('Shear stress imposto: ', 's'));
fileID = fopen(filename, 'wt');

%% stop button
fig = uifigure('Position',[675 180 200 100],'Name','Tasto interruzione esecuzione
programa');
sb = uibutton(fig,'state','text','STOP','FontName','Time New Roman','FontSize',24,...
   'Fontweight','bold','BackgroundColor','r','Position',[50 30 100 40]);

%% showing real time graph
figure (1);
grid on;
set (1, 'Name', 'Grafico acquisizione valore pressori');
title ('Acquisizione valori pressori', 'Fontsize', 16, 'Color','#D95319');
```

```
xlabel ('t_{seconds}', 'FontSize', 12, 'Color', 'k');
ylabel ('Pressure (mmHg)', 'FontSize', 12, 'Color', 'k');
% set graph axes
xlim([0 inf]);
axis 'auto y';

%% plot and save .txt files
tic
while true
    % reading voltage values from RedPitaya analog pin 2
    VoltageValue(y)=str2num(query(s,'ANALOG:PIN? AIN2'));.
    % Voltage to pressure conversion
    i(y) = (VoltageValue(y)-0.03906)./0.013;
    fprintf(fileID,'%f\n', i);
    r(j) = i(y);
    % moving average filter
    P = movmean (r,5);
    % updates graph with now point
    addpoints(h, toc, P(j));
    drawnow
    % Stop instructions
    stop_state = sb.Value;
        if stop_state
            break;
        end
    % save calculated mean values
    j = j+1;
    y=y+1;
end
saveas(1, [filename '.png'], 'png');
toc
fprintf (fileID, '\n%f\n', toc);
fclose(fileID);
fclose(s);
delete(s);
clear s
```

C.3. Pressure measurement analysis

```
% This code process the pressure data adquired from the pressure sensor and
% estimate deltaP, Pmax, AUC

clc, clear all

%% Input data
t0=0;
tf = 240; % The experiment lasts 4 min = 240 s
%select the txt file containing the pressure data and load the data in an array
[filename, path] = uigetfile('.txt');
mydata = load([path filename]);
%save separately extention and name of the file
[filepath,name,ext] = fileparts(filename);
%identify experiment final time which is the last row of the txt file and create P and t
arrays
time=mydata(end)
newdata=mydata;
newdata(end)=[];
P2=newdata;
t2 = linspace(t0,time,length(P2))';

%% curve starts when p starts to increase, cut the initial part
plot(t2, P2, '-');
xlabel('t [s]','FontName','Times New Roman','FontSize',12,'Fontweight','bold');
ylabel('p [mmHg]','FontName','Times New Roman','FontSize',12,'Fontweight','bold');
title('identify when p starts increasing');
[tstart, Pstart] = ginput(1)

istart = find( t2 > tstart, 1, 'first');
t1=t2(istart:end);
t=t1-tstart;
P1=P2(istart:end);
time=t(end);
P0=P1(1);
P1=P1-P0;
```

```
%% Aggregation curve
% Cut the curve at 4 min
if time > tf
   iend = find(t > tf, 1, 'first');
   t(iend:end)=[];
   P1(iend:end)=[];
end
%% Ask the user for the shear stress to colour differently the curve after general
stabilization time

figure()
plot(t, P1, '-');
xlabel('t [s]','FontName','Times New Roman','FontSize',12,'Fontweight','bold');
ylabel('p [mmHg]','FontName','Times New Roman','FontSize',12,'Fontweight','bold');
title({'', name, ''}, 'FontName','Times New Roman','FontSize',12,'Fontweight','bold');
button = questdlg('Is the shear stress 42.75?', 'Jump finder', 'YES', 'NO','NO');
close

if strcmp(button, 'YES') == 1
   stab_time=110;
   istab = find( t > stab_time, 1, 'first');
   tstab=t(istab)
   Pstab=P1(istab)

else if strcmp(button, 'NO') == 1
        stab_time=70;
        istab = find( t > stab_time, 1, 'first');
        tstab=t(istab)
        Pstab=P1(istab)
   end
end

% Reduce noise by applying a moving average filter and convert seconds to min
P = movmean(P1,5);

%% AUC and dP
% define baseline (where the plateau before p increases again starts)%
tbaseline=t(1:istab);  %time till the starting of the aggregation point, start of the
baseline
```

```
Pbaseline=P(1:istab);
Pbline=[Pbaseline; Pbaseline(end)*ones(length(t)-length(tbaseline),1)];
% t and Pbline determine the curve of the baseline
Pmax = P(end)      % P after aggregation at 4 min
% total Area Under the Curve estimated by trapezoidal numerical integration
AUCtot = (trapz(t,P));
AUCbline = (trapz(t,Pbline)); % Area under the baseline curve
AUC = AUCtot-AUCbline; % Area between aggregation curve and baseline
AU=Pmax-P(istab);

% Plot and show the final aggregation curve and the test parameters
plot(t(1:istab), P(1:istab), 'r-');
xlabel('t [s]','FontName','Times New Roman','FontSize',12,'Fontweight','bold');
ylabel('p [mmHg]','FontName','Times New Roman','FontSize',12,'Fontweight','bold');
title({'', name, ''}, 'FontName','Times New Roman','FontSize',12,'Fontweight','bold');
hold on
plot(t(istab:end), P(istab:end), 'b-');

%% Save
% Save the figure, the curve, Pmax and AUC data
set(gcf,'PaperPosition', [0 0 10 7]);
set(gcf,'PaperSize', [10 7]);
saveas(gcf,[path '\' name '.png'],'png');

fileID = fopen([path '\' name '_DATA.txt'],'w');
fprintf(fileID,'\n%6s\n\n', name);
fprintf(fileID,'%6s %12s\n\n', 'Data', 'Value');
fprintf(fileID,'%6s %12.2f\n', 'dP  [mmHg]  ', AU);
fprintf(fileID,'%6s %12.2f\n', 'AUC [mmHg*s]', AUC);
fprintf(fileID,'%6s %12.2f\n', 'P_max [mmHg]', Pmax);
fclose(fileID);
%close
```

List of Figures

List of Tables

Acknowledgments

I warmly thank prof. Alberto Redaelli that gave me the opportunity to carry out this project.

A big thank you to Silvia Bozzi that helped me and followed me along this path.

My heartfelt thanks to Tatiana Mencarini, I couldn't have hoped for a better tutor. Thanks for being there since day one, helping me to reach this goal.

To Mariangela Scavone, whose amazingly wide knowledge will always impress me, and to Mariagrazia Calogiuri, who's been my (dis)adventure mate for a bit, go my gratitude.

I'd also like to thank Dr. Slepian, who welcomed me to the UofA and gave me the amazing opportunity of doing research in his lab.

To Daniel and Yana, you've been my family for a while, I can't thank you enough. Thanks for all the support, for all the laughs, and for being there in the good and the bad moments. You've made this journey special.

The biggest thanks to my family, you're my rock and to you goes all my love. Just, thanks.